The Dissertation Committee for Nathan David McTigue Certifies that this is the approved version of the following dissertation:

TROPHODYNAMICS OF THE BENTHIC FOOD WEBS IN THE CHUKCHI AND BEAUFORT SEAS, ALASKA

Committee:

_____

Kenneth H. Dunton, Supervisor

_____

Edward Buskey

_____

James McClelland

_____

Zhanfei Liu

_____

Lee Cooper

TROPHODYNAMICS OF THE BENTHIC FOOD WEBS IN THE CHUKCHI AND BEAUFORT SEAS, ALASKA

by

Nathan David McTigue, B.S.

Dissertation

Presented to the Faculty of the Graduate School of

The University of Texas at Austin

In Partial Fulfillment

Of the Requirements

For the Degree of

Doctor of Philosophy

The University of Texas at Austin

December 2013

Dedication

This work is dedicated to my dearest wife Kathryn who has shown me unending support and love during this journey.

Acknowledgements

A considerable amount of work and support from others has made this work possible. I thank the captain and crews of the *R/V Arctic Seal*, *R/V Alpha Helix*, and *R/V Moana Wave* for their logistical support during oceanographic expeditions. I greatly appreciate the diligent work of colleagues at three stable isotope facilities including Patty Garlough at University of Texas Marine Science Institute, Norma Haubenstock and Tim Howe at University of Alaska Fairbanks, and Dr. Joy Matthews at University of California Davis. Many thanks to Shuting Liu for operating the instrumentation for pigment analysis. I am indebted to Kim Jackson for her support both in the laboratory and emotionally. Travis Bartholomew also provided assistance in the laboratory. Many people have provided help to develop the ideas and concepts presented here, whether in the field, lab, or office. The list includes Chris Wilson, Afonso Souza, Eric Hersh, Sarah Wallace, Joe Stachelek, Dana Sjostrom, Kelly Darnell, Tara Connelly, and Phil Bucolo. Susan Schonberg provided the expertise and tenacity to identify taxa analyzed in this research. The UTMSI Statistics Club provided statistical help. I thank my committee members for their positive feedback and constructive criticism during this learning process. I especially thank Zhanfei Liu for opening his laboratory to me for sample analysis. Funding for this research was provided by Bureau of Ocean Energy Management, Shell Exploration, the National Science Foundation GK-12 program, the E.J. Lund Fellowship, the UTMSI A.S.P.I.R.E. grant, and the David Bruton, Jr. Endowment Fund Fellowship.

TROPHODYNAMICS OF THE BENTHIC FOOD WEBS IN THE CHUKCHI AND BEAUFORT SEAS, ALASKA

Nathan David McTigue, Ph.D.
The University of Texas at Austin, 2013

Supervisor: Kenneth H. Dunton

The Chukchi and Beaufort Sea shelves host diverse and productive seafloor ecosystems important for carbon and nitrogen cycling for the Arctic Ocean. The benthic food web transfers energy from primary producers to high trophic level organisms (e.g., birds, fish, and mammals), which are important for cultural practices and subsistence hunting by Native Alaskans. This work focuses on the trophic ecology of arctic food webs through use of several different approaches. First, variation in the natural abundance of stable carbon and nitrogen isotopes facilitated the identification of trophic pathways and, subsequently, allowed the comparison of trophic guilds and food webs from the Chukchi and Beaufort Seas. Compared to water column and sedimentary organic matter end-members, second trophic level grazers and suspension feeders were conspicuously ^{13}C-enriched throughout the Chukchi Sea, which supports the hypothesis that microbial degradation of organic matter occurred prior to metazoan assimilation. Second, food web recovery from disturbances caused by exploratory oil drilling at the seafloor that had occurred approximately 20 years prior were assessed in both the Chukchi and Beaufort Seas. Based on isotopic trophic niche overlap between organisms common to drilled and reference sites in the Chukchi and Beaufort Seas, the oil drilling sites had similar food web structure, indicating recovery from the activity associated with the drilling process. Third, photosynthetic pigment biomarkers were used to better understand the diagenetic process, specifically focusing on how both microbial and metazoan grazing pathways degrade organic matter in relation to seasonal sea ice retreat in the Chukchi Sea. The benthic macrofaunal and microbial food web caused rapid

degradation of organic matter upon the initial pulse of microalgal food sources to the seafloor. These diagenetic pathways are linked to the ^{13}C-enrichment of residual organic matter, which corresponds to the stable isotope values measured in the benthic macrofauna. Lastly, high-precision liquid chromatography and spectrophotometry were compared for estimating sedimentary pigments in the marine environment. Substantial differences in pheopigment (chlorophyll degradation products) concentrations were observed between the two techniques, suggesting the need for revisions to the monochromatic spectrophotometric equation that relates absorbance to pigment concentrations. One pheopigment, pheophorbide, was found to interfere with the accuracy of the spectrophotometric equation and caused the overestimation of pheopigments.

Table of Contents

List of Tables

List of Figures

Introduction

Natural abundance stable isotopes have become a premier tool to explore trophic ecology of the world's marine ecosystems. The application of stable isotopes to trace organic matter flow and to define trophic positioning in a food web relies on two principles. First, stable isotope ecology relies on the tenet that the stable isotope ratios (e.g., $^{13}C/^{12}C$ or $^{15}N/^{14}N$ expressed in standardized δ notation in parts per thousand) of a consumer proportionally reflect its food sources given specific trophic enrichments (Fry et al., 1978; Fry and Sherr, 1984). Typically, stable carbon isotopes fractionate very little (0-2‰) during trophic transfer and link the consumer to ultimate energy resources (DeNiro and Epstein, 1978; Peterson and Fry, 1987), whereas stable nitrogen isotopes exhibit higher fractionation between trophic steps (3-4‰) and provide a means for trophic positioning (Vander Zanden and Rasmussen, 2001). Despite some variation in trophic enrichment factors (Post, 2002), stable carbon and nitrogen isotopes, in tandem, can elucidate energy flow and structure in a food web (Jardine et al., 2006). Therefore, it is possible to assign each organism to a trophic position based on its ^{15}N-enrichment compared to a baseline value, typically the $\delta^{15}N$ value of a first trophic level primary producer or particulate organic matter (POM). The contribution of food sources to the diet of a consumer can be inferred by assuming the consumer $\delta^{13}C$ value directly reflects one or an averaged combination of $\delta^{13}C$ values of organic matter sources.

The second principle to successfully use stable isotopes to describe trophodynamics requires that primary producers (or organic matter sources) are isotopically distinct in order to decipher the contribution of each source to the food web. The $\delta^{15}N$ values for primary producers reflect their ultimate inorganic nitrogen source and can distinguish the importance of isotopically disparate inorganic nitrogen pools (e.g., McClelland et al., 1997). $\delta^{13}C$ values of producers vary based on both the signature of the inorganic carbon source and the fractionation that occurs during enzyme-mediated carbon fixation during photosynthesis (Maberly et al., 1992). Terrestrial plants that use the C_3 photosynthetic pathway possess relatively ^{13}C-depleted values for primary

producers (~-28‰) since their pool of atmospheric CO_2 is more depleted (-8‰) than dissolved inorganic carbon (DIC) in the ocean (~0‰) (Peterson and Fry, 1987). Marine phytoplankton $\delta^{13}C$ values typically range from -24 to -22‰, while marine macroalgae can span a relatively wide range, e.g., from ^{13}C-depleted *Bostrychia* sp. (-30.7‰) and *Phycodrys antarctica* (-33.7‰) to relatively ^{13}C-enriched *Ulva* sp. (-15.3‰), *Ulothrix* sp. (-13.2‰), and *Laminaria solidungula* (-16.5 to -13.6‰) (Dunton and Schell, 1987; Dunton, 2001; Machas et al., 2003). Seagrasses, with $\delta^{13}C$ values reported for *Thalassia testudinum* (-10.0‰), *Posidonia oceanica* (-14‰), *Halodule wrightii* (-13.6 to -10.6‰), and *Zostera marina* (-15.0 to -7.9‰), are another ^{13}C-enriched carbon source for estuaries compared to phytoplankton (Fourqurean et al., 1997; Peterson, 1999; Pinnegar and Polunin, 2000; Moncreiff and Sullivan, 2001). *Spartina* spp., which utilize the C_4 photosynthetic pathway, provide ^{13}C-enriched organic matter (-15.4 to -12.7‰) for marsh food webs compared to phytoplankton and upland plants (Currin et al., 1995; Deegan and Garritt, 1997; Kwak and Zedler, 1997). Benthic microalgae can become ^{13}C-enriched compared to suspended microalgae (i.e., phytoplankton) since the benthic boundary layer from which they obtain DIC has less exchange with the total DIC pool, thus facilitating less ^{13}C discrimination during fixation (France, 1995; Doi et al., 2010). Unique to polar regions, sea ice algae represent another carbon source for the food web. Similar to benthic microalgae, the boundary layer of sea ice and the essentially closed-pool brine channels that house the microalgae can allow less ^{13}C discrimination during fixation, but sea ice algae range in $\delta^{13}C$ from -25 to -14‰ (Hobson et al., 2002; McMahon et al., 2006; Gradinger et al., 2009). Finally, deep sea food web studies have shown that benthic consumers become ^{13}C-enriched compared to surface POM values after assimilating the surface-derived organic matter after it has undergone microbial breakdown that causes subsequent ^{13}C-enrichment due to the degradation and release of ^{13}C-depleted compounds like lipids (Wakeham et al., 1997; Iken and 405, 2001; Nyssen et al., 2002; Mincks et al., 2008).

The Chukchi and Beaufort Seas represent unique marine habitats that lack some of the above-mentioned primary producers. The systems are devoid of ^{13}C-enriched

marsh plants, seagrasses, and macroalgae except for a kelp bed that exists in the eastern Beaufort Sea near Stefansson Sound isolated from the study sites in this research. Instead, the systems are dominated by inputs of water column primary production (Sakshaug, 2004; Wassmann and Reigstad, 2011). Perplexingly, benthic consumers in the Chukchi Sea span a wide range of $\delta^{13}C$ values, including second trophic level organisms that are 4-6‰ more ^{13}C-enriched than phytoplankton (>20μm), POM, and sedimentary organic matter, three food web end-members targeted in this research (Chapter 1). Phytoplankton indeed entrains the ^{13}C-depleted consumers, but unmeasured in this research, a ^{13}C-enriched organic matter source must also contribute to the food web as a carbon source to account for the ^{13}C-enriched values of many second trophic level consumers. Seemingly confounding, if the ^{13}C-enriched organic matter source exists in the sediments, it must be in small concentrations since the bulk sedimentary organic matter $\delta^{13}C$ values, despite being slightly more ^{13}C-enriched than the water column end-members (Chapter 1), do not account for the consumer values. Consumers, then, must continually remove the ^{13}C-enriched fraction as it is produced since its signal is diluted against the remaining organic matter. Potential candidates are sea ice algae, microbial biomass and by-products, or benthic microalgae.

Sea ice algae represent an initial pulse of organic matter for benthic food webs during ice retreat, but sea ice algae have been shown to be less important than phytoplankton to the benthic carbon budget in arctic ecosystems. Hobson and Welch (1992) investigated the food web structure of Lancaster Sound in the Canadian Archipelago to find that the system was POM-based, despite the presence of ice algae and kelp. The authors commented on the lack of "discernable patterns" in the food web based on $\delta^{13}C$ since second trophic level deposit feeders were considerably ^{13}C-enriched compared to POM. In a Chukchi Sea study, Budge et al. (2008) demonstrated 0-61% (mean=24%) of consumer carbon was derived from ice algae compared to other primary producers using compound specific stable isotope analysis on fatty acids. In the Northeast Water Polynya off the coast of Greenland, Hobson et al. (2002) ascribed the enriched $\delta^{13}C$ values of benthic consumers, compared to ^{13}C-depleted pelagic organisms,

to the input of isotopically heavier ice algae but did not rule out the potential for boundary layer effects (benthic microalgae) or microbial and meiofaunal degradation of organic matter also attributing to the consumer values.

Lovvorn et al. (2005) measured suspended POM, ice POM, and sedimentary OM end-members in the north-central Bering Sea, but benthic organisms were more ^{13}C-enriched than any measured organic matter source. The authors reasoned that microbial degradation, which can cause ^{13}C-enrichment of organic matter, occurred prior to macrofaunal assimilation. In another Bering Sea study in summer, the microbial processing of organic matter was implicated for the ^{13}C-enriched value for the deposit feeding bivalve *Yoldia limatulata* (-17.3‰) compared to the ^{13}C-depleted phytoplankton (-23.3‰) (McConnaughey and McRoy, 1979).

Although historically overlooked in the Arctic (Cahoon, 1999), benthic microalgae have been increasingly appreciated as a source of organic matter to shallow benthic food webs (Glud et al., 2009). Benthic microalgae were estimated to account for 96% of total primary production in Young Sound, Greenland at depth of 5 m, and still contributed 51% of total primary production at 30 m (Glud et al., 2002). Off Point Barrow, Alaska, benthic microalgae were measured at 3% (Horner and Schrader, 1982) and 76% (Matheke and Horner, 1974) of total primary production. Herman et al. (2000) used bulk natural abundance stable isotopes to show that benthic deposit and interface feeders were ^{13}C-enriched compared to their measured organic matter sources including bulk sedimentary organic matter. To resolve the mismatch between consumer and organic matter source, isotope labels were applied to benthic microalgae within the sediments to show that some of the ^{13}C-enriched organisms preferentially assimilated benthic microalgae from the sediments, and the ^{13}C-enriched isotopic signal of the benthic microalgae was diluted within bulk sedimentary organic matter.

Sea ice algae were the least viable possibility for a ^{13}C-enriched end-member in these studies based on the variety of literature-based stable isotope values for the producers (-25 to -14‰) and the isotopic turnover window of fauna (see Chapter 1 Discussion). Benthic microalgae presented another viable option given their generally

^{13}C-enriched isotopic signatures compared to their suspended counterparts (France, 1995; Doi et al., 2010). In an initial pursuit of this possibility, chlorophyll *a* and accessory pigments, including chlorophyll degradation products (pheopigments), were quantified in the sediments throughout the study site to assess microalgal biomass and "freshness" of the sediment organic matter (Chapter 3). Throughout the Chukchi Sea, high concentrations of chlorophyll *a* were present in sediments, and high chlorophyll:pheopigment ratios suggested the presence of viable cells. Although attempted, diatoms isolated from sediments were unsuccessfully measured for stable isotope values. However, since total organic carbon (TOC) in the sediments was highly correlated with both chlorophyll *a* and fucoxanthin (a diatom biomarker) concentrations, then the microalgae in sediments are likely a major constituent of the stable isotope values of bulk sedimentary organic matter, which was relatively ^{13}C-depleted compared to consumers. Still, it is possible that benthic microalgae in the Chukchi Sea sediments are viable, given that 1% of surface irradiance reaches 25% of the Arctic Ocean shelves (Gattuso et al., 2006), and dark-adapted benthic diatom assemblages require between 2-30 μmol photons m^{-2} s^{-1} (Gomez et al., 2009) and have been reported to subsist with as little as 0.1 μmol photons m^{-2} s^{-1} (McGee et al., 2008). In our study area, light attenuation (*k*) was measured at 0.12, 0.11, and 0.07. With these coefficients, 9 μmol photons m^{-2} s^{-1} of photosynthetically active radiation (PAR) reaches 50 m if surface irradiance was 1300 μmol photons m^{-2} s^{-1}. Importantly, at such low light and temperature levels, growth rate is extremely low (Karsten et al., 2006). Since photosynthesis occurs slowly at low light conditions, isotopic fraction during photosynthesis (ε_p) is higher than in high PAR environments (Rau et al., 1996). Therefore, the photosynthetic benthic diatom assemblages on the Chukchi and Beaufort Sea shelves would possess more ^{13}C-depleted values than those in temperate and tropical environments despite boundary layer effects. Hecky and Hesslein (1995), who isolated benthic microalgae (epilithon, epipelon, etc.) from tropical, temperate, and arctic lakes, showed that although all lakes had approximately the same δ^{13}C-DIC values, the benthic microalgae showed a δ^{13}C gradient from most ^{13}C-enriched values in tropical lakes to the most ^{13}C-depleted values

in the Arctic. For these reasons, benthic microalgae were not at the forefront of hypotheses surrounding the ^{13}C-enriched benthic consumers in the Chukchi Sea.

Instead, the microbial degradation of organic matter and subsequent ^{13}C-enrichment seemed more likely responsible for the unaccounted organic matter source, as was implicated in deep-sea food web studies (Iken and 405, 2001; Mincks et al., 2008; Bergmann et al., 2009b). This hypothesis is counterintuitive since bulk sedimentary organic matter was a relatively ^{13}C-depleted end-member. However, if the ^{13}C-enriched fraction of organic matter is continually removed by grazing, the ^{13}C-enriched signal will not be captured by our stable isotopic analysis that essentially measures standing stock of carbon sources. Hansen and Josefson (2004) showed that viable diatoms are not broken down and assimilated in animal guts, but rather pass through undigested. This provides a possible mechanism for non-selective deposit feeders to consume all organic matter in sediments, but since live microalgae are not digested, only degraded organic matter and other microbial by-products are assimilated instead. This hypothesis was pursued in this dissertation to account for the wide range of δ^{13}C values exhibited by the food web.

This research approaches the above hypothesis in several different ways. In Chapter 1, the food web consumers are divided into *a priori* trophic guilds to determine if feeding type can elucidate the organisms by which the ^{13}C-enriched organic matter is incorporated into the food web. Chapter 2 compares organisms from the Chukchi and Beaufort Seas and respective food web end-members to demonstrate the presence of a ^{13}C-enriched end-member in the Chukchi Sea. The diagenesis of organic matter is described in Chapter 3 by using chlorophyll and pheopigments as proxies for freshness and degradation of microalgae, and pheopigment concentrations were correlated to stable isotope values of sediment organic matter and the snow crab *Chionoecetes opilio*. Lastly, Chapter 4 examines and revises the spectrophotometric method to measure pheopigments, an indicator of organic matter degradation and potential ^{13}C-enrichment.

Chapter 1

Trophodynamics and organic matter assimilation pathways in the northeast Chukchi Sea, Alaska

Abstract

Trophic linkages in the northeast Chukchi Sea shelf were analyzed based on the stable carbon and nitrogen isotopic analysis of 39 species collected in 2009 and 2010. To decipher organic matter assimilation pathways, benthic fauna were first categorized into nine trophic guilds based on their physical location in the seabed (epibenthic, surface, or subsurface), feeding mode (suspension feeder, deposit feeder, predator, or scavenger), and food source (suspended particulate organic matter, phytoplankton, zooplankton, sediment, microflora, meiofauna, or macrofauna). A discriminant function analysis (DFA) determined that feeding modes were predicted by stable isotope values at an overall classification success rate of 42%, although classification success of each individual guild varied from 0 to 66%. In some instances, stable isotopes classified trophic guilds incorrectly more often than correctly, suggesting high trophic redundancy in the system. A striking pattern was observed where the $\delta^{13}C$ values of individuals in some trophic guilds, ranging from about -23 to -17‰, were substantially more ^{13}C-enriched than representative end-members, which includes phytoplankton (-24.0‰), suspended particulate organic matter (-24.3‰), and bulk sediment organic matter (-23.3‰). Near-seafloor suspended particulate organic matter was significantly ^{13}C-enriched compared to suspended particulate organic matter of near surface waters ($p<0.05$), and bulk sedimentary organic matter was more ^{13}C-enriched than overlying phytoplankton at seven of ten stations. This suggests the presence of an unmeasured ^{13}C-enriched end-member that is a product of biogeochemical alteration and reworking by the sediment microbial community. Although the microbial community is difficult to quantify using bulk stable isotope analytical techniques, these results indicate it cannot be overlooked as a critical component and avenue through which large amounts of reduced carbon are assimilated by a rich and diverse arctic shelf food web.

1. Introduction

Recent declines in sea ice extent and duration (Perovich, 2011) are lengthening the open-water season for marine primary producers in arctic ecosystems (Arrigo et al., 2008). Typically, the retreating ice edge fosters an intense phytoplankton bloom in the Chukchi Sea that is largely ungrazed by a zooplankton population that is still low in abundance in early spring (Coyle and Cooney, 1988; Sakshaug and Slagstad, 1992). The earlier onset of open water with ice retreat over the past decade has led to contrasting projections for pelagic primary production. Kahru et al. (2011) and Saitoh et al. (2002) argued that phytoplankton blooms would occur earlier, potentially yielding less production due to lower light availability during the arctic spring compared to early summer. However, open-water blooms occurring later in the season are under increased grazing pressure by zooplankton (Coyle and Pinchuk, 2002). New evidence (Arrigo et al., 2012) suggests that thin (0.5-1.8 m) first-year sea ice permits sufficient light transmission to sustain intense phytoplankton blooms prior to open water events. The change in timing of the phytoplankton bloom is important since the productivity of benthic consumers is tightly coupled to pelagic primary production (Grebmeier et al., 1988; Dunton et al., 1989; Grebmeier et al., 1989; Dunton et al., 2005; Iken et al., 2010).

Several studies have addressed the organic matter assimilation pathways in benthic food webs within high latitude marine systems in the Alaskan Arctic (McConnaughey and McRoy, 1979; Dunton and Schell, 1987; Dunton et al., 1989; Lovvorn et al., 2005; Iken et al., 2010; Feder et al., 2011; Dunton et al., 2012), but few detail the northeast Chukchi Sea, which is now an area of increased interest because of its enormous potential for offshore oil and natural gas exploration and production (Gautier et al., 2009). Tracing assimilation pathways from primary producers is essential to understand how high trophic level organisms (e.g., marine mammals, birds, fish), important for cultural and subsistence hunting practices of native Alaskan communities obtain their ultimate energy sources (Lovvorn et al., 2003; Highsmith, 2006). The assimilation pathways that lead to apex predators are particularly of interest since their ultimate energy sources (primary producers) are heavily dependent on and regulated by

sea ice dynamics. Although a multitude of studies relate climate change effects to primary producers in arctic ecosystems (Arrigo et al., 2008; Kahru et al., 2011; Wassmann and Reigstad, 2011), few approach the problem by addressing how organisms with different feeding modes may be affected (Sun et al., 2009).

Stable isotope analyses are used to identify the ultimate sources of carbon that are critical components of consumer diets and track the transfer of assimilated organic matter among organisms. Because of the consistent, stepwise fractionation or enrichment exhibited by carbon and nitrogen isotopes during biological processing, these analyses are reliable tools to investigate food web dynamics (Fry and Sherr, 1984). $\delta^{13}C$ values between source and consumer change approximately 0-2‰ per trophic step (DeNiro and Epstein, 1978; DeNiro and Epstein, 1981; Post, 2002). Since ultimate sources of carbon often have distinct $\delta^{13}C$ signatures, and fractionation per trophic step is small, stable carbon isotopes can act as tracers of ultimate carbon sources from origin consumer. Stable nitrogen values ($\delta^{15}N$) of organisms become enriched by 3-4‰ per trophic step (DeNiro and Epstein, 1981). Consequently, $\delta^{15}N$ values are used to model species' trophic position in a food web (Vander Zanden and Rasmussen, 2001; Post, 2002). Stable isotope analysis provides an advantageous tool for the Chukchi Sea system because it not only incorporates a long-term, integrated trophic position for organisms, but also distinguishes between food source assimilation versus ingestion as indicated by gut contents analysis. Moreover, organic matter assimilation pathways also represent the avenues that contaminants, like polycyclic aromatic hydrocarbons (PAHs) or heavy metals associated with oil and natural gas development, are transferred and biomagnified in the food web (Rasmussen et al., 1990; Hoekstra et al., 2003; Fox et al., in press).

It is useful to explore the functional role of different organismal groups when investigating the biological processing of organic matter within an ecosystem. Studies that have used the trophic guild approach, in concert with stable isotope analyses, were able to describe organic matter assimilation pathways in food webs in the Mediterranean suprabenthos (Fanelli et al., 2009b), tropical estuaries (Abrantes and Sheaves, 2009), temperate latitudes (Reum and Essington, 2008), arctic deep sea (Bergmann et al.,

2009a), and on the Antarctic shelf (Mintenbeck et al., 2007; Gillies et al., 2012). We grouped organisms, regardless of taxonomic lineage, into trophic guilds, or groups of organisms that exploit the same resource(s) in a similar manner (Root, 1967). By incorporating functional morphology (i.e., feeding mode), it is possible to elucidate the pathways by which organic matter is processed and passed to higher trophic levels. This approach is useful since marine food webs often represent a "trophic continuum" (i.e., a cascade of non-integer trophic levels) rather than a food web with discrete trophic levels (France et al., 1998).

The results presented here represent a subset of interdisciplinary studies conducted during the Chukchi Sea Offshore Monitoring in Drilling Area: Chemical and Benthos (COMIDA:CAB) project that was designed to establish baseline chemical and biological characteristics for the northeast Chukchi Sea. The goal of this study was to determine major avenues of organic matter assimilation for the benthic food web. Specifically, I asked if stable isotope values of primary consumers in separate trophic guilds can discriminate major avenues of organic matter assimilation. I hypothesized that trophic guilds will exhibit high trophic redundancy, measured by isotopic niche overlap, if they assimilate organic matter resources from the same ultimate carbon and nitrogen sources.

2. Methods

2.1 Study area and sample collection

Our sampling stations in the COMIDA study area in the northeastern Chukchi Sea were positioned between the Alaska coastline and 169°W, and from approximately 68.9°N to 72.4°N (Figure 1.1). Samples were collected between 27 July and 12 August 2009 and 25 July and 16 August 2010 aboard the vessels *R/V Alpha Helix* and *R/V Moana Wave*, respectively. Stations were chosen using a hexagonal tessellation technique to ensure random selection and even distribution of stations (White et al., 1992). Mean station depth was 42 ± 7 m ($\bar{x}$ ± SD, n = 50), excluding Station 50 in Barrow Canyon (130 m). The region is dominated by Bering Shelf-Anadyr Water,

although the Alaska Coastal Water likely influenced some of the easternmost stations, including Stations 1, 4, and 14 (Coachman et al., 1975). Hydrographic parameters of temperature and salinity were measured using a YSI Data Sonde 6690 (YSI, Yellow Springs, OH). Conductivity was calibrated at 10,000 and 50,000 μS (Ricca Chemical Company, Arlington, TX). Bottom temperatures during both sampling years averaged ~0 °C, and bottom water salinities ranged from 30.0 to 33.6. Although warmer bottom waters (1-6 °C) predominated in the southern study area (stations 1, 105, 2, 3, 6, 7, and 14), salinity showed no strong spatial pattern.

Preceding water collection, a Data Sonde cast at each station determined the structure of the pycnocline. A peristaltic pump attached to weighted, metered Tygon tubing was used to collect water at surface, intermediate, and near-bottom depths for suspended particulate organic matter (SPOM). Vertical plankton tows using 20 and 335 μm mesh nets (Sea Gear, Melbourne, FL) were used to collect phytoplankton and zooplankton, respectively, from near bottom depths to the surface. Prior to sample filtration, any visible zooplankton were removed from SPOM and phytoplankton samples, and samples were vigorously shaken to ensure no settling had occurred. SPOM size class was defined by the 0.7 μm retention size of the GF/F filters. Phytoplankton was defined as particulates retained by the 20 μm net mesh size. Visual microscopy inspections revealed concentrated microalgae in phytoplankton samples with few, if any, other particulates. Calanoid copepods were isolated from zooplankton by hand using a transfer pipette for filtration. Replicate samples of SPOM, phytoplankton, and copepods were filtered onto 25 mm GF/F filters (Whatman, Buckinghamshire, UK) that were previously combusted at 450°C for 24 hours to remove trace organic material. All filtered samples were dried at 60°C and stored in opaque vials.

A van Veen grab (0.1 m^2) was used to collect benthic infauna (see Schonberg et al., in press). Benthic epifauna were collected using a 3.05 m plumb-staff beam trawl with a 7 mm mesh and a 4 mm cod-end liner (see Ravelo et al., in press). Infauna and epifauna samples were sieved through 1 mm mesh and washed with ambient surface seawater to remove extraneous organic matter and sediment. Organisms were kept in

holding tanks with running ambient seawater to allow small organisms to evacuate gut contents prior to isotopic analysis. Faunal organisms were keyed to lowest taxonomic level possible, usually species, in the field. When possible, muscle tissue was extracted from the organism (e.g., gastropods, bivalves, large arthropods, and fish) following IACUC protocols. Small organisms (e.g., amphipods and polychaetes) were kept whole. Labeled samples were dried on board ship at 60°C in aluminum dishes.

Sediment samples for biological and chemical analyses were collected at all stations from van Veen grabs. A 60 cm^3 syringe barrel (2.6 cm diameter, 10 cm depth) was used to extract sediment for porewater ammonium analysis. A 20 cm^3 syringe barrel (1.8 cm diameter, 2 cm depth) was used to collect undisturbed surface sediment for stable carbon and nitrogen isotope analysis of organic matter. Sediment aliquots were placed in either pre-labeled Whirl-pak bags (Nasco, USA) or pre-labeled Falcon tubes (BD, USA) and immediately frozen in darkness. Filters, tissue samples, and sediment were transported to the University of Texas Marine Science Institute (UTMSI) for stable isotope preparation and analysis.

2.2 Sample analyses

Stable isotopic analyses were performed on benthic fauna, zooplankton, filtered water samples, and sediments. To remove carbonates that would skew stable carbon isotope analysis, a subsample of faunal tissues (particularly calcifying organisms and small, whole organisms) and sediments were soaked in 1 *N* HCl until bubbling stopped, then rinsed in deionized water and dried at 60°C to a constant weight. SPOM and phytoplankton filters were repeatedly wetted with H_2PO_4 for 24 hours prior to analysis. Tissue subsamples, sediment subsamples, and replicate filtered samples prepared for stable nitrogen isotope analysis were not subjected to acidification. Muscle tissue excised from organisms that contained non-calcifying structures or shells were not acidified.

Dried tissue samples were manually homogenized with a mortar and pestle and weighed in tin capsules to the nearest 10^{-6} g. Samples were analyzed on an automated

system for coupled $\delta^{13}C$ and $\delta^{15}N$ measurements using a Finnigan MAT Delta Plus mass spectrometer attached to an elemental analyzer (CE Instruments, NC 2500) at UTMSI, a PDZ Europa ANCA-GSL elemental analyzer interfaced to a PDZ Europa 20-20 isotope ratio mass spectrometer (Sercon Ltd., Cheshire, UK) at UC Davis, or a Thermo Delta V Plus interfaced with a Costech ESC 4010 elemental analyzer using a ConfloIII system at University of Alaska Fairbanks. Samples were combusted at 1020°C and injected into the mass spectrometer with continuous flow. Isotopic ratios are denoted in standard δ notation relative to carbon and nitrogen standards of VPDB and atmospheric N_2, respectively, where

$$\delta X=[(R_{sample}/R_{standard})-1] \times 1000. \quad (1)$$

X is either ^{13}C or ^{15}N of the sample and R corresponds to the $^{13}C/^{12}C$ or $^{15}N/^{14}N$ ratio. Instrumental analytical error was ±0.15‰ and analytical sample error was ±0.20‰, based on internal standards from the U.S. National Institute of Science and Technology and the International Atomic Energy Agency. Lipids were not extracted from samples prior to analysis. Although we found most consumer tissues were more ^{13}C-enriched than expected, many organisms possessed relatively high C:N values, a possible indicator of high lipid content (see Post et al., 2007). To assess whether lipids were important, we selected 14 species from seven phyla that possessed a relatively high range of both C:N ratios (>4) and $\delta^{13}C$ values (>2‰) to determine if those individuals with high C:N ratios possessed depleted $\delta^{13}C$ values. We individually regressed $\delta^{13}C$ values from each of the 14 species by their C:N ratios. We found no inverse relationship between the two indices in these species, which indicated that lipid extraction would not have altered $\delta^{13}C$ values ($r^2 < 0.33$). Other studies have found that lipid content in arctic benthic organisms did not confound $\delta^{13}C$ values (Graeve et al., 1997; Iken et al., 2010) and that C:N ratios and $\delta^{13}C$ values are not correlated (Dunton et al., 2012).

Trophic level (TL) was calculated using an equation incorporating $\delta^{15}N$ values of consumers, a baseline food source, and a calculated enrichment factor:

$$TL = [(\delta^{15}N_{consumer} - \delta^{15}N_{SPOM}) / 3.4]+1 \quad (2)$$

A trophic enrichment factor of 3.4 was calculated based on the average difference of $\delta^{15}N$ between the suspension feeding amphipod *Ampelisca macrocephala* (11.1±0.5‰) and phytoplankton (7.7±0.3‰). *A. macrocephala* individuals consistently had $\delta^{13}C$ values that signify high dependence on phytoplankton carbon (Table 1.1). Although this determination was based on only one consumer-diet relationship, the estimated enrichment factor was applied to all consumers in the Chukchi Sea. However, the value is in close agreement with other arctic benthic food web enrichment factors reported for the Canadian archipelago (Hobson and Welch, 1992; 3.8), the Bering Strait and Southern Chukchi Sea (Iken et al., 2010; 3.4), and the nearshore shelves and estuarine lagoons of the Beaufort Sea (Dunton et al., 2012; 3.4). We calculated a carbon isotopic trophic enrichment factor of ~0.4‰ between *A. macrocephala* (-23.6±0.4‰) and phytoplankton (-24.0±0.4‰). In contrast, Dubois et al. (2007) reported mean enrichment factors of +2‰ for $\delta^{13}C$ in bivalves based on a controlled feeding study. A metadata analysis by Post (2002) showed that despite mean and mode $\delta^{13}C$ enrichment factors falling between 0 and +1‰, some values ranged up to +4‰. To account for such interspecies variation, we employed a 2‰ trophic enrichment factor for $\delta^{13}C$ in this study.

Sediment cores collected for porewater ammonium analysis were thawed and centrifuged at 5000 rpm for 20 min to separate porewater from the sediment. Porewater was decanted and prepared for analysis using the phenolhypochlorite (or indophenol blue) method (Solórzano, 1969). Samples were read against a blank on the Shimadzu UV-2401PC spectrophotometer at 640 nm.

2.3 Ice cover data

Shapefiles of daily ice cover at resolutions down to 50 m^2, provided courtesy of the National Ice Center (NIC), were projected onto a basemap containing all sampling stations in ArcMap 10.0 (ESRI). The NIC defines the demarcation between ice coverage

and the marginal ice zone (MIZ) as 8/10ths ice cover. This line was tracked daily to determine the day that each station was initially covered by <80% sea ice to determine the approximate date of ice algal deposition.

2.4 Statistical analyses

To ensure adequate replication, only species with $n \geq 4$ were assigned a trophic guild classification based on the coding scheme of Macdonald et al. (2010). The scheme classifies arctic benthic species by food source (epibenthic, surface, subsurface), food type/size (sediment, suspended particulate organic matter, benthic microflora, benthic meiofauna, benthic macrofauna, phytoplankton, or zooplankton), and feeding mode (deposit feeder, detritus feeder, suspension feeder, predator, scavenger, grazer, or browsers, see Table 1.2 for acronym codes). Species were classified into 25 specific feeding guilds based on taxonomic data from Macdonald et al. (2010), the World Register of Marine Species (Appeltans et al., 2012), and other primary literature sources (see Table 1.1). Data for a species' genus or closely related genus were used if species-specific data were not available.

Feeding mode data were converted to a binary matrix, where rows and columns represented species and feeding guild components, respectively (descriptors listed in Table 1.2). Organisms were grouped by a binary hierarchical cluster protocol using Ward's method in the *MASS* package for R, where distance on the x-axis (dissimilarity) is equal to the proportion of difference between the binary matrices that defines each species. Using the *pamk* function from the *fpc* package for R (Hennig, 2010), we determined the number of significant clusters of organisms that exist when partitioned around group medoids of each trophic guild at $\alpha = 0.05$ (Kaufman and Rousseeuw, 1990). The *fpc* package (Flexible Procedures for Clustering) provides various clustering techniques and cluster validation procedures. The *pamk* function was used since it first determines the number of significant clusters using algorithms that iteratively minimize the distance between multivariate medians (medoids), then subsequently partitions data around the medoids.

Prior to performing the discriminant function analysis, we tested the null hypothesis that there is no difference between mean stable isotope values (i.e., dual isotopic centroid) between each significant cluster, or trophic guild using multivariate analysis of variance (MANOVA). We used the MANOVA test statistic Pillai's Trace since it is appropriate for small unequal sample groups (*n*). A quadratic discriminant function analysis (DFA) with cross-validation was used to determine if stable carbon and nitrogen isotope values could accurately classify individuals into *a priori* trophic guild assignments (Jepsen and Winemiller, 2002). A DFA is considered an extension of a MANOVA, but instead of testing the null hypothesis that groups differ in classification variables, DFA describes the variables that maximally discriminate among groups. Cross-validation (in this case, jackknife validation) systematically omits a single data point in the entire dataset and groups the remaining data based on the *a priori* classifications. The omitted data point is then re-plotted and reclassified into the best-fitting group, regardless if it is correct or incorrect with respect to its *a priori* grouping. Once the procedure is conducted for every observation in the dataset, a jackknifed reclassification success rate for each *a priori* group is used to quantify the accuracy of the discriminant function, i.e., the rate at which data are distinct in multivariate (or bivariate) space. Cross-validation provides the rate and identity of the groups to which the data were misclassified. A quadratic DFA was used instead of its linear counterpart because it is free of assumptions regarding homogeneity of covariance matrices.

Classification success rates were employed to examine the similarity of resources assimilated by each trophic guild, where high classification error implies overlapping isotopic values (niche) between trophic guilds. Prior to analysis, we determined if the discriminant function was capable of classifying the data at a better-than-random rate using an iterative routine provided by White and Ruttenberg (2007) in Matlab 6.1. Each individual data point (defined by $\delta^{13}C$ value on the x-axis and $\delta^{15}N$ on the y-axis) was randomly assigned membership to a group, and the jackknifed reclassification success rate for the new data was calculated for 1000 iterations. All other statistical analyses were performed in R 2.14.0 (http://www.r-project.org). The area of niche space occupied by

each guild was calculated using the convex hulls created in ArcMap 10.0 (ESRI) after the methods described in Layman et al. (2007a).

3. Results

3.1 Sources of organic matter

Slight but significant differences existed between the stable carbon isotope values of phytoplankton and sediments at the same stations. A comparison of mean $\delta^{13}C$ values of phytoplankton (± 95% confidence intervals; $n = 2$) and sediments ($n = 1$) from stations where both were collected revealed that organic matter within sediments at seven of ten stations was more ^{13}C-enriched than phytoplankton in the overlying water column (Figure 1.2). The mean $\delta^{13}C$ values for near-surface SPOM (-24.7 ± 0.2‰) and near-bottom SPOM (-23.8 ± 0.2‰) were similar to the mean value for phytoplankton collected in the vertical tow (-24.0 ± 0.4‰), but the phytoplankton mean $\delta^{15}N$ value (7.7 ± 0.3‰) was more enriched than near-surface SPOM (6.2 ± 0.4‰) and near-bottom SPOM (4.6 ± 0.5‰).

All sediment samples (top 2 cm) were pooled to form one sediment end-member value since interstation and interannual variation of values was small (SD < 1‰). For values averaged over all stations, bulk organic matter within sediments was similar to phytoplankton with a $\delta^{15}N$ value of 7.4‰ and a $\delta^{13}C$ value of -23.3‰ (Table 1.1). The mean porewater ammonium concentration was 154 ± 73 μM.

3.2 Trophic guild assignment and classification success rate

Identical species collected at the same stations occupied in both the 2009 and 2010 field seasons were compared to determine if interannual stable isotope value variation precluded the aggregation of datasets. Our analyses revealed that neither $\delta^{15}N$ values nor $\delta^{13}C$ values varied significantly ($p > 0.05$) for any species among the two years based on a Student's *t*-test for paired samples. Therefore, all organisms collected in 2009 and 2010 were pooled by species and treated as a single population.

A total of 433 individuals (39 species in eight phyla) were collected in sufficient replication ($n \geq 4$) to test the hypothesis that organisms within separate trophic guilds obtain organic matter through unique trophic pathways. Cluster analysis provided evidence that the 39 species were represented by nine significantly different guilds of organisms that corresponded well to their feeding modes (Table 1.3; Figure 1.3). While each guild consisted of organisms that had feeding modes at least 90% similar, some guilds contained solely organisms with identical feeding modes (e.g., EP-Su-pom in Guild 1, SR-Pr/Sc-mac in Guild 7, etc.). The main compartmentalization made by the clustering routine divided organisms into suspension feeder, deposit feeder, and predator/scavenger guilds (Figure 1.3).

A MANOVA showed that both classification variables ($\delta^{13}C$ and $\delta^{15}N$) significantly differed between trophic guilds ($p<0.0001$); therefore, testing the hypothesis with a DFA was appropriate. We were also able to reject the null hypothesis that the observed classification success rates obtained from a DFA were no better than that expected by random chance ($p = 0.001$). Stable carbon and nitrogen isotope values successfully discriminated feeding guilds at an overall 42% accuracy (Table 1.4). The highest classification rate of 66% was for the guild of surface predators on macrofauna (SR-Pr-mac), while the lowest classification success rate of 0% was for the guild of subsurface predators on macrofauna (SS-Pr-mac). SS-Pr-mac was most often misclassified as either surface predator/scavengers (SR-Pr/Sc-mac) or epifaunal zooplankton predators (EP-Pr-zoo) at 46% and 32%, respectively. SR-Pr-mac was also misclassified as SR-Pr/Sc-mac at a rate of 23%, while SR-Pr/Sc-mac was misclassified as SR-Pr-mac in 16% of instances. The suspension feeder group EP-Su-pom was successfully classified 44% of the time, but was misclassified as the deposit-feeding group SR-De-sed/pom/mic at a higher rate of 49%. Organisms within EP-Su-pom, which included the bivalves *Astarte borealis* and *Serripes groenlandicus*, the amphipod *Ampelisca macrocephala*, the bryozoans *Alcyonidium gelatinosum*, *Carbasea carbasea*, and *Eucratea loricata*, and the ascidians *Boltenia ovifera* and *Molgula griffithsii*, were never misclassified as any predatory or scavenger guild. SR-De-sed/pom/mic was

successfully classified at a rate of 46% but was misclassified as EP-Pr-zoo 28% of the time, SR-Pr/Sc-mac 11% of the time, and SS-De-sed/pom/mic, EP-Su-phy/zoo, and EP-Su-pom less than 10% of the time.

3.3 Trophic guild extent in niche space

Quantification of bivariate isotopic space (on a $\delta^{13}C$ versus $\delta^{15}N$ biplot) occupied by a trophic guild is one way to assess the guild's isotopic niche, a depiction of the resources utilized by an organism. Isotopic niches are not necessarily synonymous with trophic niches, but they represent an ecological proxy conveyed in stable isotope values (Layman et al., 2012). Relative positions of isotopic niches can provide valuable information about how trophic guilds assimilate carbon and nitrogen resources from their environments.

The spatial extent of each guild's isotopic niche space was highly variable (Table 1.5, Figure 1.4). The $\delta^{15}N$ range for trophic guilds varied from 5.2 to 12.5‰. All trophic guilds exhibited a $\delta^{15}N$ range spanning about two trophic levels based on a trophic step of 3.4‰, except for SR-De-sed/pom/mic, which occupied three trophic levels. The $\delta^{13}C$ range for the nine trophic guilds spanned from 3.9 to 7.5‰, values indicative of multiple, isotopically distinct carbon source assimilation. Overall, niche space area ranged from 13.8 to 59.7 square units. The amount of niche space overlap between each trophic guild is represented in the discriminant function analysis classification success rate (Table 1.4).

Two trophic guilds expected to occupy different niche space based on their feeding modes, epibenthic suspension feeders of SPOM (EP-Su-pom) and subsurface deposit feeders of sediments, SPOM, and microflora (SS-De-sed/pom/mic), occupied similar isotopic niches. Each guild occupied a similar amount of area (27.9 and 23.9 square units, respectively) and exhibited similar $\delta^{15}N$ range (5.9 and 7.3‰, respectively) and $\delta^{13}C$ range (6.9 and 5.6‰, respectively) (Table 1.5). Taxa within the EP-Su-pom guild were successfully classified at a 44% rate, while those of the SS-De-sed/pom/mic guild were successfully classified 28% of the time (Table 1.4). Taxa in both guilds were misclassified as surface deposit feeders of sediment, SPOM, and microflora (SR-De-

sed/pom/mic) at rates higher than their own classification success rates (49% for EP-Su-pom and 50% for SS-De-sed/pom/mic).

Faunal organisms were widely dispersed in isotopic space, but most organisms were more ^{13}C-enriched than the three measured end-members (Figure 1.5). Only three of the thirty-nine benthic consumer species analyzed in this study (*Echinarachnius parma*, *Ampelisca macrocephala*, *Ocnus glacialis*) possessed ^{13}C-depleted values less than -22‰ that might reflect phytoplankton, SPOM, or sediment. Verified by low trophic guild classification rates (Table 1.4), taxa showed high dispersion within isotopic space with no clear spatial patterns related to trophic guild. The ^{13}C-enriched values of most organisms were not traced back to SPOM, phytoplankton, or bulk sedimentary organic matter, even assuming a maximum expected ^{13}C enrichment of 2‰ for every 3‰ enrichment for ^{15}N (Fry and Sherr, 1984; Vander Zanden and Rasmussen, 2001; Dubois et al., 2007).

4. Discussion

4.1 ^{13}C-enriched organic matter assimilation decoupled to ^{15}N-enrichment

Despite the large numbers of samples analyzed and species surveyed, we were unable to clearly discern isotopic end-members within the Chukchi Sea food web. Phytoplankton and SPOM δ^{13}C values were situated between -25 and -22‰ with few outliers. Based on a maximum enrichment of 2‰ per trophic step for δ^{13}C, direct consumption of phytoplankton or the measured bulk sedimentary organic matter end-member was not a likely explanation for the enriched δ^{13}C values observed in consumers (Figure 1.5). For example, the second trophic level bivalve *Yoldia hyperborea* exhibited a fairly enriched δ^{13}C value of -18.0‰ that can be explained by one of several mechanisms: *Y. hyperborea* assimilated a carbon source (or mean carbon sources) more ^{13}C-enriched than our observed end-members, or it exhibits a strikingly high δ^{13}C trophic enrichment factor of at least +4‰ and directly assimilated measured carbon sources. This trend was reflected in the other seven bivalve species analyzed in the Chukchi Sea (Table 1.1). Apart from the bivalves, calanoid copepods and bryozoans posed as other

striking examples of grazers separated by up to 4.8 and 3.6‰, respectively, in $\delta^{13}C$ from their potential food resources in the water column.

Based on the absence of an obvious end-member value, it seems possible that an unidentified organic matter resource posed as a significant carbon source to the Chukchi Sea food web. While ice algae are reported to have varying $\delta^{13}C$ values from -25‰ to -14‰ (Hobson et al., 2002; McMahon et al., 2006; Gradinger, 2009), the late summer sampling period of this study prevented the acquisition of ice algae samples for stable isotope analyses. However, ice algae are not considered a likely potential carbon source to the benthic consumers in this study based on their rapid consumption upon deposition (McMahon et al., 2006; Sun et al., 2007), and the nearly complete absence of ice during the late summer months when our sampling was conducted (Cavalieri et al., 2009; Cavalieri et al., 2010). The stable isotopic value of an organism represents the integrated assimilation of all organic matter sources within an isotopic turnover window. One estimate of isotopic turnover for organismal tissue (~20 days) was measured in arctic amphipods (Kaufman et al., 2008). Arctic bivalves exhibited marked changes of $\delta^{13}C$ in tissues four weeks after an isotopically distinct dietary change (McMahon et al., 2006). Assuming the isotopic ratios measured in organism tissues reflect organic matter assimilated approximately four weeks prior, values reported here represent food resources assimilated from late June and early July. In 2009, the southernmost stations in the study area became ice free in mid-June (20-50 days prior to sampling). The ice edge retreated beyond our northernmost stations by mid-July (18-46 days prior to sampling), except in the Hanna Shoal area where sea ice, possibly eddied, remained until the fourth day of August (less than a week prior to our occupation) (see supplementary data for detailed list).

To determine if potentially recent ice algae deposition caused notable ^{13}C-enrichment in organism tissues, we tested whether species from stations that had been ice free for more than 30 days prior to sampling were isotopically different than common species from stations that had been ice covered within 30 days of our occupation (supplementary data). We found that the $\delta^{13}C$ values of benthic organisms were not

different for those that had experienced ice retreat 4 to 30 days before sampling versus those that had experienced ice retreat >30 days before sampling (Student's *t*-test, p = 0.70).

Lalande et al. (2007) confirmed that POC flux to the benthos in the Chukchi Sea near Barrow Canyon was greater in open water conditions than during ice cover. The authors also demonstrated that stable carbon isotopic values of the organic matter from all depths in ice covered or open water conditions were less than -22‰. Therefore, although sea ice algae can possess extremely ^{13}C-enriched values, phytoplankton and other particulate matter in the water column can dilute the ice algal isotopic signature. Furthermore, SPOM and phytoplankton from all depths during the open water sampling of this study had $\delta^{13}C$ values less than -22‰, except for four of 102 measurements that were between -20.3 and -21.2‰. We assume, based on these ancillary data, that in late summer there was no residual ice algal isotopic signal in our samples.

Benthic diatoms represent another potential Chukchi Sea primary producer available at shallow sites (Matheke and Horner, 1974; Horner and Schrader, 1982). Although we were able to isolate diatoms from the sediments following Blanchard (1990), we were unable to reliably measure their stable isotopic values. Mounting evidence suggests that viable microphytobenthos exist on the Arctic (Glud et al., 2009) and Antarctic (Gilbert, 1991) shelves, and future studies should consider them as a potential organic matter source.

Because of the strong coupling of benthic processes to pelagic productivity (Grebmeier et al., 1988; Grebmeier and Barry, 1991; Dunton et al., 2005), bulk organic matter in Chukchi Sea sediments largely reflected stable isotope values of water column primary producers (Table 1.1). Upon close examination, however, sediment $\delta^{13}C$ values at seven out of ten stations were more ^{13}C-enriched than the 95% confidence interval surrounding mean phytoplankton values when compared on a station-by-station basis (Figure 1.2). This pattern was consistent with previous findings by Iken et al. (2005) who found that sediments were slightly ^{13}C-enriched relative to phytoplankton carbon. The pattern indicates that either an organic matter source other than settled phytoplankton was

present within the sediments or some unidentified process is causing ^{13}C-enrichment of organic matter within the benthos.

Mean $\delta^{13}C$ values for near-bottom SPOM (-23.8 ± 0.2‰) and sediment organic matter (-23.3 ± 0.1‰) were not end-members that independently explained the ^{13}C-enriched benthic fauna values. Instead, we attribute the enriched $\delta^{13}C$ values of both deposit and suspension feeders at multiple trophic levels to organic matter routed through the microbial food web. Isotopic fractionation associated with microbial processes (Macko et al., 1987; Coffin et al., 1990) has been invoked by other polar studies as an intermediate trophic step to explain the mismatch of ^{13}C-enriched fauna to their relatively ^{13}C-depleted ultimate organic matter resources (e.g., McConnaughey and McRoy, 1979; Lovvorn et al., 2005; Mincks et al., 2008). The concept of the microbial community providing a major carbon subsidy to benthic fauna, which is supported by the current study, is described in further detail by Lovvorn et al (2005).

Although microbial metabolism produces ^{13}C-enriched cells, products, and substrate via respiration of ^{13}C-depleted CO_2, it can either enrich, deplete, or have no effect on ^{15}N depending on the chemical nature of the substrate (Macko and Estep, 1984; Hoch et al., 1994). Since the Chukchi Sea sediments measured in this study show replete stores of ammonium (154 ± 73 μM), it was expected that microflora assimilated $^{14}NH_4^+$ faster than $^{15}NH_4^+$ since the DIN pool was not limiting. In fact, ^{15}N isotopic fractionation (ε) of bacterial biomass can span from -16 to -22‰ when cultured on media within the nitrogen concentrations of the Chukchi Sea sediments (Hoch et al., 1994). This provides an explanation for how microbial processing can enrich organic matter in ^{13}C but not ^{15}N. In this way, benthic fauna potentially assimilate ultimate organic nitrogen transformed from both "old" nitrate upwelled from the North Pacific Ocean advected through the Bering Strait (Walsh et al. 1989) and "regenerated/new" nitrogen from autochthonous remineralization processes in sediments (Rowe and Phoel, 1992). Dual nitrogen source assimilation pathways may contribute to the high benthic biomass in the Chukchi Sea (Grebmeier et al., 1988; Grebmeier et al., 1989; Dunton et al., 2005; Bluhm et al., 2009; Iken et al., 2010).

A significant fingerprint of bacterial fatty acids in the Chukchi Sea sediments in the study area suggested that appreciable bacterial biomass exists in the sediments that likely fuel an active microbial food web (K. Taylor and R. Harvey, pers. comm.). A recent study provided evidence that organic matter from freshly deposited microalgae was rapidly converted into bacterial biomass in arctic sediments (Sun et al., 2009). Furthermore, Hansen and Josefson (2004) suggested that deposit feeders digest and assimilate only dead, degraded microalgae compared to living diatoms that pass through herbivore guts and remain viable. We hypothesize that sedimentary organic matter processed by the microbial community provides a labile fraction of organic matter to the macrofaunal food web in the form of degraded microalgae, microbe-derived organic matter (by-product), or the microbes themselves. One of two scenarios may explain the inability of our isotopic analyses to pinpoint the labile, ^{13}C-enriched fraction of sedimentary organic matter: either the ^{13}C-enriched organic matter is rapidly assimilated by benthic consumers and no inventory exists in the sediments, or this ^{13}C-enriched fraction is such a small proportion of total organic matter that its ^{13}C-enriched signature was diluted in the larger pool of ^{13}C-depleted organic matter.

4.2 Discriminant function analysis of isotopic niche space

The low to moderate classification success rates of each trophic guild using stable carbon and nitrogen isotope ratios suggest that the Chukchi Sea benthic communities exhibit a moderate to high degree of trophic redundancy. Trophic guilds did not predict distinct pathways of organic matter assimilation. The high rate of misclassification reveals that trophic guilds overlap in isotopic niche space and assimilate the same resources despite their differing morphological adaptations to acquire organic matter.

The high misclassification rate between surface and subsurface deposit feeding guilds (Table 1.4) provides evidence that organic matter on the surface of sediments is isotopically similar to the organic matter buried within sediments that is accessible to subsurface feeders. The similarity of surface and subsurface trophic pathways reflect the high bioturbation activities that bury organic matter in Chukchi Sea sediments (Hansen

and Josefson, 2001; Pirtle-Levy et al., 2009) and a sedimentation rate of about 0.1cm yr^{-1} (Fox et al., in press). Although the two guilds feed in separate horizons within the sediments, sources of assimilated organic matter are essentially equivalent. It was unexpected, however, that suspension feeders and deposit feeders would be misclassified as each other since their feeding morphology suggests they obtain organic matter from different parts of the ecosystem.

Mechanistically, deposit feeders can obtain phytoplankton carbon after its settlement to the sediments, since zooplankton and benthic suspension feeders do not completely graze the seasonal pulse of fresh phytomaterial (Coyle and Cooney, 1988; Lovvorn et al., 2005). Bottom currents and/or bioturbation events may suspend sediments and associated organic matter allowing suspension feeders to capture organic matter normally buried in the sediments, including the ^{13}C-enriched carbon source reflected in suspension feeder tissues. Alternatively, novel feeding strategies may have evolved to obtain organic matter. On the Antarctic shelf, the soft coral *Gersemia antarctica* employs a scraping "inch worm" movement to obtain microalgae from undisturbed sediments in order to supplement its suspension feeding of planktonic prey (Slattery et al., 1997). In this instance, an organism with suspension feeding morphology is capable of directly obtaining organic matter from the sediments. The degree to which novel feeding strategies are employed by Chukchi Sea benthic fauna is unknown, but the possibility may be supported by the trophic redundancy exhibited by trophic guilds.

Of the predatory trophic guilds, the surface macrofaunal predators (SR-Pr-mac) were successfully classified at the highest rate of all nine guilds at 66%. Although predatory guilds exhibited an equally wide $\delta^{13}C$ and $\delta^{15}N$ range as other guilds, their $\delta^{15}N$ values reached relatively high values that did not overlap with other guilds. The highest trophic level organisms in the community (i.e., predatory gastropods, sea stars, crabs, etc.) possessed the most enriched $\delta^{15}N$ and $\delta^{13}C$ values of the benthic fauna. As a result, the discriminant function for this guild yielded a high classification rate. The SR-Pr-mac guild was still misclassified as surface predators and scavengers on macrofauna (SR-

Pr/Sc-mac) 23% of the time, which was not surprising since scavengers comprise the highest trophic levels with predators.

Within the entire study area, few species' stable carbon isotope values fell near phytoplankton, SPOM, or sediment organic matter on a $\delta^{13}C$:$\delta^{15}N$ biplot (Figure 1.5). Three species (the tube-dwelling amphipod *Ampelisca macrocephala*, the sea cucumber *Ocnus glacialis*, and the sand dollar *Echinarachnius parma*) fell within depleted $\delta^{13}C$ and depleted $\delta^{15}N$ space near the identified end-members of the food web. Since this amphipod and sea cucumber are suspension feeders and sand dollars are deposit feeders, we expected these organisms and all the other organisms in their respective trophic guilds to fall near phytoplankton, SPOM, and sediment end-members. However, the bulk of the organisms in the food web occupied isotopic niche space that was more enriched in $\delta^{13}C$ than the sampled end-members. The majority of species defined as suspension and deposit feeders fell near each other in isotopic space.

4.3 Redefining trophic guilds

The trophic redundancy measured in the Chukchi Sea benthic fauna suggests that organisms assimilate the same ultimate carbon and nitrogen sources despite differing feeding modes. Broader classifications of groups based on feeding mode may elucidate underlying general trends of trophodynamics, since specific classifications were too narrowly defined (see previous section). Instead of relying on iterative statistic routines to determine significant clusters in multivariate datasets (e.g., the *pamk* function used in this study), Leakey et al. (2008) chose to run systematic discriminant function analyses by manually varying the number of feeding mode-based trophic guilds and number of discriminant factors to achieve the most accurate, meaningful classification rate for their groups of estuarine fish.

When applying this strategy to the current dataset, a linear trend ($r^2 = 0.94$) appeared to negatively correlate the number of trophic guilds to the sum of classification success of the DFA (Figure 1.6). Stable carbon and nitrogen isotopes most accurately classified trophic guilds when only two guilds (suspension feeders and non-suspension

feeders) were used, which is a gross oversimplification for the benthos. "Non-suspension feeders" is much too inclusive to categorize the diverse morphologies of benthic consumers (e.g., a subsurface deposit feeding polychaete and a predatory gastropod obviously belong to separate guilds morphologically). However, it is plausible to consider two guilds based on ultimate organic matter resources if one group assimilates sedimentary organic matter reworked by the microbial community and the other group assimilates suspended, non-reworked organic matter. Yet, the range of $\delta^{13}C$ values exhibited by the suspension feeder guilds identified in this study spanned ~7‰, a much larger range than that reflected in our measured, non-reworked end-members. To verify the appropriate number of feeding mode-based trophic guilds that existed within the Chukchi Sea benthos, we applied another trophic guild determination technique that relies on stable isotope ratios to determine unknown feeding mode characteristics (Abrantes and Sheaves, 2009). Here, we analyzed how many significant clusters exist within dual stable isotope space based on Bray-Curtis similarity distances between all individuals.

We found three significantly different clusters based on stable carbon and nitrogen isotope values. We compared the composition of individuals in the three groups clustered by stable isotope values to the composition of three groups clustered by feeding mode (a quadratic DFA with cross-verification was employed to determine if the individuals grouped by stable isotope values were accurately discriminated by feeding mode; Table 1.6). The predatory feeding mode guild was similar to the isotopic guild of highly ^{13}C- and ^{15}N-enriched organisms (84% agreement). In this case, the general predatory feeding mode (EP/SR/SS-Pr/Sc-mac/zoo) coincides with distinct stable isotopic space (enriched $\delta^{13}C$ and $\delta^{15}N$ values). Less agreement existed between suspension and deposit feeders and their stable isotopic ratios. However, this was not surprising in light of the trophic redundancy and wide range of $\delta^{13}C$ values exhibited by both guilds. An important distinction illuminated by the cross-verification was that suspension feeders were never mistakenly classified as predators, and the opposite held true as well. Although they obviously differed in feeding mode, the stable isotopic space of

suspension feeders and predators was coincidently distinct. Deposit feeders showed 22% agreement between the two clustering methods, but the wide range of both $\delta^{13}C$ values (ultimate carbon source) and $\delta^{15}N$ values (trophic level) exhibited by deposit feeders caused poor discrimination. Despite unique suspension- and deposit-feeding morphological adaptations to acquire organic matter from the marine ecosystem, benthic fauna in the Chukchi Sea ultimately depend on the same resources. Using this classification of trophic guilds to describe organic matter assimilation pathways, the northeast Chukchi Sea food web during the open water summer season consisted of suspension and deposit feeders that obtained their ultimate organic matter resources through microbial processing (Figure 1.7). Although three species provided isotopic evidence of fresh phytoplankton carbon assimilation, this connection was weak among entire trophic guilds. Predators and scavengers obtained their organic matter resources from lower trophic level organisms and remained isotopically distinct as high trophic level organisms.

We have provided further evidence to support the hypothesis that the pathways highlighted here provide a major avenue for organic matter assimilation, and we emphasize the importance of a potential link between the benthic microbial and the macrofaunal food webs in the Arctic (McConnaughey and McRoy, 1979; Lovvorn et al., 2005; Dunton et al., 2012). Many intricacies exist in the Chukchi Sea benthos and require integrated studies regarding the importance of each organic matter source for the various benthic consumers, the longevity of organic matter in the sediments, and the complicated dynamics of the microbial and meiofaunal food web in the Chukchi Sea. Although the bulk isotope values reported here show major overlap of trophic niches, compound-specific stable isotope analysis may provide further insights to the pathways that transfer organic matter through the food web in terms of ice algae, microphytobenthos, and the microbial food web.

Table 1.1. $\delta^{15}N$ and $\delta^{13}C$ values (mean ± SE) of taxa collected from the Chukchi Sea in summer 2009 and 2010. Guild assignment described in Table 1.4 (see section 2.4). C:N ratio is expressed as mol/mol. References for feeding mode determination are superscripted: 1) Macdonald et al. (2010), 2) Ellers and Telford (1984), 3) Crawford and Jorgenson (1993), 4) Appeltans et al. (2012), and 5) Dennard et al. (2009). *n*: number of samples analyzed

Taxonomic group or species	*n*	$\delta^{15}N$ (‰)	$\delta^{13}C$ (‰)	C:N	Guild Assignment	Trophic Guild	Fig. 6 Label
Near-surface SPOM	26	6.2±0.4	-24.7±0.2				
Near-seafloor SPOM	22	4.6±0.5	-23.8±0.2				
Phytoplankton	25	7.7±0.3	-24.0±0.4				
Sediment bulk organic matter	80	7.4±0.1	-23.3±0.1				
Calanoid copepods	17	11.1±0.2	-21.6±0.4				
CNIDARIA							
Anthozoa							
Gersemia rubiformis	9	12.5±0.4	-20.3±0.2	9.2±0.9	2	EP-Su-zoo[1,4]	1
Hydrozoa							
Sertularia sp.	6	11.8±0.3	-20.51±0.2	5.6±0.4	6	EP-Pr-zoo[1]	2
SIPUNCULA							

Table 1.1 cont.

Golfingia margaritacea	6	12.4±0.3	-17.6±0.3	3.6±0.0	5	SR-Dt[1]	3
ANNELIDA							
Polychaeta							
Arcteobia anticostiensis	6	14.1±0.4	-20.2±0.5	5.2±0.2	9	SR-Pr-mac[1]	5
Brada nuda	4	14.0±0.2	-19.1±0.2	4.4±0.6	3	SR-De-sed/pom/mic[1]	4
Cistenides hyperborea	7	13.1±0.2	-21.07±0.6	6.7±1.2	4	SS-De-sed/pom/mic[1]	8
Maldane sarsi	36	14.6±0.2	-19.2±0.1	4.6±0.1	4	SS-De-sed/pom/mic[1]	6
Nephtys ciliata	9	15.1±0.2	-18.60±0.4	5.5±0.3	8	SS-Pr-mac[1]	7
Praxillella gracilis	5	13.4±0.5	-18.5±0.5	4.5±0.3	4	SS-De-sed/pom/mic[1]	9
MOLLUSCA							
Bivalvia							
Astarte borealis	7	12.1±0.3	-19.5±0.3	4.8±0.2	1	EP-Su-pom[1]	10
Ennucula tenuis	33	9.7±0.1	-19.7±0.1	4.9±0.1	4	SS-De-mic[1]	11
Macoma calcarea	14	9.4±0.3	-19.1±0.5	5.5±0.2	3	SR-De-sed/pom/mic[1]	12

Table 1.1 cont.

Macoma moesta	6	10.3±0.3	-19.7±0.4	5.2±0.1	3	SR-De-sed/pom/mic[1]	13
Musculus discors	8	10.5±0.3	-19.6±0.3	4.5±0.1	2	EP-Su-pom/zoo[1]	14
Nuculana pernula	12	10.5±0.2	-18.9±0.3	4.6±0.1	3	SR-De-sed/pom/mic[1]	15
Serripes groenlandicus	4	10.7±0.5	-19.5±0.5	4.0±0.2	1	EP-Su-pom[1]	16
Yoldia hyperborea	8	9.0±0.4	-18.0±0.3	4.0±0.0	4	SS-De-sed/pom/mic[1]	17
Gastropoda							
Cryptonautica affins	4	11.8±1.0	-16.4±0.3	4.1±0.0	8	SS-Pr-mac[1]	18
Neptunea heros	42	16.2±0.2	-17.2±0.2	4.3±0.1	9	SR-Pr-mac[1]	19
Plicifusus kroeyeri	13	16.9±0.2	-16.8±0.2	4.2±0.0	9	SR-Pr-mac[1]	20
Nudibranchia							
Tochuina tetraquetra	4	17.0±0.1	-18.5±0.1	4.6±0.5	7	SR-Pr/Sc-mac[4]	21
ARTHROPODA							
Amphipoda							
Ampelisca macrocephala	8	11.1±0.5	-23.6±0.5	9.3±0.6	1	EP-Su-pom[1]	22
Decapoda							
Argis lar	7	15.8±0.1	-16.6±0.2	3.6±0.0	7	EP-Pr/Sc-zoo[1,4]	23

Table 1.1 cont.

Chionoecetes opilio	32	15.1±0.2	-18.4±0.2	4.6±0.1	7	SR-Pr-mac[1]	24
Hyas coarctatus	4	15.8±0.2	-18.6±0.3	5.0±0.2	7	SR-Pr/Sc-mac[4]	25
Pagurus sp.	8	13.7±0.4	-17.6±0.6	3.8±0.2	5	SR-Om-mac[1]	26
ECHINODERMATA							
Asteroidea							
Leptasterias polaris	6	15.3±0.6	-17.9±0.9	9.0±1.9	7	SR-Pr/Sc-mac[4]	27
Ophiuroid							
Gorgonocephalus eucnemis	9	15.0±0.7	-19.4±0.4	22.4±3.1	6	EP-Pr-zoo[1]	28
Ophiura sarsii	14	12.7±0.7	-18.8±0.3	41.4±5.9	5	SR-Om-mic[1]	29
Echinoidea							
Echinarachnius parma	7	8.0±0.3	-22.1±0.3	48.0±8.2	4	SS-De-mic[2]	30
Holothuroidian							
Ocnus glacialis	11	12.0±0.4	-22.7±0.3	12.4±0.6	2	EP-Su-pom/phy[4]	31
Psolus chitonoides	11	12.8±0.6	-21.8±0.1	16.7±3.4	2	EP-Su-pom/phy/zoo[1]	32
BRYOZOA							

Table 1.1 cont.

Alcyonidium gelatinosum	4	10.3±0.3	-20.4±0.4	7.6±0.6	1	EP-Su-pom/phy[1]	33
Carbasea carbasea	7	11.7±0.5	-20.2±0.3	10.9±1.2	1	EP-Su-pom[1]	34
Eucratea loricata	4	10.5±0.1	-19.8±0.8	8.9±0.9	1	EP-Su-pom[1]	35
CHORDATA							
Tunicata							
Ascidiacea							
Boltenia ovifera	7	10.2±0.4	-20.7±0.1	9.0±0.8	1	EP-Su-pom[1]	36
Molgula griffithsii	4	10.3±0.6	-20.9±0.0	11.3±4.3	1	EP-Su-pom[1]	37
Vertebrata							
Pisces							
Boreogadus saida	38	15.4±0.1	-20.0±0.2	4.1±0.0	6	EP-Pr-mac/zoo[3]	38
Hippoglossoides robustus	9	14.3±0.3	-18.1±0.5	3.8±0.1	6	EP-Pr-mac/zoo[5]	39

Table 1.2. Coding acronyms for trophic guilds described by Macdonald et al. (2010). Descriptors from each category are joined to describe a trophic guild, e.g. EP-Su-pom represents an epibenthic suspension feeder of SPOM size class particulates.

Food Source	
EP	epibenthic
SR	surface
SS	subsurface
Feeding mode	
De	deposit feeder (ingests sediments)
Dt	detritus feeder (does not ingest sediments)
Su	suspension feeder
Pr	predator (live prey)
Sc	scavenger (carrion)
Br	browser (tears/gathers)
Om	omnivore
Food type/size	
sed	sediment
pom	suspended particulate organic matter
mic	benthic microflora
mei	benthic meiofauna >500 μm
mac	benthic macrofauna <500 μm
phy	phytoplankton
zoo	zooplankton

Table 1.3. Trophic guild clusters identified for the benthic food web of the Chukchi Sea based on the hierarchical clustering routine described in Section 2.5. Acronym coding scheme derived from Table 1.2.

	Trophic Guild Acronym	Guild Classification
1	EP-Su-pom	epibenthic suspension feeder on SPOM size class
2	EP-Su-phy/zoo	epibenthic suspension feeder on phytoplankton and zooplankton
3	SS-De-sed/pom/mic	subsurface deposit feeder on sediment, SPOM, and microflora
4	SR-De-sed/pom/mic	surface deposit feeder on sediment, SPOM, and microflora
5	SR-Om/Sc-mac	surface omnivore and scavenger on macrofauna
6	EP-Pr-zoo	epibenthic predator on macrofauna
7	SR-Pr/Sc-mac	surface predator and scavenger on macrofauna
8	SS-Pr-mac	subsurface predator on macrofauna
9	SR-Pr-mac	surface predator of macrofauna

Table 1.4. Quadratic discriminant function analysis (DFA) classification success rate matrix. The percent classification rates by which stable C and N isotopes predicted trophic guild membership are shown. Shaded cells indicate percent of correct classifications. The numbers above each column correspond to the trophic guild number. Non-grayed numbers across a row correspond to the misclassification rate. Hyphens represent a 0% reclassification rate.

		Reclassified as (%)								
	Trophic Guild	1	2	3	4	5	6	7	8	9
1	EP-Su-pom	44	3	4	49	-	-	-	-	-
2	EP-Su-phy/zoo	28	28	3	28	-	13	-	-	-
3	SS-De-sed/pom/mic	11	-	28	50	-	8	3	-	-
4	SR-De-sed/pom/mic	2	5	8	46	-	28	11	-	-
5	SR-Om/Sc-mac	4	-	12	42	13	4	21	-	4
6	EP-Pr-zoo	3	3	-	11	2	63	18	-	-
7	SR-Pr/Sc-mac	-	-	-	2	4	18	60	-	16
8	SS-Pr-mac	-	-	8	-	8	32	46	-	8
9	SR-Pr-mac	-	3	-	-	-	8	23	-	66

Table 1.5. Ranges, extent, and area of the niche space occupied by each trophic guild for Chukchi Sea benthic organisms on a $\delta^{13}C$: $\delta^{15}N$ biplot. Refer to Table 1.3 for full names of each trophic guild. Range is defined as difference between maximum and minimum values, and represents the span of isotopic niche space occupied by each guild in each axis direction. Units are ‰ except for niche space area, which are square units.

Trophic Guild	$\delta^{15}N$ (‰) Minimum	$\delta^{15}N$ (‰) Maximum	$\delta^{15}N$ (‰) Range	$\delta^{13}C$ (‰) Minimum	$\delta^{13}C$ (‰) Maximum	$\delta^{13}C$ (‰) Range	Niche Space Area (‰^{2})
EP-Su-pom	8.2	14.0	5.9	-25.2	-18.3	6.9	27.9
EP-Su-phy/zoo	9.6	15.7	6.1	-24.0	-18.5	5.6	22.6
SS-De-sed/pom/mic	7.3	14.6	7.3	-22.4	-16.8	5.6	23.9
SR-De-sed/pom/mic	6.9	19.4	12.5	-23.2	-16.8	6.4	59.7
SR-Om/Sc-mac	8.9	17.4	8.5	-20.7	-15.7	5.0	29.6
EP-Pr-zoo	10.7	18.4	7.7	-23.8	-16.4	7.5	31.0
SR-Pr/Sc-mac	12.6	17.8	5.2	-21.5	-15.4	6.1	20.2
SS-Pr-mac	9.8	16.7	6.9	-19.8	-15.9	3.9	13.8
SR-Pr-mac	12.8	19.2	6.4	-22.7	-15.3	7.3	19.7

Table 1.6. Cross-validation matrix comparing the composition similarity of trophic guilds grouped by stable isotope values using Euclidean hierarchical clustering and feeding mode information. The percentage value represents how well organisms that were grouped into a guild by stable isotope values were discriminated by their *a priori* feeding mode-based trophic guild.

		Guilds determined by stable isotope ratios		
	Degree of ^{15}N-enrichment	*High*	*Moderate*	*Moderate*
	Degree of ^{13}C-enrichment	*High*	*High*	*Moderate*
Determined by feeding mode	*Predatory Guild*	84%	16%	0%
	Deposit Feeder Guild	11%	22%	67%
	Suspension Feeders	0%	45%	55%

Table 1.7. Date of ice retreat and date surveyed for stations occupied in 2009 and 2010. Stations sorted from least to most days elapsed each sampling year. Ice retreat data provided courtesy of the National Ice Center (NIC).

Station Number	Date Occupied	Date of Ice Retreat	Days elapsed between ice retreat and sampling
43	8-Aug-2009	4-Aug-2009	4
39	9-Aug-2009	4-Aug-2009	5
44	8-Aug-2009	3-Aug-2009	5
42	10-Aug-2009	4-Aug-2009	6
45	10-Aug-2009	4-Aug-2009	6
25	3-Aug-2009	22-Jul-2009	12
27	4-Aug-2009	22-Jul-2009	13
46	10-Aug-2009	28-Jul-2009	13
40	10-Aug-2009	24-Jul-2009	17
31	9-Aug-2009	22-Jul-2009	18
32	9-Aug-2009	22-Jul-2009	18
37	7-Aug-2009	20-Jul-2009	18
36	6-Aug-2009	18-Jul-2009	19
30	11-Aug-2009	22-Jul-2009	20
33	7-Aug-2009	18-Jul-2009	20
34	7-Aug-2009	18-Jul-2009	20
47	11-Aug-2009	22-Jul-2009	20
9	29-Jul-2009	8-Jul-2009	21
15	31-Jul-2009	9-Jul-2009	22
16	1-Aug-2009	9-Jul-2009	23
17	1-Aug-2009	9-Jul-2009	23
21	6-Aug-2009	14-Jul-2009	23

Table 1.7 cont.

23	5-Aug-2009	12-Jul-2009	24
24	5-Aug-2009	12-Jul-2009	24
8	29-Jul-2009	4-Jul-2009	25
26	3-Aug-2009	9-Jul-2009	25
11	30-Jul-2009	4-Jul-2009	26
12	30-Jul-2009	4-Jul-2009	26
13	31-Jul-2009	1-Jul-2009	30
3	28-Jul-2009	25-Jun-2009	33
6	29-Jul-2009	30-Jun-2009	34
7	29-Jul-2009	30-Jun-2009	34
14	31-Jul-2009	25-Jun-2009	36
29	3-Aug-2009	25-Jun-2009	39
2	27-Jul-2009	15-Jun-2009	42
48	11-Aug-2009	30-Jun-2009	42
4	28-Jul-2009	15-Jun-2009	43
50	12-Aug-2009	25-Jun-2009	48
1	27-Jul-2009	7-Jun-2009	50
46	5-Aug-2010	4-Aug-2010	1
105	27-Jul-2010	14-Jun-2010	13
103	25-Jul-2010	9-Jun-2010	16
106	28-Jul-2010	20-May-2010	39
107	29-Jul-2010	18-May-2010	42
108	5-Aug-2010	24-Jun-2010	42
1013	5-Aug-2010	21-Jun-2010	45
1030	6-Aug-2010	22-May-2010	45
49	4-Aug-2010	19-Jun-2010	46

Table 1.7 cont.

21	7-Aug-2010	20-Jun-2010	48
47	4-Aug-2010	17-Jun-2010	48
22	31-Jul-2010	10-Jun-2010	51
39	6-Aug-2010	10-Jun-2010	57
50	3-Aug-2010	5-Jun-2010	59
48	3-Aug-2010	28-May-2010	67
11	30-Jul-2010	9-Jun-2010	71
1014	1-Aug-2010	19-May-2010	74
1010	10-Aug-2010	21-May-2010	81

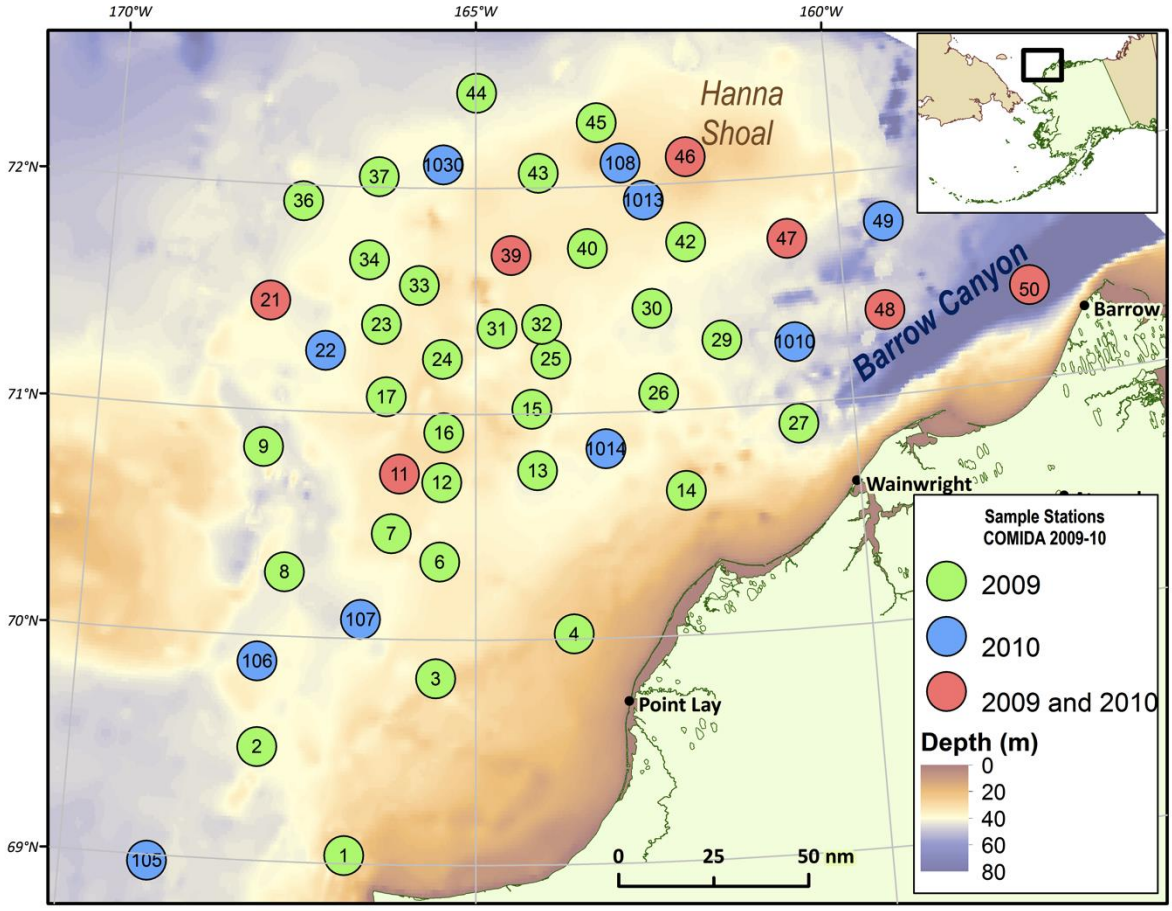

Figure 1.1. Location of sampling stations in 2009 and 2010 with respect to the bathymetry of the northern Chukchi Sea.

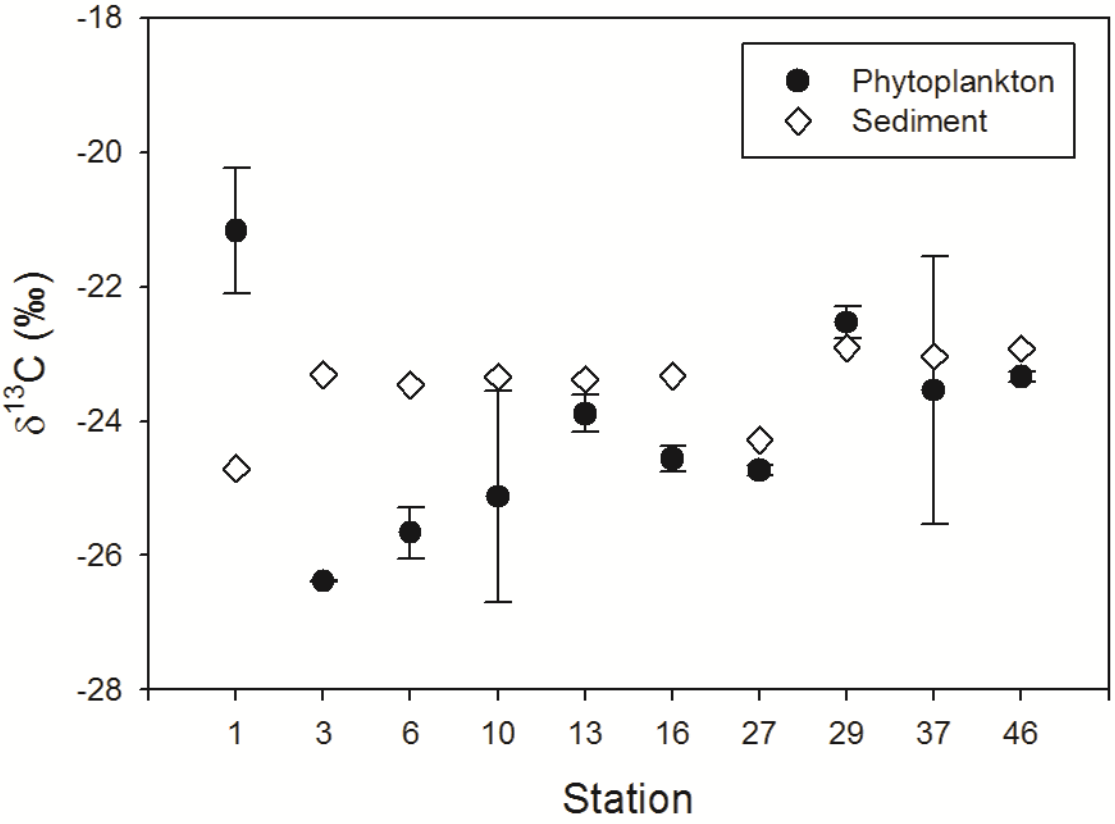

Figure 1.2. Comparison of mean phytoplankton $\delta^{13}C$ values (± 95% confidence intervals) to $\delta^{13}C$ values of sediment at stations where both were collected. Sediment organic matter is more ^{13}C-enriched than the 95% confidence interval around mean phytoplankton values at all but three of the ten stations.

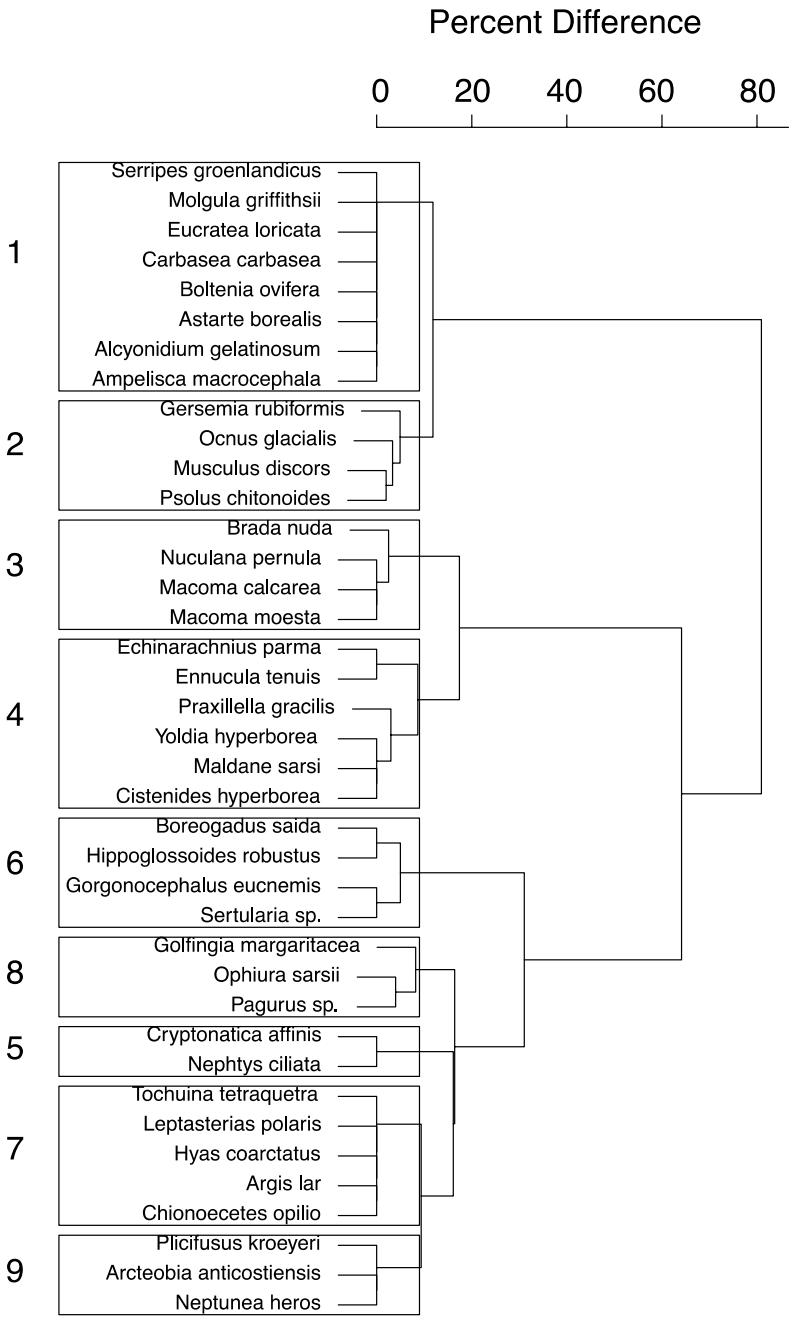

Figure 1.3. Cluster analysis based on binary feeding mode matrix for benthic fauna. Significantly different groups ($\alpha = 0.05$) are outlined in boxes. Species are denoted on the y-axis; the x-axis corresponds to proportion of difference between species. Numbers on y-axis refer to trophic guilds (see Table 3 for acronym definition): 1) EP-Su-pom, 2) EP-Su-phy/zoo, 3) SS-De-sed/pom/mic, 4) SR-De-sed/pom/mic, 5) SR-Om/Sc-mac, 6) EP-Pr-zoo, 7) SR-Pr/Sc-mac, 8) SS-Pr-mac, 9) SR-Pr-mac.

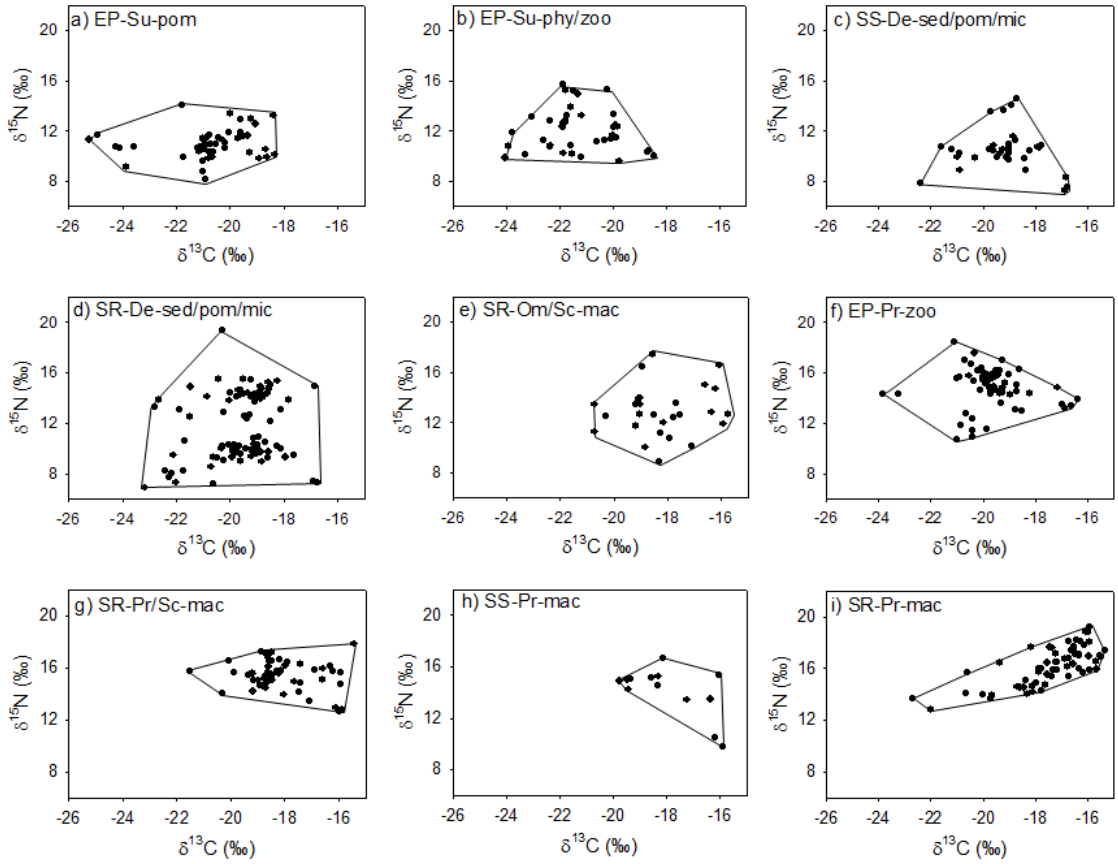

Figure 1.4. Convex hulls representing the extent of niche space occupied on $\delta^{13}C$ vs. $\delta^{15}N$ biplots for the nine trophic guilds.

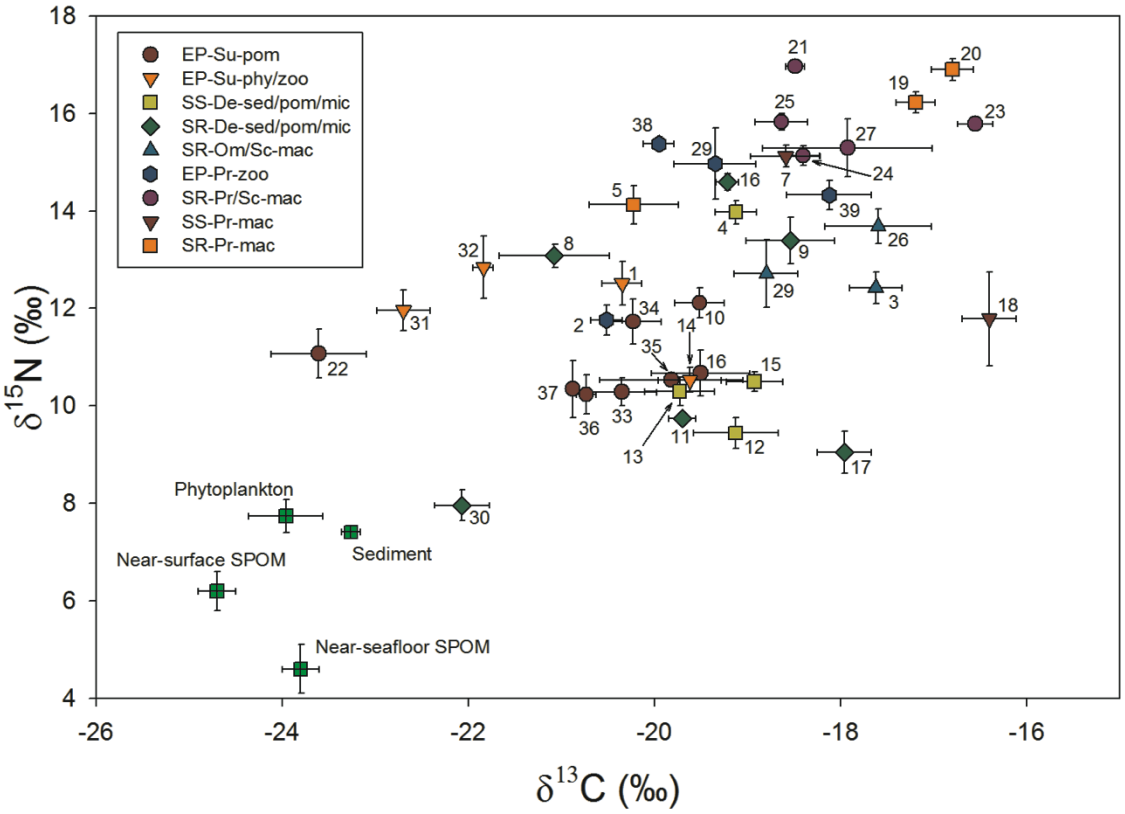

Figure 1.5. $\delta^{13}C$ vs. $\delta^{15}N$ biplot depicting isotopic niche space for primary and secondary consumers collected in the northern Chukchi Sea. Values are $\bar{x} \pm SE$ (*n* is denoted in Table 1). Numbers refer to specific species listed in Table 1. Species guild membership is denoted by symbol color and shape. Food web end-members are noted in green squares.

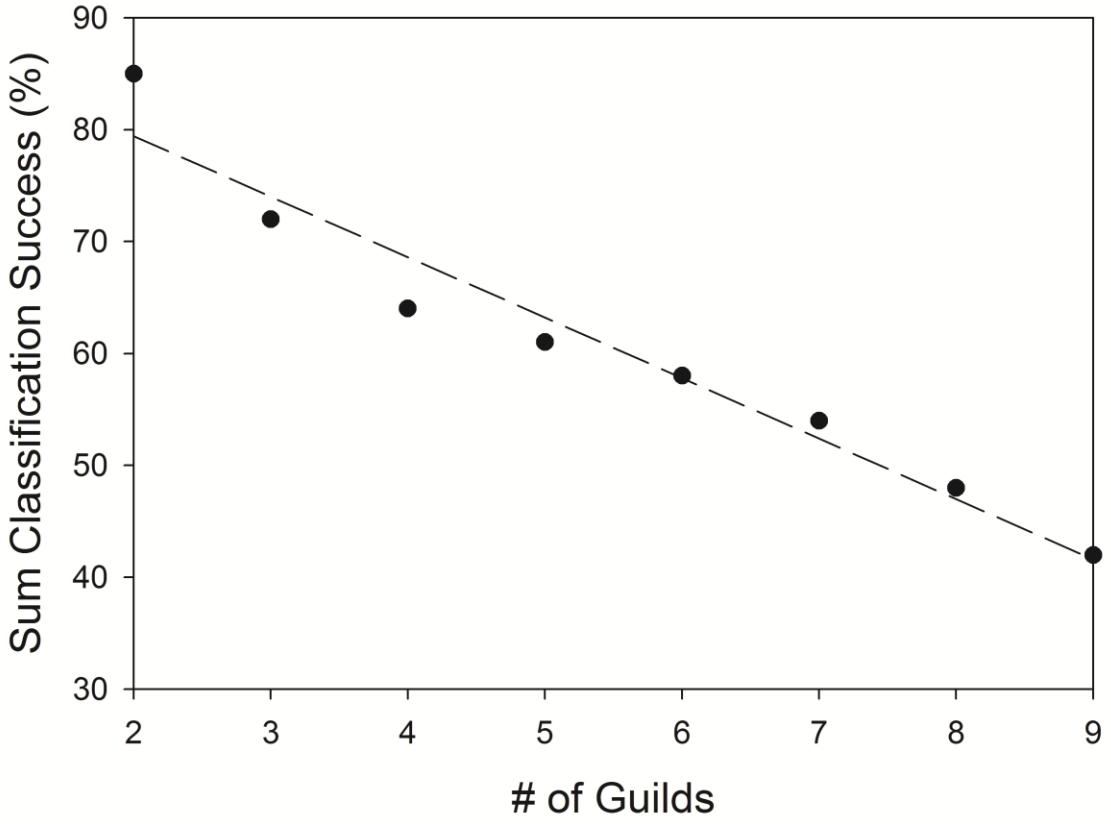

Figure 1.6. Results of the quadratic discriminant function analysis (DFA) using different number of trophic guilds based on feeding mode. Species were grouped into guilds by systematically decreasing the number of clusters on the hierarchical similarity tree. Values represent the sum of classification success (%) for the entire DFA.

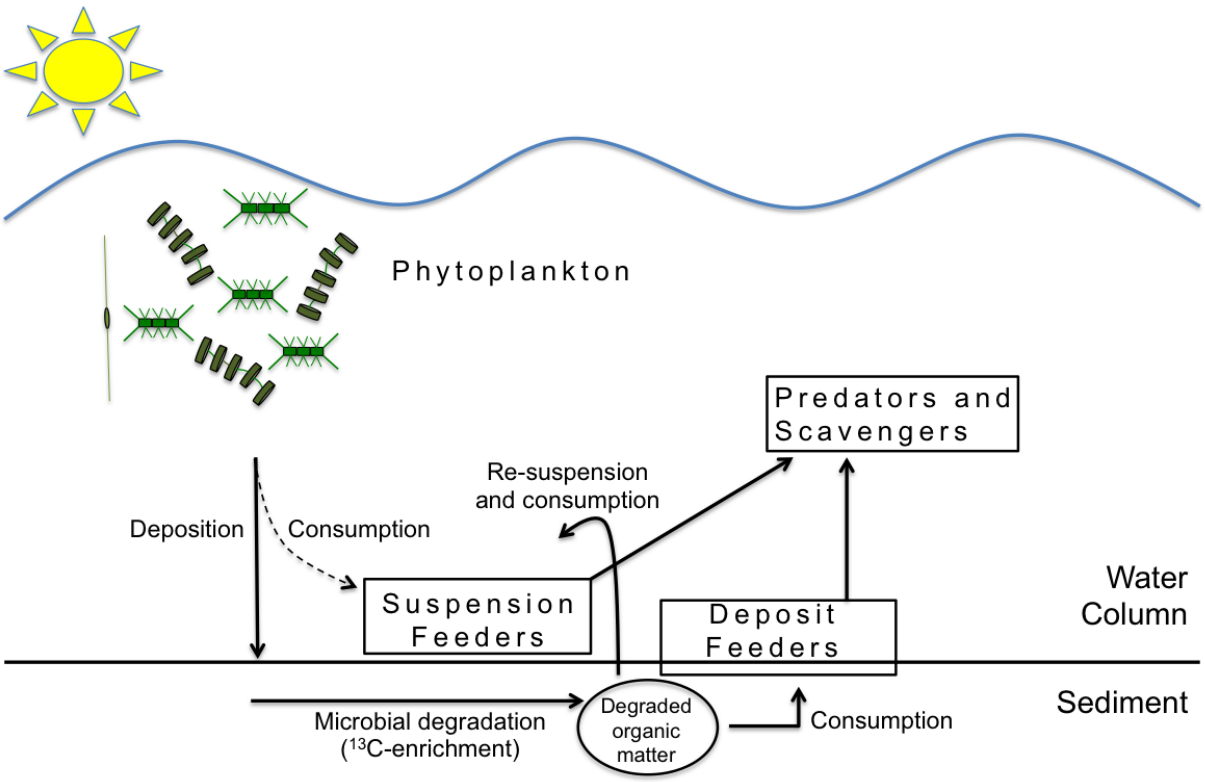

Figure 1.7. Conceptual diagram depicting the major pathways of organic matter assimilation from primary producers in the water column to high trophic level predators and scavengers.

Chapter 2

Food Web Structure and Function in Exploratory Oil Drilling Sites in the Chukchi and Beaufort Seas, Alaska

Abstract

Exploratory oil wells drilled in the Chukchi and Beaufort Seas between 1985 and 1990 were revisited in 2008, 2009, and 2010 to assess the long-term impacts of drilling activities on food web structure and energy flow. Stable carbon and nitrogen isotopes were employed to assess differences in food web structure and organic matter sources between drilled and non-drilled (reference) sites by comparing the isotopic values of species common to both sites. Thirteen species were collected in sufficient replication for dual stable isotope pairwise (species-by-species) comparisons in the Chukchi Sea and twelve organisms were compared in the Beaufort Sea. Of these, only the bivalve *Yoldia hyperborea* was significantly different in stable isotope values between drilled and non-drilled sites in the Chukchi Sea (MANOVA, $p=0.022$). Statistical differences for *Y. hyperborea* between sites may have resulted from low replication ($n=4$) since intra-station variation of stable carbon isotope values for *Y. hyperborea* was greater than differences between sites, stable nitrogen isotope values were overlapping between sites, and differences of stable carbon isotope values between groups was less than instrument analytical error (0.2‰). Carbon and nitrogen stable isotope values for the food web end-members sedimentary organic matter and suspended particulate organic matter were not significantly different between reference and drilled sites in each sea, which translated to similarity in food web function. Stable carbon and nitrogen isotope values of organisms in drilled sites were essentially identical to those that had not experienced drilling activities in the control sites. Lastly, food web structure and function between the Chukchi and Beaufort Seas was compared. Common organisms to both systems were significantly different in stable carbon and nitrogen isotope values (MANOVA, $p<0.001$) since sedimentary organic matter and particulate organic matter were different between the systems (MANOVA, $p<0.05$). The different isotopic signals of the end-members was transferred through the respective food webs, causing organisms common to both systems to possess different isotopic composition. Despite differing isotopic values, the food web function in each system is similar in the way energy is transferred to higher trophic level organisms through groups of lower trophic level organisms.

1. Introduction

The Chukchi and Beaufort Sea shelves not only possess a potential >10 billion barrels of oil and >100 trillion ft^3 of undiscovered natural gas reserves beneath the seafloor (Gautier et al. 2009), but also host some of the most productive food webs in the pan-Arctic shelf system (Cota et al., 1996; Grebmeier et al., 2006; Bluhm et al., 2011). The heightened interest in extracting these natural resources from within the marine environment has encouraged efforts to identify the impacts of drilling activities on the benthic marine communities, and food web dynamics. Drilling activities, particularly the discharge of drilling muds and formation cuttings, can bury benthic communities or cause contamination adversely impacting the long-term survivability and proliferation of a healthy benthic community (Coull and Chandler, 1992). The fate of potential anthropogenic contamination from oil and natural gas exploration are of particular interest since high concentrations of volatile organic compounds, including polycyclic aromatic hydrocarbons (PAHs) and heavy metals associated with drilling muds, may impair endocrine, reproductive, and nervous systems in marine organisms (Walker et al., 2006).

Trophic transfer of contaminants is of particular concern. Toxic compounds move from a lower to a higher trophic level during heterotrophy, and often result in the concentration, or biomagnification, of contaminants at the higher trophic levels, especially fish and marine mammals that are used by native subsistence hunters in Alaska (Rasmussen et al., 1990; Fisk et al., 2001; Hoekstra et al., 2003). Thus, the food web structure, defined as how organisms and food web end-members are arranged in isotopic bivariate space, conceptualizes how contaminants are transferred through a system. Careful examination of any differences between food web structure in undisturbed sites versus those previously occupied for oil and gas exploration can be used to determine whether drilling disturbances have lasting effects on food web function. For these purposes, function is defined as the flow of materials and processing of energy in an ecosystem dependent upon the overlying food web structure (Naeem, 1998).

Although the effects of oil and gas drilling and oil spills in the marine environment have been a topic of interest, few studies have approached ecosystem function recovery from a perspective of food web structure (Trefry et al., 2013). Considerable work has explored the toxicological and reproductive impacts of pollutants associated with oil and gas drilling by exposing meso- or microcosms to concentrations of toxins that are likely encountered in the

environment (Carman et al., 1997; Nayar et al., 2005; Hjorth et al., 2007; Jensen and Carroll, 2010). Other studies have evaluated the impacts of actual oil spills on ecosystems following such events (Feder and Blanchard, 1998; Sanchez et al., 2006; Velando et al., 2010; Chanton et al., 2012; McCall and Pennings, 2012). Assessments of community recovery have measured species abundance, richness, and diversity between impacted and reference (baseline) sites, or when possible, before and after the disturbance in the impacted location (Davies et al., 1984; Olsgard and Gray, 1995; Borja et al., 2003). In this study, we used stable isotopic data from benthic organisms collected from both previously-drilled and reference sites in a comparative analysis to assess the longevity of the effects of exploratory drilling to the food web. Since no baseline stable isotope data exist from these sites before it was explored, long-lasting disturbance must be assessed by comparing the current state of the food web in drilled sites to adjacent pristine reference sites. Differences measureable by stable isotope analysis will exist between the two sites if the drilled sites contain toxic substances associated with exploratory drilling like PAHs or heavy metals that have prevented food web end-members to grow and provide energy to consumers.

The application of stable isotopes to assess food web function is advantageous because it not only incorporates a long-term average food web position for organisms but also distinguishes between organic matter assimilation versus ingestion (Fry and Sherr, 1984). The application of stable isotopes in food web studies is based on the predictable step-wise enrichment of $\delta^{13}C$ and $\delta^{15}N$ values between food source and consumer. Stable carbon isotopes fractionate little to none between food and consumer (0-2‰), making them ideal for tracing isotopically distinct ultimate carbon sources since consumer $\delta^{13}C$ values will reflect those of the ultimate carbon sources (DeNiro and Epstein, 1978; Dubois et al., 2007). For nitrogen, ^{15}N enrichments occur with trophic level rather consistently at 3-4‰ (DeNiro and Epstein, 1981; Vander Zanden and Rasmussen, 2001). Consequently, $\delta^{15}N$ values for organisms are used to model its trophic position in a community. The bivariate positioning of data on a $\delta^{13}C$:$\delta^{15}N$ biplot, or isotopic space, yields pertinent information about the trophic niche a species occupies. This information can further elucidate trophic differences between species at different sites, different species at the same site, or between two different food webs (Bearhop et al., 2004; Layman et al., 2007a; Newsome et al., 2007; Hammerschlag-Peyer et al., 2011). Using bivariate stable isotope space

also allows food web function to be described by the relationship of organisms along a linear regression that can be attributed to energy transfer (Fanelli et al., 2009a).

Between 1989 and 1990 exploratory oil wells were drilled at survey areas in the northeastern Chukchi Sea denoted as Klondike, Burger, and Crackerjack (hereafter, drilled sites) in the northeast Chukchi Sea (Figure 2.1). Two sites in the coastal Beaufort Sea (Camden Bay) denoted as Hammerhead 1 and 2 were occupied during 1985 and 1986, respectively (Figure 2.2). The three sites in the Chukchi Sea were occupied during an oceanographic research cruise in 2009 and the Beaufort Sea sites in 2008 and 2009 to determine the current food web structure and detect any long-lasting effects of drilling activities on the biological community. The food web end-members (suspended particulate organic matter (POM) and sedimentary OM) and the benthic macrofauna of the drilled sites in the Chukchi Sea were compared to baseline data collected during the COMIDA:CAB project (Chukchi Sea Offshore Monitoring in Drilling Area: Chemical and Benthos; http://comidacab.org/) that took place in 2009 and 2010 (hereafter, reference stations). The drilled Beaufort Sea sites were compared to surrounding reference sites occupied during the cruises.

The purpose of this study was to determine if long-lasting disturbances (e.g., seafloor community burial by drilling muds, exposure to toxic substances) associated with exploratory drilling activity existed in the contemporary benthic food web. Assuming the reference sites are undisturbed Chukchi and Beaufort Sea communities, we accomplished these goals by making comparisons of stable isotope values of consumers in drilled sites to reference sites. This study tests the hypothesis that if the effects of drilling have prevented or altered the growth of food web end-members, then the stable isotope composition of food web consumers will be significantly different between drilled and reference sites.

2. Methods

2.1 Study area and sample collection

Samples were collected from 13 stations at Klondike site, 14 stations at Burger site, and 9 stations at Crackerjack site on 13-15 August 2009 aboard the *R/V Alpha Helix* (Figure 2.1). Stations at each drilled site were situated within 250 m of the historic well. Reference stations (55) were sampled July – August 2009 and July – August 2010 aboard the *R/V Alpha Helix* and *R/V Moana Wave*, respectively. Hammerhead 1 was occupied August 2009**,** and Hammerhead 2

was occupied from August 2010 aboard the *R/V Arctic Seal* and *R/V Alpha Helix*, respectively (Figure 2.2). During the Beaufort Sea cruises, 33 reference stations were also occupied to collect baseline data for the area, as detailed in Trefry et al. (2013). Stations were chosen using a hexagonal tessellation technique to ensure random selection and even distribution of stations (White et al., 1992).

A peristaltic pump attached to weighted, metered Tygon tubing was used to obtain water to collect suspended POM from near-surface and near-bottom depths. Vertical tows with a 20 μm mesh plankton net (Sea Gear, Melbourne, FL) were used to collect phytoplankton for stable isotope analyses. Suspended POM and plankton samples were filtered through 25 mm diameter GF/F filters (Whatman, Buckinghamshire, UK) that were previously combusted at 450°C for 24 hours to remove trace organic material. Prior to sample filtration, any visible zooplankton were removed from suspended POM and phytoplankton samples, and samples were vigorously shaken to ensure no settling had occurred. Suspended POM size class was defined by the 0.7 μm pore size of the GF/F filters. Phytoplankton was defined as particulates retained by the 20 μm net mesh size. After removing any visual zooplankton or particulates, microscopy inspections revealed concentrated microalgae in phytoplankton samples. Filters were then dried at 60°C and stored in opaque vials.

Undisturbed surface sediments were extracted with a core liner (1.8 cm diameter, 2 cm depth) from a 0.1 m^2 van Veen grab for stable carbon and nitrogen isotope. Sediment aliquots were placed in pre-labeled Falcon tubes (BD, USA) and immediately frozen in darkness.

The contents of van Veen grabs were sieved through 1 mm mesh and washed with ambient seawater to clean infauna from extraneous organic matter and sediment. Faunal organisms were keyed to lowest taxonomic level, usually species, in the field. When possible, muscle tissue was excised from the organism (e.g. gastropods, bivalves, large arthropods, and fish). Small organisms were kept whole. Tissues were dried at 60°C in aluminum trays in the shipboard drying oven. All water column, sediment, and faunal samples were transported to The University of Texas Marine Science Institute (UTMSI) for preparation for stable isotopic analysis.

2.2 Stable Isotope Analysis

Prior to analysis for stable carbon isotopic ratios, filtered samples (i.e. suspended POM, phytoplankton) were acidified in H_2PO_4 for 24 hours. Whole organisms, sediments, and faunal tissues that contained calcareous structures were homogenized and then split into two portions. One aliquot was soaked in 1 *N* HCl until bubbling stopped, rinsed with deionized water, and dried at 60°C for stable carbon isotope analysis. The second aliquot used for stable nitrogen isotope analysis was not subjected to acidification. All tissues were manually homogenized with a mortar and pestle. Lipids were not extracted from samples prior to analysis.

All samples were analyzed on an automated system for coupled $\delta^{13}C$ and $\delta^{15}N$ measurements using a Finnigan MAT Delta Plus mass spectrometer attached to an elemental analyzer (CE Instruments, NC 2500) at UTMSI, a PDZ Europa ANCA-GSL elemental analyzer interfaced to a PDZ Europa 20-20 isotope ratio mass spectrometer (Sercon Ltd., Cheshire, UK) at the University of California Davis, or a Thermo Delta V Plus interfaced with a Costech ESC 4010 elemental analyzer using a ConfloIII system at the University of Alaska-Fairbanks. Samples were combusted at 1020°C and injected into the mass spectrometer with continuous flow. Isotopic ratios are denoted in standard δ notation relative to carbon and nitrogen standards, PDB and atmospheric N_2, respectively, where

$$\delta X=[(R_{sample}/R_{standard})-1] \times 1000.$$

X is either ^{13}C or ^{15}N of the sample and R is the corresponding ratio $^{13}C/^{12}C$ or $^{15}N/^{14}N$. Instrumental analytical error was ±0.20‰ based on internal standards casein and gluatamic acid used at UTMSI, peptone used at UAF, or nylon, bovine liver, and glutamic acid used at UC Davis. Laboratory working standards were checked against standards issued from the U.S. National Institute of Science and Technology and the International Atomic Energy Agency.

2.3 Statistics

Statistical analyses were computed using R 2.14.0 (http://www.r-project.org/). All data met the assumptions of linear models based on graphical assessment of homoscedasticity and the normal distribution of residuals. Organisms common to both reference and drilled stations were compared for differences in $\delta^{13}C$ and $\delta^{15}N$ values. Multivariate analysis of variance (MANOVA)

was used to test if dual stable isotope values were different for species in reference and drilled stations. Only species with $n \geq 3$ were used since n must be greater than the number of independent variables in MANOVA (i.e., $\delta^{13}C$ and $\delta^{15}N$ values). Outcomes of MANOVA pairwise tests were subjected to Bonferroni corrections. We used the MANOVA test statistic Pillai's Trace since it is robust against unequal sample sizes (n). Analysis of variance (ANOVA) or *t*-tests were used to determine if significant differences existed between univariate factors. Analysis of covariance (ANCOVA) was used to test significant differences between linear regressions. Prior to statistical analysis, we tested the assumption that organisms collected from the Beaufort Sea in 2008 and 2009 did not differ in $\delta^{13}C$ and $\delta^{15}N$ values using MANOVA. We used species that were collected in sufficient replication ($n \geq 3$) for both years at reference sites, including *Ampelisca macrocephala*, *Astarte* sp., *Diastylis* sp., *Ennucula tenuis*, *Haploops* sp., *Lumbrineris fragilis*, *Maldane sarsi*, *Nephtys ciliata*, and *Nuculana* sp. A similar interannual comparison was conducted for reference sites in the Chukchi Sea for organisms collected in 2009 and 2010 (see Chapter 1 for description of analysis). For all tests, α was set to 0.05.

3. Results

3.1 Food web end-members

3.1.1 Chukchi Sea sites

Suspended POM stable carbon and nitrogen isotope values from drilled sites were pooled and compared to overall suspended POM values from all reference stations in the northeast Chukchi Sea (Table 2.1). No significant differences were measured between the two groups (MANOVA, F=0.840, p=0.438). Dual stable carbon and nitrogen stable isotopes of sedimentary OM were not significantly different between the two groups (MANOVA, F=1.256, p=0.291). Molar C:N ratios were not significantly different between groups (ANOVA, F=1.862, p=0.177).

3.1.2 Beaufort Sea sites

Stable carbon and nitrogen isotopes of suspended POM from all depths between drilled and reference sites were not significantly different (MANOVA, F=1.679, p=0.212). Sedimentary OM was not different between the two groups (MANOVA, F=1.377, p=0.260) for stable carbon and nitrogen isotopes.

3.2 Stable isotope composition of fauna

3.2.1 Chukchi Sea

We measured the $\delta^{13}C$ and $\delta^{15}N$ values of 151 individual organisms consisting of 32 species from the drilled sites (Table 2.1). Between drilled and reference sites, 22 species or genera were common to both and, subsequently, compared for differences in stable isotopes. Overall, the distribution of dual carbon and nitrogen isotopes pooled from all 22 taxa was not different between sites (MANOVA, F=0.271, p=0.763). Of the 22 common taxa, 13 were collected in sufficient replication ($n \geq 3$) to be tested for differences in stable isotope values by a pairwise (organism-by-organism) approach (denoted by asterisks in Table 1). Excluding the bivalve *Yoldia hyperborea*, no significant differences were measured for dual stable carbon and nitrogen isotopes for any organisms after Bonferroni corrections (Figure 2.3). Dual stable isotope values for *Y. hyperborea* were significantly different (MANOVA, F=14.45, p=0.022). Further analyses revealed that $\delta^{13}C$ values for *Y. hyperborea* were driving the significant differences in isotopic space (ANOVA, F=12.78, p=0.005) whereas $\delta^{15}N$ values were overlapping between drilled and reference sites (ANOVA, F=0.277, p=0.61).

All organisms from the drilled and reference sites, regardless of taxonomy, were plotted on a $\delta^{13}C$:$\delta^{15}N$ biplot, and linear regressions were made for both groups. The slopes of the regression lines from the reference dataset ($y=0.99x + 32.6$, $r^2=0.36$) and the drilled sites dataset ($y=0.82x + 28.1$, $r^2=0.32$) were not significantly different (ANCOVA, interaction term, F=1.926, p=0.122) (Figure 2.4).

3.2.2 *Beaufort Sea*

There was no difference between $\delta^{13}C$ and $\delta^{15}N$ values between 2008 and 2009 for reference site organisms except for *M. sarsi* (p=0.043). However, this value of *p* is only slightly lower than α. Also, considering the $\delta^{13}C$ values (mean±SD) for organisms collected in 2008 were -22.8±0.7 and in 2009 were -22.1±0.4, there are no real isotopic differences between the groups. There were no significant differences in $\delta^{15}N$. Therefore, all samples collected from both years were treated as one population.

The stable carbon and nitrogen isotope values from 617 individuals from drilled and reference sites from the Beaufort Sea were used to investigate differences in stable isotopes between the two groups (Table 2.2). In total, 72 species were analyzed from both reference and

drilled sites. Of these, 12 were collected in sufficient replication ($n \geq 3$) from both drilled and reference sites to conduct pairwise tests for differences in dual stable isotope values (see section 3.2.1) (Figure 2.5). After applying Bonferroni corrections, no significant differences existed between drilled and reference organisms (MANOVA, $p>0.05$).

To include all analyzed organisms for comparison, regardless of taxonomy or replication, linear regressions for all organisms were compared from drilled and reference sites (Figure 2.6). The slope for the drilled site organism regression ($y=1.04x + 34.0$, $r^2=0.43$) and the reference site organisms ($y=0.91x + 31.0$, $r^2=0.45$) were not significantly different (ANCOVA, $F=1.515$, $p=0.219$).

4. Discussion

4.1 Food web function in drilled sites

Populations of benthic fauna in drilled sites are equivalent to organisms from reference sites in stable carbon and nitrogen composition throughout the Chukchi and Beaufort Seas. We found no indication that stable isotopes differed between drilled and reference sites based on stable carbon and nitrogen isotopes from the Chukchi and Beaufort Seas. The results of our MANOVA indicated that organisms from drilled and reference sites occupied similar trophic niches in the two sites.

Since isotopic niche space was formally described as a quantifiable metric to elucidate ecosystem function (Bearhop et al., 2004), isotopic niches have become increasingly employed to compare trophodynamics within or between populations (Layman et al., 2007b; Hammerschlag-Peyer et al., 2011). Newsome et al. (2007) identified the major shortcomings of isotopic niches as potentially yielding misleading results and/or giving inaccurate estimates of trophic width. The former concern is important to consider if the end-members of the systems under comparison are isotopically disparate. The end-members measured between drilled and reference sites in each separate sea were not significantly different with respect to their $\delta^{13}C$ and $\delta^{15}N$ values, providing a comparable baseline for organisms at both sites. Trophic widths can vary considerably between species based on their stable isotope ranges (e.g., insect larvae and mammals; see Newsome et al. 2007) making inter-species comparisons problematic. We circumvented these limitations by making isotopic niche comparisons only between the same species.

The bivalve *Y. hyperborea* was the only organism in the entire study that possessed statistically different stable isotopic values between drilled and reference sites (Figure 2.3). The four individuals measured from Chukchi Sea drilled sites were less ^{13}C-enriched than their reference site counterparts. There are several explanations for this difference. Hypothetically, *Y. hyperborea* individuals would be less ^{13}C-enriched between the two sites if organic matter sources were isotopically disparate. We reject this notion since organic matter sources, particularly sediment organic matter, were not isotopically different between sites. *Y. hyperborea* is described as a subsurface deposit feeder of sediments, POM, and microflora by Macdonald et al. (2010). Other organisms identified by Macdonald et al. (2010) that belong to this trophic guild analyzed in the present study (*Maldane sarsi*, *Praxillella* sp., *Ennucula tenuis*) did not show significant differences in isotopic values between sites. Therefore, the differences observed in *Y. hyperborea* must be attributed to other factors besides their sedimentary food resources. Essentially, the MANOVA determined significant differences between groups if there was no bivariate overlap of groups in isotopic space. Although *Y. hyperborea* did not display overlap, values of individuals were remarkably similar. Two individuals from the drilled sites possessed values of -19.0‰, while two individuals from reference sites possessed values of -18.9 and -18.8‰. Furthermore, the intra-station isotopic variation observed for this species was up to 0.7‰ for two individuals at the reference station 1013 that possessed δ^{13}C values -18.8 and -18.1‰. Compounding the intra-station variation, the analytical error for stable isotope analyses was 0.2‰. We suspect that the significant differences detected by the MANOVA are an artifact of low replication (n=4 for drilled sites) in consideration of the natural variation associated with stable isotopes and that individuals in the two groups are $\leq$ 0.2‰ different.

The linear regression of the δ^{13}C:δ^{15}N biplots of all organisms was another metric used to assess differences in the dual stable isotope values between drilled and references sites in the Chukchi and Beaufort Seas. The metric did not require identical taxa like the pairwise tests, but rather assessed how isotopic space was filled. Since the range of stable carbon and nitrogen isotope values of organisms from the two sites overlapped, the interaction term of ANCOVA can detect differences in food web function. Regression lines would differ if organisms were not transferring energy through the food web in the same manner (e.g., utilizing alternative food resources or routing energy through different trophic guilds in the food web). Since the slope of the two regression lines for the drilled and reference sites from either the Chukchi and Beaufort

Seas were not significantly different, the populations within each sea can be considered the same with respect to of their trophodynamics.

The correlation coefficients of both regressions for Chukchi Sea organisms were relatively low (r^2=0.36 for the reference sites and 0.32 for the drilled sites). Correlation coefficients have been used to assess if food webs assimilate a sole organic matter resource or multiple sources with disparate isotopic values, where high correlation represents one organic matter source (Fanelli et al., 2009a). The drilled and reference sites in the Chukchi Sea showed almost equal variance, which indicated that they assimilated multiple, isotopically-disparate end-members in a similar manner. At the Chukchi Sea drilled sites, the measured end-members sedimentary OM and suspended POM were both similar in isotopic composition implying strong deposition of water column production to the benthos (Figure 2.7). The amphipod *Ampelisca macrocephala* and the hermit crab *Pagurus rathbuni* possessed relatively depleted $\delta^{13}C$ values that indicated a strong reliance on sedimentary OM and suspended POM. The depleted $\delta^{13}C$ values of *A. macrocephala* might also be partially attributed to lipid content since individuals at both drilled and reference sites possessed relatively high C:N ratios (Table 2.1), a proxy for lipid content (Post et al., 2007). All other organisms in the food web possessed relatively enriched $\delta^{13}C$ values (>-21‰) compared to the measured end-members (Figure 2.7). This trend has been observed in previous studies in the Chukchi and Bering Sea and described in great detail (e.g., Lovvorn et al., 2005, Chapter 1). The relatively ^{13}C-enriched benthic fauna values have been attributed to the assimilation of organic matter that has been substantially amended by microbial processes. We observed this enrichment pattern in organisms collected at both drilled and reference sites.

At the Beaufort Sea drilled sites, food web end-members also reflected each other, but sedimentary OM was more ^{13}C- and ^{15}N-depleted than suspended POM (Figure 2.8). The broad taxonomic groups of organisms appeared functionally similar to those in the Chukchi Sea food web. Bivalves and amphipods were the lowest trophic level organisms, although they were shifted toward the relatively ^{13}C-depleted end-members compared to the Chukchi Sea bivalves. Polychaetes spanned a wide range of $\delta^{13}C$ and occupied two trophic levels. The highest trophic level consumers were the gastropod *Plicifusus kroyeri*, the decapods *Pagurus* and *Pandalus*, a Nemertean, a Priapulid, and the seastar *Leptasterias groenlandica*. The amphipods from the *Anonyx* genus were conspicuously more enriched in ^{15}N and ^{13}C than other amphipod species

measured in this study. In other observations, the amphipod *Anonyx nugax* demonstrated distinct shifts in trophic level, where adults >10 mm occupy a higher trophic level than smaller individuals of the same species (Dunton et al., 2012). Our data correspond well with values of *Anonyx* sp. from other Beaufort Sea locations.

The Beaufort Sea sites showed slightly tighter correlation of consumers around a linear regression than the Chukchi Sea organisms (r^2=0.45 for reference sites and 0.43 for drilled sites). Both drilled and reference site organisms showed almost the same scatter around the regression line, which alludes not only to the same dependency on isotopically disparate organic matter sources but also that these groups of organisms from the same population (Figure 2.6). The results of the ANCOVA also demonstrated that the linear regressions were not significantly different. The lower tropic level organisms, like the amphipods, bivalves, and bryozoans, reflected the $\delta^{13}C$ value of sedimentary OM and suspended POM. Assuming a 1‰ trophic enrichment factor for $\delta^{13}C$ and a 3‰ trophic enrichment factor for $\delta^{15}N$, some of the $\delta^{13}C$ values for the higher trophic level organism are too enriched to be ultimately obtained from either sedimentary OM or suspended POM. Processes like those hypothesized to occur in the Chukchi Sea may be responsible for the shifts in consumer stable isotope values on the Beaufort Sea shelf.

Food web function can appear unaltered between sites if the community exhibits high trophic redundancy. Trophic redundancy buffers the effects of disturbance since species that perform equivalent roles in the food web can be removed from a system without apparent alterations in function because other taxa are able to compensate for changes in community structure (Walker, 1992; Woodward et al., 1995). The northeast Chukchi Sea exhibits high trophic redundancy based on the numerous omnivorous and plastic feeding guilds that can exploit varying organic matter sources (Chapter 1). We showed that 13 organisms from the Chukchi Sea (Figure 2.3) and 12 organisms from the Beaufort Sea (Figure 2.5) occupied overlapping trophic niches, which supported our claim of food web function recovery.

Ideally, the impacted sites would have been assessed for baseline conditions before drilling activities occurred. Additionally, to facilitate assessment, occupation of the drilled sites immediately following the disturbance would definitively describe the degree of impact experienced from drilling activities. Since these data were not collected, drilled sites were assumed to be measurably different at one point in time. Because our data were collected 20

years post-disturbance, this constrains the minimum amount of time we can assert is needed for system recovery. If site recovery assessment was addressed at multiple, shorter intervals (e.g., annually), then a more accurate timeframe could be applied to food web function recovery.

Lastly, any long-lasting effects from drilling activities that would measurably separate them from reference sites may have been expunged by large-scale impacts of a changing climate in the Arctic (ACIA, 2005), such as alterations in sea ice thickness, extent, and duration (Arrigo et al., 2008). Changes in sea ice regime ultimately impact primary production (Kahru et al., 2011; Perovich, 2011), which may have cause the food web function of both drilled and reference sites to converge to a new baseline within the past two decades. Thus, any differences previously recognizable as the effects from drilling may no longer exist if both drilled and reference sites have since experienced the same large-scale disturbance. The assessment of this possibility is beyond the scope of our study, but it is worth noting in the context of current arctic changes in the biological community. Based upon our assessment of long-term biological impacts on a community in previously drilled sites, the food webs in drilled and reference sites were not different based on stable isotope analysis of end-members and fauna.

4.2 Comparison of Chukchi and Beaufort Sea food webs

By combining both reference and drilled site organisms to form two composite populations from the Chukchi and Beaufort Seas, we were able to compare the adjacent populations in terms of isotopic niche space. Following the comparison routine above for species found in both seas, we found little to no trophic niche overlap (Figure 2.9). After Bonferroni corrections, 12 pairwise comparisons of dual stable isotope values of organisms common to both the Chukchi and Beaufort Seas were all significantly different (MANOVA, $p<0.001$). *Macoma* sp. displayed some overlap in dual isotope space where some of the most ^{13}C-enriched organisms from the Beaufort Sea were equally or more enriched than the most ^{13}C-depleted organisms from the Chukchi Sea. In most cases, however, there was a very distinct separation of stable isotopic space where organisms from the Beaufort Sea occupied more ^{13}C- and ^{15}N-depleted space while Chukchi Sea organisms occupied more ^{13}C- and ^{15}N-enriched space.

Examination of end-members between these systems revealed that sedimentary OM was significantly different in $\delta^{13}C$ and $\delta^{15}N$ (MANOVA, $p<0.0001$). Comparison of both carbon and

nitrogen stable isotope values for suspended POM revealed significant differences (MANOVA, p=0.0458), but we further investigated differences between the two groups since *p* was slightly smaller than α. One-way ANOVA revealed that $\delta^{13}C$ for suspended POM was different between the two seas (p=0.017), but $\delta^{15}N$ was not (p>0.05). The sedimentary OM sources in the Chukchi and Beaufort Seas appeared to cause the dramatic differences in isotopic trophic niche space occupied by organisms common to both systems (Figure 2.9).

Sediments are repositories for organic matter, particularly on shallow shelves. The nearshore Beaufort Sea sites were different in sources of organic matter from the offshore Chukchi Sea sites, as preserved in their sediments and evident in the food web signal. Appreciable contributions of organic matter are provided to the Arctic Ocean and its surrounding seas by freshwater runoff (Raymond et al., 2007). In the coastal Beaufort Sea, between 50 and 75% of carbon in marine sediments are terrestrial in origin (Macdonald et al., 2004). The terrestrial organic matter signal (depleted $\delta^{13}C$ values) in our Beaufort Sea sites was likely from the Canning River, which empties into Camden Bay. Suspended POM $\delta^{13}C$ values were also different between the Chukchi and Beaufort sites. Since $\delta^{15}N$ values were not significantly different, all suspended POM in the Beaufort sites cannot be entirely attributed to river runoff. The low-nutrient, low-salinity Alaska Coastal Current (ACW) moves northward along the entire Alaskan coast and continues eastward after Point Barrow, whereas the Chukchi Sea sites are overlaid mostly by the Bering Shelf Anadyr Water (BSAW) that lacks substantial freshwater inputs (Coachman et al., 1975; Walsh et al., 1989). These disparate water masses and the organic matter associated with them supplement the organic matter available to consumers. Their signals are transferred through the entire food web and are responsible for such dramatic differences in stable isotopic values between adjacent systems (Figure 2.9). However, as per the recommendations by Newsome et al. (2007), we cannot assess differences in isotopic trophic niche since the end-members are different for the two systems. Although organisms common to both systems possessed different stable isotope composition, their trophic niche or function can still be the same in each system. Similarities in the position of organisms in food webs in the Chukchi (Figure 2.7) and Beaufort Seas (Figure 2.8) suggests that the systems transfer organic matter to high trophic level organisms in a similar manner despite the differences in the ultimate organic matter sources that provide energy to the system.

Table 2.1. Stable carbon and nitrogen isotopic values, C:N (mol:mol) values, and *n* values for end-members and taxa collected at drilled and reference sites in the Chukchi Sea. Asterisks denote organisms used for pairwise comparisons. Numbers in second column refer to the labels in Figure 2.7. [1]Aggregate of *P. gracilis* and *P. praetermissa*. [2]Aggregate of *A. borealis* and *A. montagui*. [3]Aggregate of *M. calcarea* and *M. moesta*.

Taxonomic group or speices	Drilled Stations					Reference Stations			
	Fig. 2.7 Label	*n*	δ^{13}C±SE (‰)	δ^{15}N±SE (‰)	C:N±SE (mol:mol)	*n*	δ^{13}C±SE (‰)	δ^{15}N±SE (‰)	C:N±SE (mol:mol)
Suspended POM		85	-24.3±0.1	5.4±0.2		6	-24.2±0.2	5.1±0.3	
Sediment POM		27	-23.4±0.1	6.9±0.1	10.1±1.1	48	-23.2±0.1	7.2±0.2	9.2±0.2
NEMERTEA									
Cerebratulus sp.	1	1	-18.7	12.1	4.5	3	-15.4±1.2	13.6±0.2	4.1±0.0
SIPUNCULIDA									
*Golfingia margaritacea**	2	10	-16.9±1.0	13.2±0.4	3.8±0.0	6	-17.6±0.2	12.5±0.3	3.5±0.0
PRIAPULIDA									
Priapulis caudatus	3	2	-18.1±0.9	15.3±0.7	4.5±0.1				
ANNELIDA									
Polychaeta									
*Harmothoe imbricata**	4	6	-17.8±1.0	14.8±0.7	5.3±0.8	6	-20.2±0.4	14.1±0.3	5.2±0.2
Axiothella cantenata	5	9	-18.9±0.5	12.6±0.3	4.6±0.2				
Lumbrineris sp.*	6	6	-18.6±0.4	14.4±0.6	4.6±0.4	3	-18.8±0.0	15.8±0.5	4.5±0.2
*Maldane sarsi**	7	9	-19.0±0.7	14.2±0.6	5.2±0.5	36	-19.2±0.1	14.5±0.1	4.5±0.1
*Nephtys ciliata**	8	15	-17.7±1.0	15.2±1.3	4.3±0.1	9	-18.5±0.3	15.1±0.2	5.4±0.3
Nicomache lumbricalis	9	1	-19.6	13.0	2.3				
Onuphis parva	10	7	-18.5±0.5	11.9±0.9	4.9±0.1				
Pectinaria granulata	11	1	-20.8	11.8	3.8				
Phyllodoce groenlandica	12	2	-18.8±0.2	14.6±0.0	4.8±0.0				
Praxillella sp.*[1]	13	7	-19.0±0.8	13.2±0.9	4.9±0.2	5	-18.5±0.4	13.3±0.4	4.5±0.3

Table 2.1 cont.

*Sternaspis scutata**	14	8	-19.5±1.1	12.5±0.7	4.3±0.2	6	-19.0±0.4	13.5±0.3	4.6±0.5
Terebellides stroemi	15	2	-19.9±0.0	11.2±0.0	5.3±0.0	1	-22.2	12.2	6.5
MOLLUSCA									
Bivalvia									
Astarte sp.*[2]	16	3	-20.3±0.4	11.1±1.0	5.5±0.4	10	-19.6±0.2	11.8±0.2	4.8±0.2
Cyclocardia crebricostata	17	3	-20.0±0.4	10.1±1.0	5.8±0.3	2	-19.5±0.7	12.3±1.2	3.8±0.1
*Ennucula tenuis**	18	17	-20.1±0.6	9.1±0.8	5.4±0.4	33	-19.7±0.1	9.7±0.1	4.8±0.1
Liocyma fluctuosa	19	2	-20.7±0.4	12.6±0.9	5.1±0.4	20	-19.3±0.3	9.6±0.2	5.4±0.2
Macoma sp.*[3]	20	7	-20.4±0.9	9.1±2.1	5.9±0.3	12	-18.9±0.3	10.4±0.1	4.5±0.1
Nuculana pernula	21	1	-21.1	9.8	5.2	4	-19.5±0.5	10.6±0.4	4.0±0.2
*Yoldia hyperborea**	22	4	-19.6±0.7	8.6±1.0	5.2±0.4	8	-17.9±0.2	9.0±0.4	4.0±0.0
Gastropoda									
Buccinum sp.	23	1	-17.7	17.8	4.6	2	-18.1±0.6	14.3±0.1	4.6±0.1
Euspira pallida	24	5	-19.8±1.5	12.7±0.8	5.2±0.7	1	-18.3	12.3	4.3
Neptunea heros	25	2	-17.2±0.2	18.2±0.8	4.3±0.1	42	-17.1±0.2	16.2±0.2	4.2±0.1
ARTHROPODA									
Amphipoda									
*Ampelisca macrocephala**	26	9	-22.8±1.4	10.5±0.8	7.0±0.8	8	-23.6±0.5	11.0±0.4	9.2±0.6
Decapoda									
Pagurus rathbuni	27	1	-22.8	13.1	1.4	8	-17.5±0.5	13.6±0.3	3.8±0.0
ECHINODERMATA									
Ophiurida									
*Ophiura sarsii**	28	10	-18.9±0.9	11.8±1.6	18.±5.2	14	-18.7±0.3	12.7±0.6	41.4±5.9

Table 2.2. Stable carbon and nitrogen isotope values (‰), C:N ratios (mol:mol), and *n* values for end-members and taxa collected at drilled and reference sites in the Beaufort Sea. Asterisks denote organisms used for pairwise comparisons. Numbers in second column refer to labels in Figure 2.8. [1]Aggregate of *A. borealis* and *A. montagui*. [2]Aggregate of *H. laevis* and *H. tubicola*. [3]Aggregate of *M. calcarea* and *M. moesta*. [4]Aggregate of *N. radiata* and *N. pernula*. [5]Aggregate of *P. gracilis* and *P. praetermissa*. [6]Aggregate of *S. sabini* and *S. entomon*.

Taxonomic group or species	Drilled Stations					Reference Station			
	Fig. 2.8 Label	*n*	δ^{13}C±SE (‰)	δ^{15}N±SE (‰)	C:N (mol:mol)	*n*	δ^{13}C±SE (‰)	δ^{15}N±SE (‰)	C:N (mol:mol)
Suspended POM		4	-24.5±0.8	4.5±1.1		19	-24.9±0.3	5.7±0.2	
Sediment POM		20	-25.6±0.1	3.3±0.2		43	-25.3±0.1	3.4±0.1	
CNIDARIA									
Tealia sp.						1	-21.2	6.7	6.3
Unidentified anemone	1	2	-23.6±0.2	12.3±0.2	5.4±0.2	8	-23.6±0.4	13.3±0.5	5.9±0.4
NEMERTEA									
Cerebratulus sp.*	2	6	-20.9±0.7	12.8±1.0	5.36±0.7	7	-22.5±0.5	13.2±0.9	6.3±1.0
PRIAPULIDA									
Priapulus caudatus	3	1	-20.8	12.5	4.6				
ANNELIDA									
Polychaeta									
Aglaophamus malmgreni	4	4	-20.5±0.4	12.4±1.5	6.0±1.2	1	-18.6	14.9	6.2
Ampharetidae sp.	5	2	-24.5±0.4	6.9±0.0	7.8±0.9	4	-25.6±0.3	8.1±0.1	10.5±1.0
Axiothella sp.						2	-23.3±0.3	11.3±0.2	6.1±0.2
Capitella capitata						5	-24.3±0.2	8.3±0.3	7.5±0.4
Cirratulus cirratus	6	1	-22.8	9.2	5.8	8	-23.5±0.3	9.2±0.4	7.3±0.6
Euchone analis	7	3	-24.0±0.4	10.2±0.4	5.6±0.1				
Eunoe sp.	8	1	-21.2	11.4	4.4	2	-21.8±1.0	14.1±2.0	5.1±0.2
Lumbrineris sp.	9	2	-21.7±0.5	13.1±1.4	5.7±1.2	13	-22.1±0.1	12.4±0.3	5.3±0.1

Table 2.2 cont.

*Maldane sarsi**	10	14	-22.3±0.2	11.1±0.3	6.5±0.1	26	-22.5±0.1	11.5±0.1	6.2±0.1
*Nephtys ciliata**	11	16	-22.0±0.3	12.1±0.3	6.7±0.4	28	-22.0±0.2	12.9±0.2	6.2±0.2
Nereis zonata	12	2	-22.0±0.3	12.8±0.6	6.1±0.8	7	-23.7±0.6	10.2±0.3	8.7±1.2
Nicolea zostericola						2	-24.7±0.8	7.6±0.4	17.9±8.0
Owenia fusiformis	13	2	-22.2±0.1	8.8±0.0	6.7±0.8				
*Pectinaria granulate**	14	11	-23.4±0.4	10.0±0.4	9.8±2.0	7	-24.8±0.3	9.0±0.7	11.5±1.7
Phyllodoce groenlandica	15	4	-21.1±0.7	11.6±0.9	6.5±1.1	4	-22.7±0.6	13.6±1.0	6.3±0.5
Praxillella sp.*[5]	16	7	-22.5±0.2	10.8±0.3	5.7±0.3	12	-22.9±0.1	10.7±0.5	5.6±0.2
Sabellidae sp.	17	1	-23.4	7.3	5.4	2	-24.5±0.1	11.3±0.5	5.7±0.1
*Sternaspis scutata**	18	6	-21.9±0.6	9.0±0.6	5.04±0.6	13	-22.7±0.2	9.7±0.5	5.6±0.2
Terrebellides stroemi						11	-24.9±0.2	8.4±0.7	10.0±0.7
Bylgides sp.	19	1	-21.2	12.1	4.9	1	-22.7	13.1	4.6
Paradiopatra parva						2	-21.6±0.4	13.9±0.7	6.0±1.0
MOLLUSCA									
Bivalvia									
Astarte sp.*[1]	20	12	-23.3±0.1	7.9±0.1	7.1±0.6	12	-23.6±0.1	8.2±0.2	6.2±0.2
Axinopsida orbiculata	21	1	-23.6	8	6.3	6	-22.8±0.3	9.8±0.1	5.4±0.2
Cyclocardia sp.						4	-22.9±0.1	10.0±0.1	5.3±0.1
*Ennucula tenuis**	22	4	-23.3±0.2	8.7±0.3	7.1±1.4	11	-24.0±0.3	8.7±0.1	7.0±0.4
Liocyma fluctuosa	23	2	-23.9±0.4	7.2±0.0	6.3±0.3	3	-23.7±0.6	7.9±0.6	7.5±0.7
Macoma sp.*[3]	24	11	-24.0±0.3	7.9±0.3	7.7±0.6	10	-24.0±0.3	7.5±0.2	7.3±0.4
Musculus discors	25	2	-24.2±0.2	7.3±0.0	8.2±0.6				
Mya truncate						1	-23.7	11.7	6.6
Nuculana sp.*[4]	26	8	-23.2±0.1	7.7±0.1	6.7±0.3	23	-23.6±0.2	7.9±0.1	6.6±0.2
Pandora glacialis						1	-24.2	8.9	5.4
Portlandia arctica	27	2	-22.9±0.2	7.8±0.6	10.0±4.0				
Thracia septentrionalis	28	10	-23.8±0.3	8.8±0.7	7.7±0.8				
Similipecten greenlandicus	29	1	-24.5	8.69	6.74	1	-24.0	8.35	12.1

Table 2.2 cont.

Gastropoda									
Cryptonatica sp.	30	1	-21.5	12.9	5.46	2	-19.8±1.8	11.3±0.9	5.7±0.1
Margarites sp.						2	-22.6±0.4	10.7±0.1	6.1±0.4
Neptunea heros	31	1	-20.6	11.5	5.03				
Plicifusus kroyeri	32	2	-21.3±0.0	13.7±0.7	4.7±0.0	1	-25.9	11.0	7.7
Retusa obtusa	33	1	-21.8	11.0	4.5				
Tachyrhynchus sp.						2	-20.1±2.1	9.6±0.9	7.2±1.0
Propebela arctica	34	1	-22.5	13	6.1	1	-23.2	10.3	6.8
Nudibranchia									
Tritonia diomedia	35	1	-23.6	13.1	5.28				
ARTHROPODA									
Amphipoda									
Aceroides latipes	36	1	-23.9	10.9	7.7				
*Ampelisca macrocephala**	37	7	-24.5±0.2	8.0±0.3	10.1±0.5	9	-25.9±0.4	8.0±0.7	11.9±1.3
Anonyx sp.	38	2	-21.8±0	15.9±0.2	6.0±6.0	4	-25.2±1.0	11.0±1.3	13.0±0.8
Byblis gaimardi	39	1	-25.2	10	7.2	9	-27.1±0.1	6.9±0.3	16.7±1.0
Caprella sp.						2	-26.0±0.5	7.5±0.5	10.3±2.0
Gammarus wilkitzkii						2	-25.8±0.1	7.1±0.2	13.6±0.2
Haploops sp.*[2]	40	9	-25.5±0.3	8.41±0.2	10.1±1.2	18	-26.4±0.3	7.62±0.2	13.1±0.8
Pardalisca sp.						1	-21.9	15.1	7.0
Paroediceros lynceus						1	-23.6	10.5	6.9
Protomedeia fasciata						4	-26.3±0.3	8.4±0.7	10.5±2.5
Cumacea									
Diastylis sp.	41	2	-24.2±0.8	7.8±1.0	17.4±0.5	19	-24.5±0.3	8.3±0.3	9.1±0.5
Decapoda									
Argis sp.	42	1	-22.9	15.0	5.1	1	-20.0	14.7	4.2
Hyas coarcticus	43	1	-21.9	11.8	13.1	1	-22.2	12.5	9.9
Pagurus sp.	44	1	-20.9	14.5	7.6				

Table 2.2 cont.

Pandalus sp.	45	1	-21.3	14.1	4.5	1	-19.8	13.3	4.3
Isopoda									
Saduria sp.[6]	46	5	-22.2±0.5	10.8±1.0	8.1±1.0	2	-23.6±0.2	7.1±1.4	9.6±1.4
Mysida									
Mysis sp.	47	1	-21.1	10.9	4.7	1	-21.9	10.8	5.8
Pycnogonida									
Pycnogonid sp.						1	-23.3	12.2	5.5
ECHINODERMATA									
Asteroidea									
Leptasterias groenlandica	48	2	-19.7±0.3	17.0±0.2	17.0±4.6				
Holothuroidea									
Cucumaria sp.						1	-23.5	13.3	6.6
Psolus chitonoides						2	-22.4±0.1	9.1±2.0	20.0±3.5
Ophiurida									
Ophiura sarsii	49	1	-23.5	10.3	7.2	1	-24.1	9.0	20.6
BRYOZOA									
Alcyonidium gelatinosum	50	1	-24.5	9.1	5.4				
Alcyonidium mamillatum						2	-22.2±0.9	9.9±0.4	3.9±0.1
Eucratea loricata	51	1	-21.8	8.9	13.2				
VERTEBRATA									
Pisces									
Lumpenus fabricii						1	-22.4	13.9	4.3

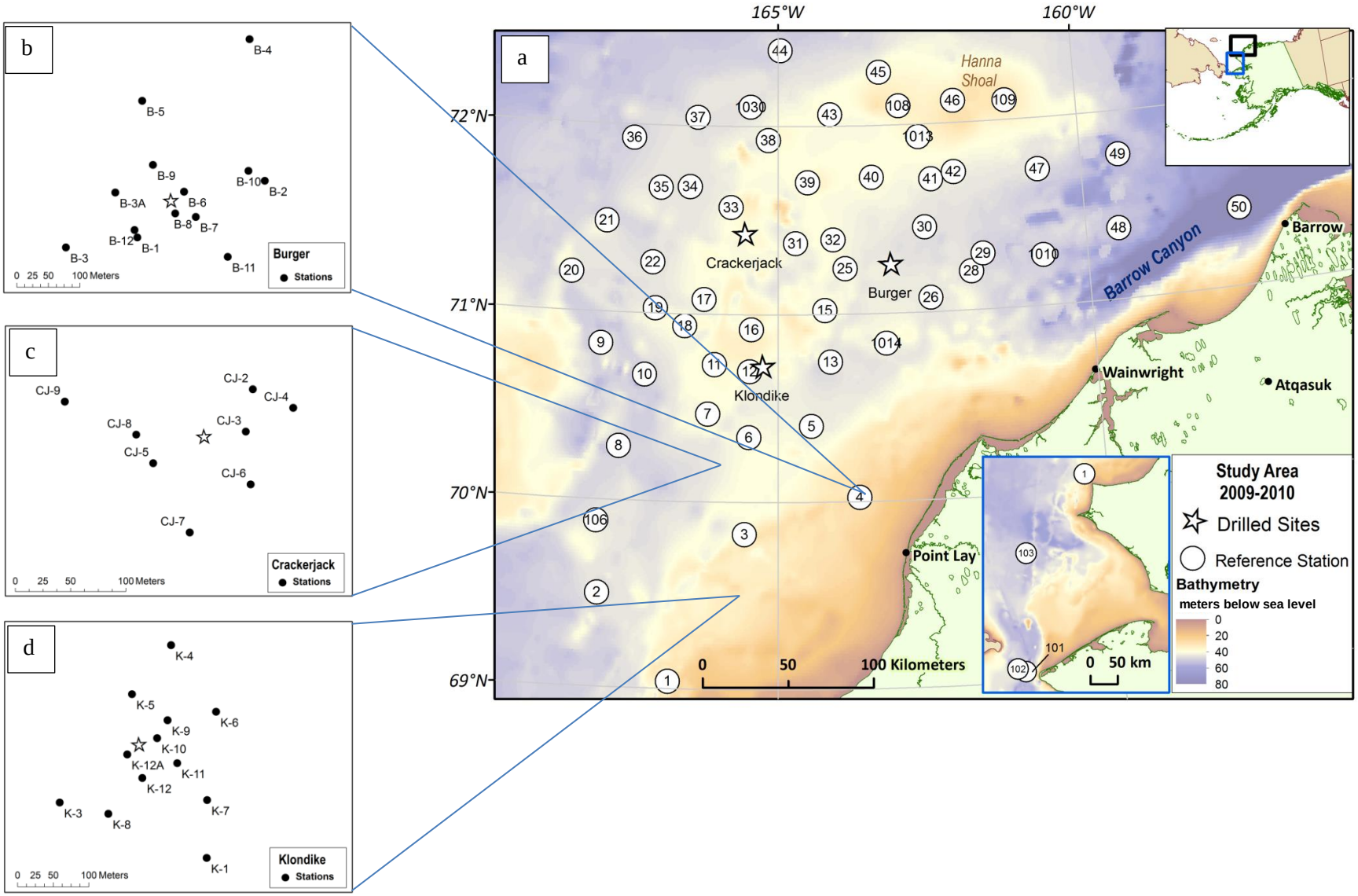

Figure 2.1. Location of Chukchi Sea study area for reference (open circles) and drilled (stars) sites. Stations for drilled sites (b) Burger, (c) Crackerjack, and (d) Klondike are subset with different scales. Stars in b-d represent the well head.

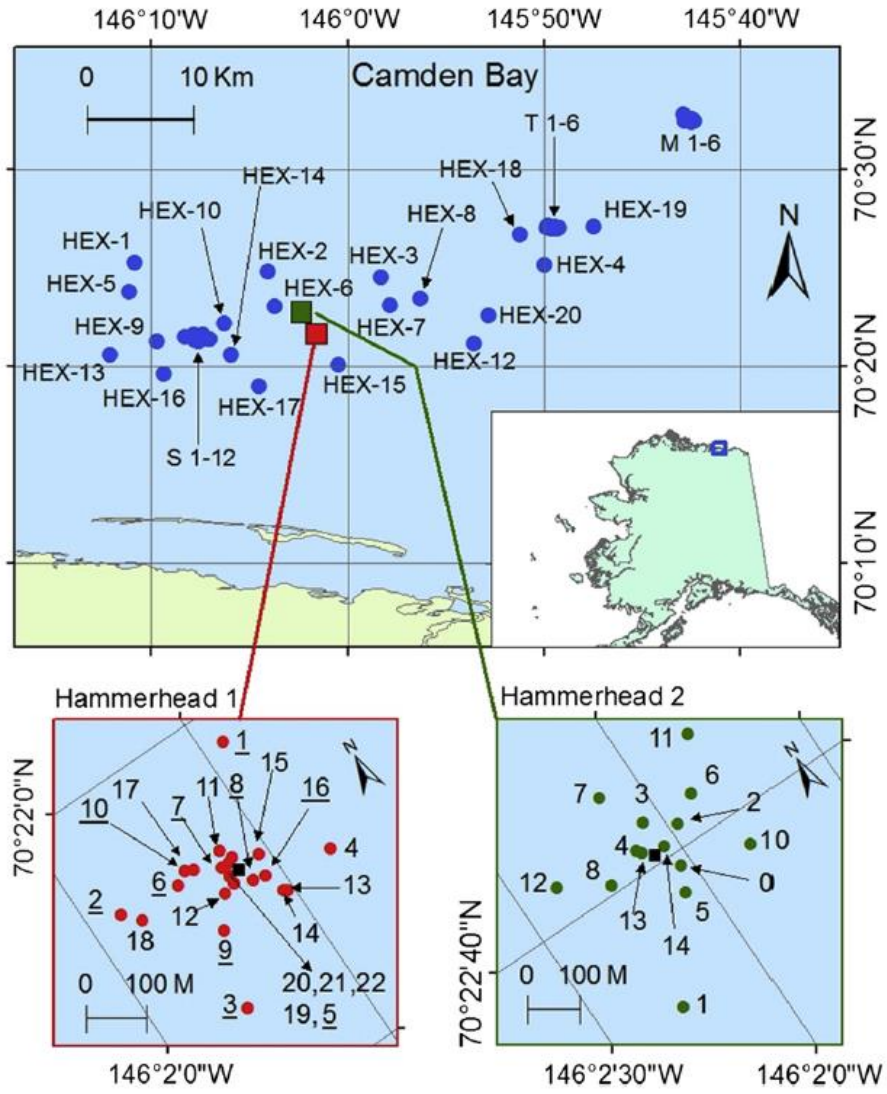

Figure 2.2. Location of study area in the Beaufort Sea (Camden Bay). Hammerhead 1 and 2 insets denote drilled stations with the black square showing the drill head. All other stations denote reference sites. From Trefry et al. (2013).

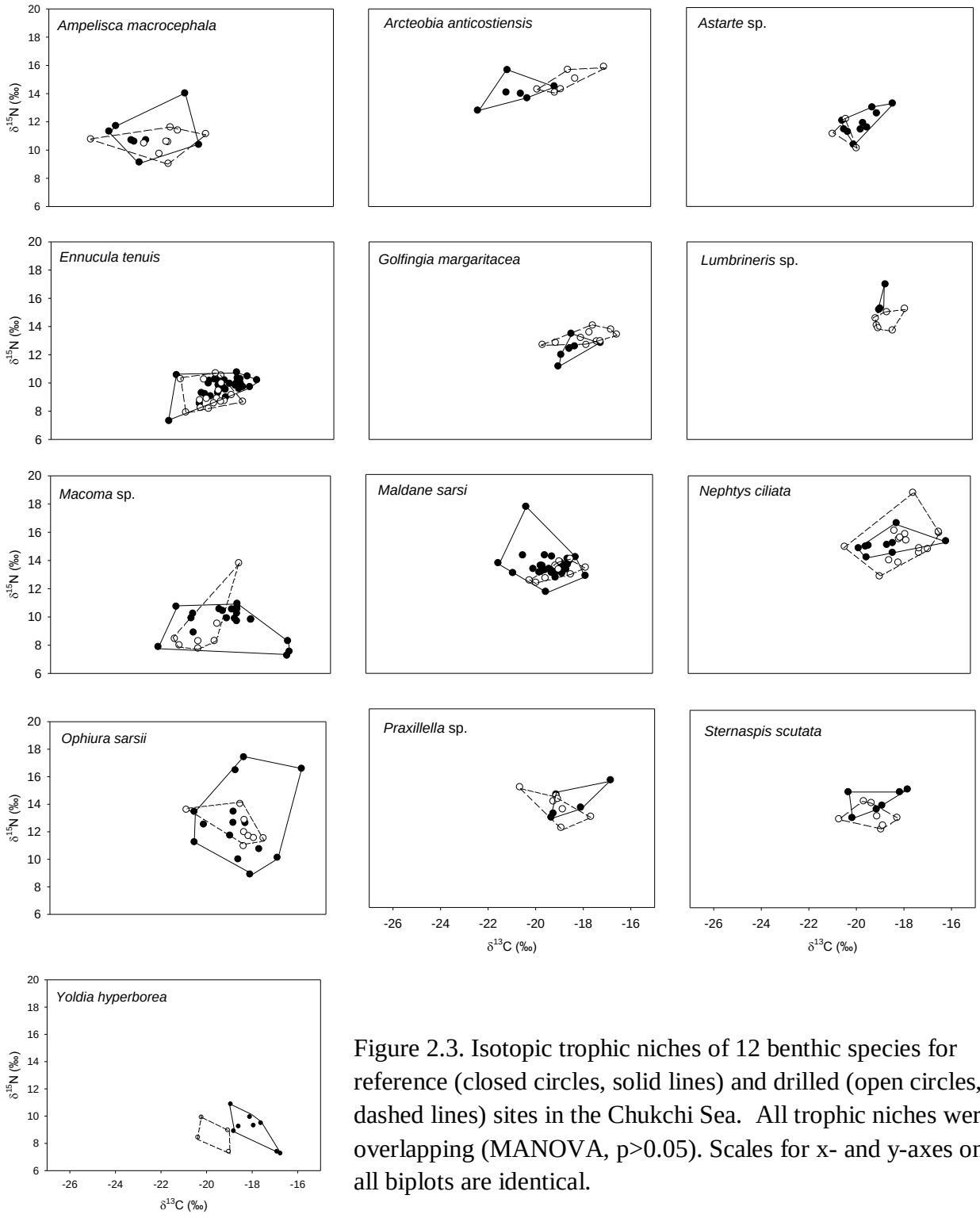

Figure 2.3. Isotopic trophic niches of 12 benthic species for reference (closed circles, solid lines) and drilled (open circles, dashed lines) sites in the Chukchi Sea. All trophic niches were overlapping (MANOVA, $p>0.05$). Scales for x- and y-axes on all biplots are identical.

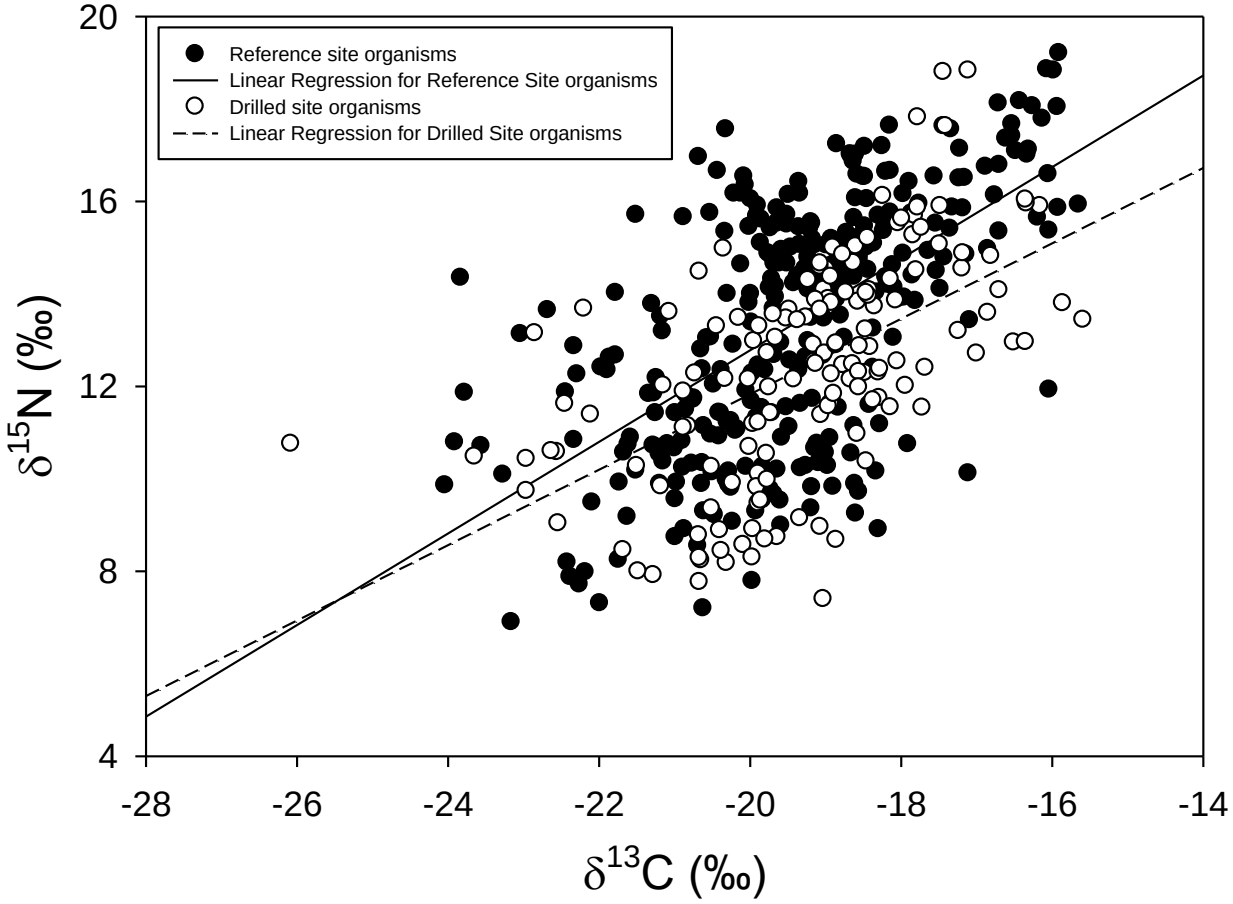

Figure 2.4. $\delta^{13}C$:$\delta^{15}N$ biplot of all benthic organisms from the Chukchi Sea analyzed from reference (closed circles) and drilled (open circles) sites. Slopes of linear regressions for reference ($y = 0.99x + 32.6$; $r^2 = 0.36$) and drilled sites ($y = 0.82x + 28.1$; $r^2 = 0.32$) were not significantly different (ANCOVA, $F=0.27$, $p=0.61$).

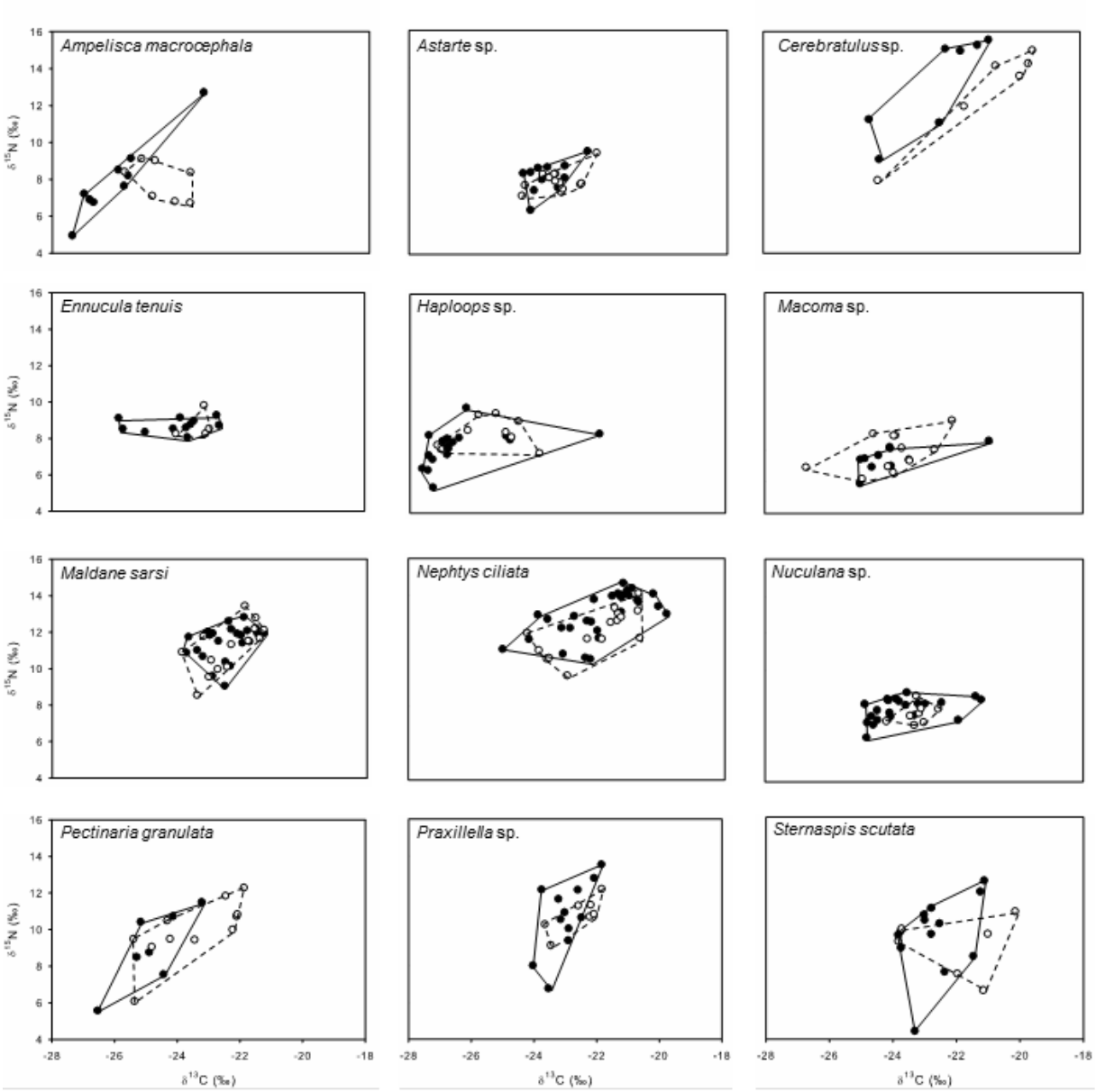

Figure 2.5. Comparison of organisms from reference (closed circles) and drilled (open circles) sites in the Beaufort Sea. Stable carbon and nitrogen isotope values were not significantly different in all comparisons (MANOVA, $p>0.05$).

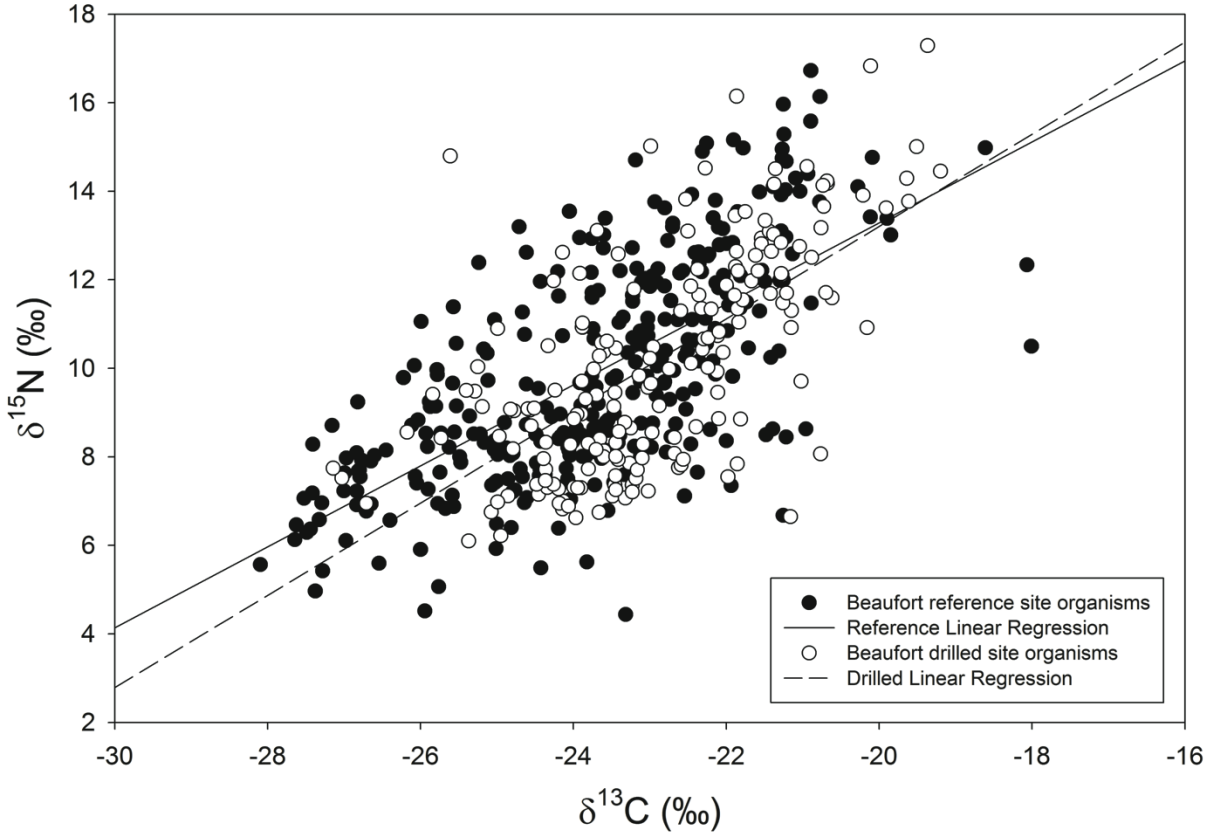

Figure 2.6. . $\delta^{13}C$:$\delta^{15}N$ biplot of all benthic organisms from the Beaufort Sea analyzed from reference (closed circles) and drilled (open circles) sites. Slopes of linear regressions for reference ($y = 0.91x + 31.0$; $r^2 = 0.45$) and drilled sites ($y = 1.04x + 34.0$; $r^2 = 0.43$) were not significantly different (ANCOVA, $F=1.52$, $p=0.22$).

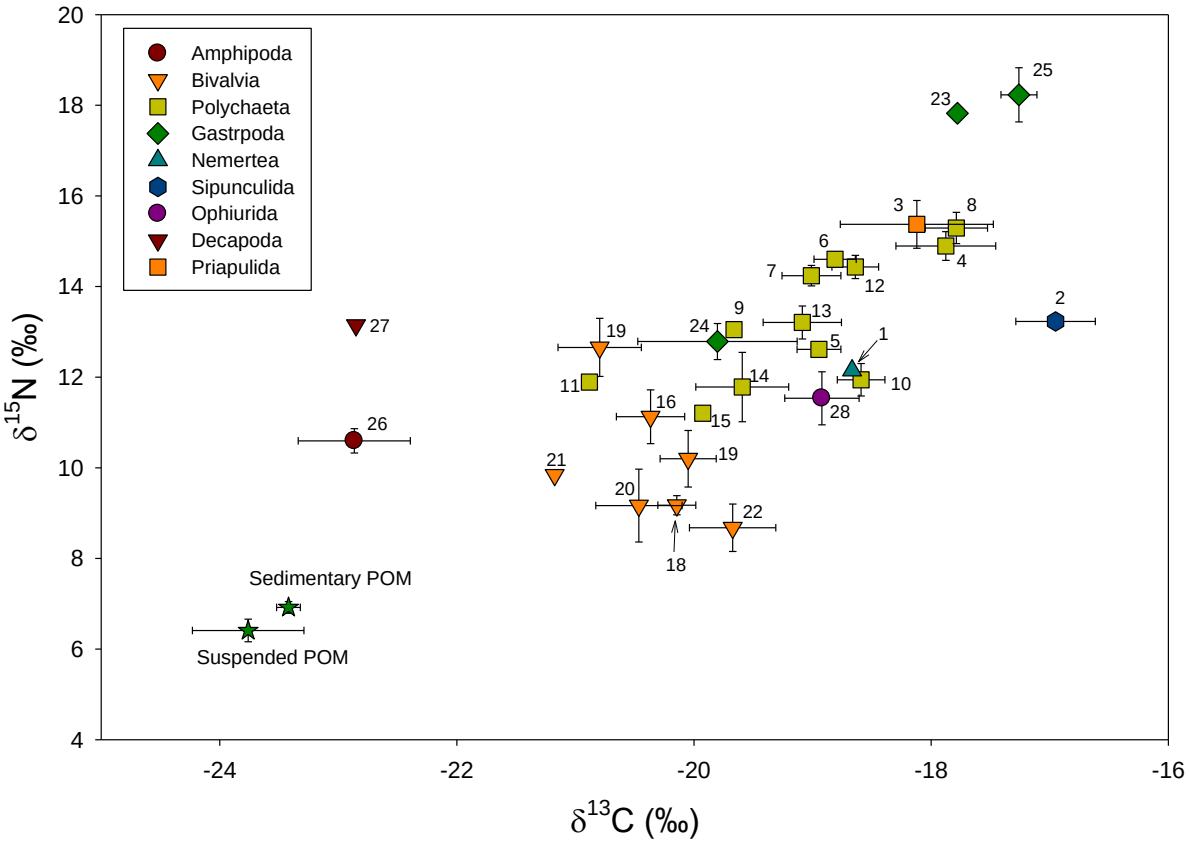

Figure 2.7. Food web structure for drilled sites in the northeast Chukchi Sea. Organism labels are denoted in Table 2.1. Data points (mean ± SE) are grouped by color and shape according to taxonomic group.

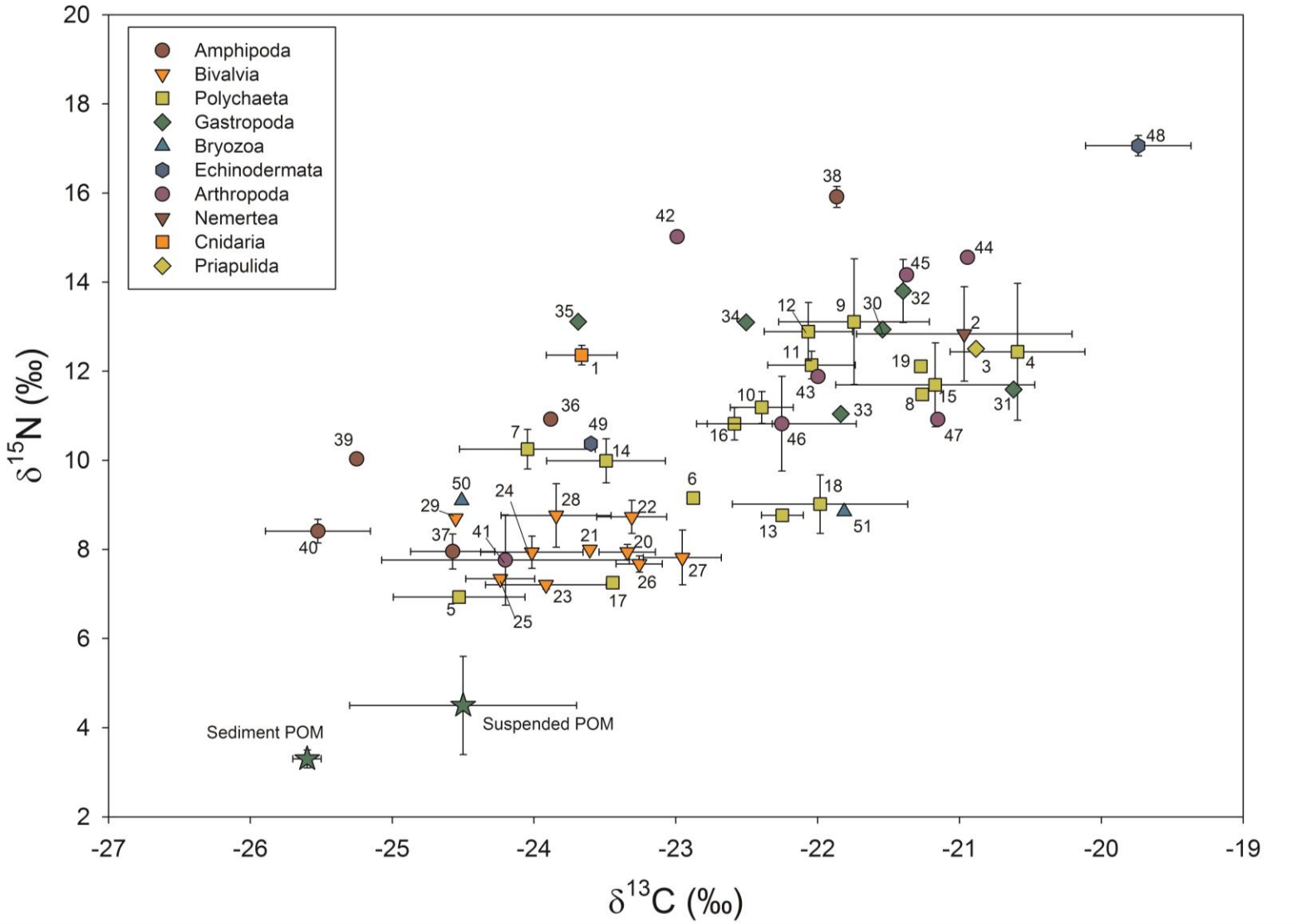

Figure 2.8. Food web structure for drilled sites in the Beaufort Sea. Organism labels are denoted in Table 2.2. Data points (mean ± SE) are grouped by color and shape according to taxonomic group.

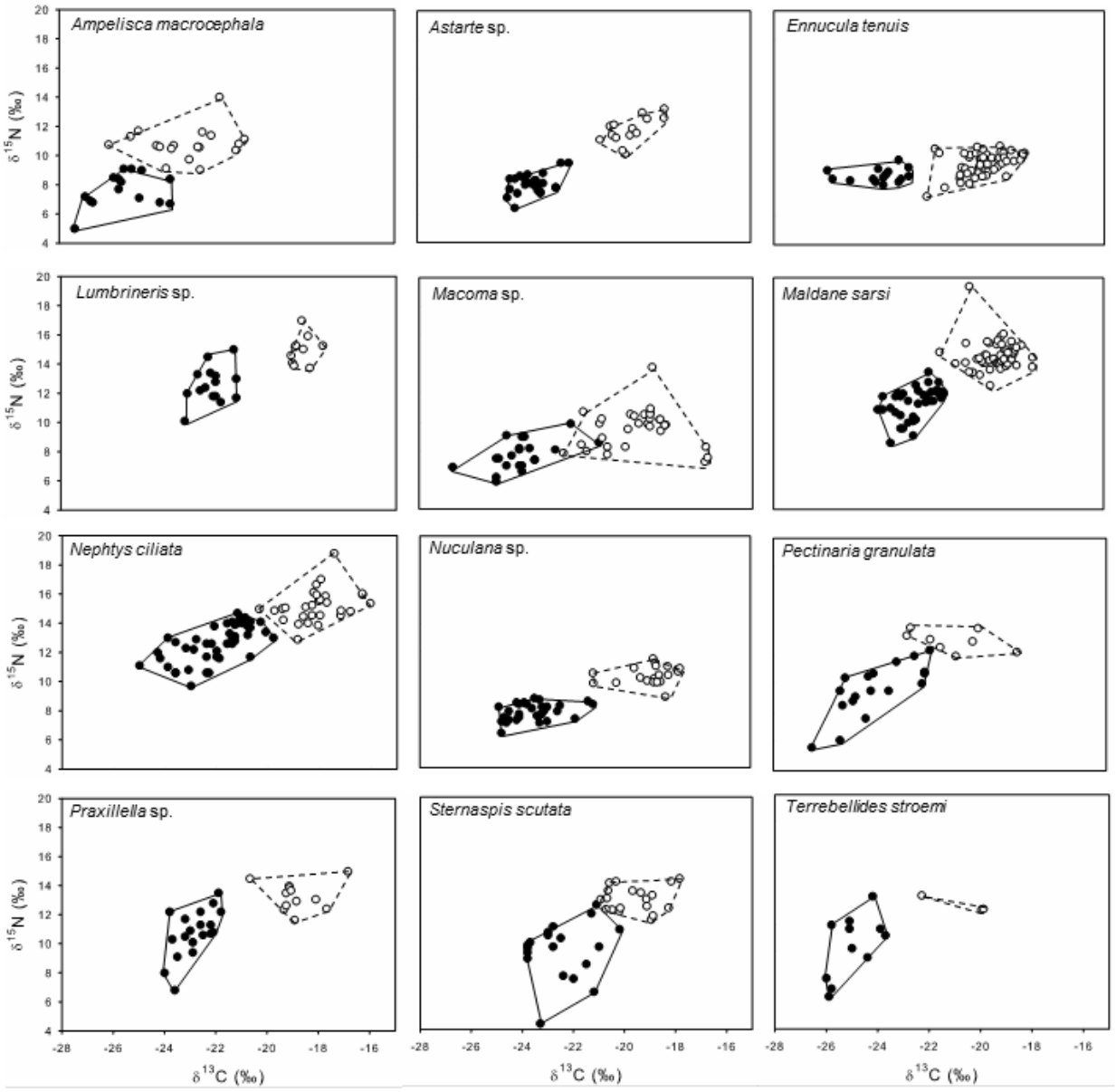

Figure 2.9. Isotopic niche space for organisms common to both the Chukchi (open circles) and Beaufort (closed circles) Seas. For all twelve pairwise comparisons, dual isotopic space was significantly different (MANOVA, $p<0.001$).

Chapter 3

Distribution of sedimentary pigments in the northeastern Chukchi Sea: ecosystem insights into pelagic-benthic coupling, the benthic food web, and microbial processes

Abstract

We measured the concentrations of chlorophyll *a*, pheopigments, and accessory pigments in sediments at 39 stations in the Chukchi Sea using high-performance liquid chromatography (HPLC) to investigate the degradation pathways of chlorophyll-containing organic matter. Chlorophyll *a* concentrations were among the highest ever recorded in marine sediments (up to 665 mg m^{-2}). Chlorophyll *a* concentrations were highest in sediments underlying the Bering Sea-Anadyr Water in the Chukchi Sea, and were much less concentrated in coastal stations under the Alaska Coastal Water. The concentrations of the pheopigments pheophytin *a*, pheophorbide *a*, and pyropheophorbide *a* indicated substantial degradative processing of organic matter that began ~2 weeks after ice retreat. However, the ratio of chlorophyll *a* to total pheopigments (chl:pheo) was >1 in most stations, which indicated that chlorophyll *a* is preserved against grazing and senescent degradation pathways despite moderate accumulation of pheopigments. The diatom biomarker fucoxanthin was found in high concentrations throughout the study area and positively correlated with chlorophyll *a* ($p<0.001$, $r=0.95$). $\delta^{13}C$ values of bulk sediment organic matter was positively correlated to concentrations of pheophytin *a* ($p<0.01$, $r=0.46$), and total pheopigment concentration was correlated to the $\delta^{13}C$ values of the epibenthic scavenging snow crab *Chionoecetes opilio* ($p<0.05$, $r=0.92$). Individual organisms collected at sediments with low pheopigment concentration reflected the stable carbon isotope value of sediment organic matter, but those found in high pheopigment concentration stations were more ^{13}C-enriched than the sedimentary organic matter. This pattern suggests that organic matter degraded by microbial and herbivorous grazing pathways produced a ^{13}C-enriched signal that was transferred to the macrofaunal food web.

1. Introduction

Sedimentary pigments provide an estimate of the amount of pelagic production exported to the benthos, and can indicate how this organic matter degrades on the seafloor (Vallentyne, 1955; Dayton et al., 1986; Morata and Renaud, 2008). The concept of pelagic-benthic coupling has received particular attention in shallow polar shelf ecosystems where a short photosynthetic growing season mediated by ice cover sustains diverse and abundant benthic faunal communities (Dunton et al., 2005; Grebmeier et al., 2006; Bluhm et al., 2009). As the polar ice pack retreats during spring, the ice edge fosters a pelagic microalgal bloom that rapidly sinks to the benthos (Carmack et al., 2004; Sakshaug, 2004).

In the Arctic, weak grazing pressure from low zooplankton abundance during spring allows a large proportion of pelagic primary producers to reach the shallow benthos, providing a major carbon subsidy to the benthic food web (Coyle and Cooney, 1988; Dunton et al., 2005). The occurence is exemplified in that benthic consumer biomass reflects the degree of primary production that occurs in the water column (Grebmeier et al., 1988). Polar shelf sediments act as repositories for the various pelagic microalgae that sink to the benthos and provide a "food bank" for benthic grazers and organic matter substrate for the microbial community (Mincks et al., 2005; Pirtle-Levy et al., 2009). It is, therefore, ecologically important to measure sedimentary pigments to assess the standing stock of benthic organic matter food resources in terms of food web dynamics.

Though a variety of different chlorophyll *a* derivatives can exist in marine sediments, the formation of these compounds depends on specific diagenetic events. Herbivorous metazoan grazing forms primarily pheophorbide *a* by cleaving the phytol chain and removing the Mg^{2+} ion from the porphyrin ring in the chlorophyll *a* molecule; pheophytin *a*, formed after Mg hydrolysis from the porphyrin ring, is predominantly a product of microbial degradation but can also be produced by metazoan and protozoan grazing (Bianchi et al., 1988; Sun et al., 1993; Cartaxana et al., 2003). The differentiation of pheopigments can provide insights into metazoan grazing versus

microbial degradation of organic matter in sediments, the latter of which has not been investigated in the Chukchi Sea using pigment biomarkers. Few studies have described concentrations of accessory pigments or pheopigments to differentiate the degradation pathways in arctic shelf sediments (Morata and Renaud, 2008, and references within; Morata et al., 2011), and currently, only spatially-limited sediment chlorophyll *a* concentrations have been measured for the Chukchi Sea using fluorometry (Clough et al., 2005; Cooper et al., 2009; Pirtle-Levy et al., 2009).

Recent studies in the Chukchi Sea have indicated that benthic fauna assimilate a carbon source that is ^{13}C-enriched relative to phytoplankton, indicating that the benthic food web is more complicated than previously conceived (Lovvorn et al., 2005; Iken et al., 2010, Chapter 1). Microbial degradative activities are shown to cause ^{13}C-enrichment of organic matter, but the extent that the arctic microbial community processes organic matter prior to macrofaunal assimilation is poorly understood despite its previously hypothesized role in benthic food web dynamics (McConnaughey and McRoy, 1979; Lovvorn et al., 2005; Sun et al., 2007). We hypothesize that major degradation processes of chlorophyll-containing organic matter that cause ^{13}C enrichment occurs before macrofaunal food web assimilation. To address this hypothesis, relationships between δ^{13}C values of both benthic invertebrates and sediments and were compared to the concentrations of pheopigments.

2. Methods

2.1 Study area and sample collection

The study area was located in the northeastern Chukchi Sea with sampling stations between the Alaska coastline and the U.S.-Russia maritime border at 169°W, and from approximately 68.9°N to 72.4°N (Figure 3.1). Samples were collected between 25 July and 16 August 2010 aboard the *R/V Moana Wave*. Stations were chosen using a hexagonal tessellation technique to ensure random selection and even distribution of stations (White et al., 1992). Station depth was 42 ± 7 m deep ($\bar{x}$ ± SD). The region is dominated by Bering Shelf-Anadyr Water (BSAW), although the Alaska Coastal Water

(ACW) influenced some of the easternmost stations, including stations 1, 4, 14, and 27 (Coachman et al., 1975).

Suspended particulate organic matter (SPOM) was concentrated by vacuum filtration onto pre-combusted 25 mm GF/F filters (Whatman, UK) from water collected at near-surface (within 2-8 m of the surface) and near-bottom (approximately 3 m above the seafloor) depths. Sediment samples for pigments, stable isotopic analyses, total organic carbon (TOC), and total nitrogen (TN) were collected using a 20 cm^3 syringe barrel (1.8 cm diameter, 2 cm depth) at all stations from undisturbed surface sediments retrieved by a van Veen grab (0.1 m^2). Sediment aliquots were placed in pre-labeled Falcon tubes (BD, USA) and immediately frozen in darkness to -20°C. Sediment was transported to the University of Texas Marine Science Institute (UTMSI, USA) and preserved at -80°C until prepared for pigment analysis.

The snow crab *Chionoecetes opilio* were collected using a 3.05 m plumb-staff beam trawl with a 7 mm mesh and a 4 mm cod-end liner. Samples washed with ambient surface water to remove extraneous organic matter and sediment. When possible, muscle tissue was extracted from the organism for stable isotope analyses. Biota and tissue samples were dried on board ship in aluminum dishes at 60°C.

2.2 Pigment analyses

Pigments targeted for analysis in the sediments were chlorophyll *a*, the pheopigments pheophytin *a*, pheophorbide *a*, pyropheophorbide *a*, and the accessory pigments chlorophyll *b*, chlorophyll *c* (defined as the sum of *c1* and *c2*), fucoxanthin, peridinin, prasinoxanthin, and 19-hex-fucoxanthin. Sediment pigments were extracted using 10 mL of 100% acetone since residual porewater in the sample dilutes the acetone concentration (Sun et al., 1991). Volume of porewater was determined by evaporation and accounted for in extract volume. Samples were sonicated in chilled water for 15 min in darkness. After centrifuging samples for 5 min at 4000 rpm, supernatant was decanted and filtered through 0.2 μm porosity nylon filters. To ensure the complete extraction of pigments from sediments, each sample was extracted twice and the extracts were

combined. If the combined extract was cloudy, the entire 20 mL was re-filtered through a 0.2 μm porosity nylon filter.

The HPLC pigment analysis followed the protocol of DHI (DHI Water and Environment, Denmark). Briefly, a binary gradient of 28 mM tetrabuyl ammonium acetate (TBA) in methanol (30%:30%, v:v) (eluent A) and methanol (eluent B) was used. Eluant B was ramped from 5% to 95% in 22 min, and held for 7 min before falling back to 5% within 2 min. A C_8 HPLC column (Agilent Eclipse XDB, 3.5 μm, 4.6 mm diameter x 150 mm length) was used, and the eluted pigment was detected by UV-vis absorbance (wavelength = 450 nm). Concentrations were determined by comparing pigment peaks of equal retention time to those of certified commercial standards (DHI, VWR, and Sigma-Aldrich, USA).

2.3 TOC, TN, and stable C and N isotopic analyses

To remove carbonates that would interfere with stable carbon isotope analysis of organic carbon, a subsample of faunal tissues (particularly calcifying organisms and small, whole organisms) and sediments were soaked in 1 *N* HCl until bubbling stopped, then rinsed in deionized water and dried at 60°C to a constant weight. Tissue and sediment subsamples prepared for stable nitrogen isotope analysis were not subjected to acidification. Muscle tissue excised from shell or exoskeleton was not acidified.

Dried tissue samples were manually homogenized with a mortar and pestle, and tissue, sediment, and filter samples were weighed in tin capsules to the nearest 10^{-6} g. Samples were analyzed on an automated system for coupled $\delta^{13}C$ and $\delta^{15}N$ measurements using a Finnigan MAT Delta Plus mass spectrometer attached to an elemental analyzer (CE Instruments, NC 2500). Samples were combusted at 1020°C and injected into the mass spectrometer with continuous flow. Isotopic ratios are denoted in standard δ notation relative to carbon and nitrogen standards of VPDB and atmospheric N_2, respectively where

$$\delta X=[(R_{sample}/R_{standard})-1] \times 1000 \quad (1)$$

and *X* is either ^{13}C or ^{15}N of the sample and R corresponds to the $^{13}C/^{12}C$ or $^{15}N/^{14}N$ ratio. Instrumental analytical error ±0.20‰ based on internal standards (casein and glutamic acid) checked against certified standards from the U.S. National Institute of Science and Technology and the International Atomic Energy Agency. We reported total nitrogen (TN) instead of total organic nitrogen (TON) since inorganic nitrogen, especially ammonium, can bind to clay minerals common to marine sediments and inflate the amount of measured N (Stein and Macdonald, 2004).

2.4 Ice Cover Data

Shapefiles of daily ice cover (resolutions to 50 m^2) provided courtesy of the National Ice Center (NIC), were projected onto a basemap containing all sampling stations in ArcMap 10.0 (ESRI). The NIC defines the demarcation between ice coverage and the marginal ice zone (MIZ) as 8/10ths ice cover. This line was tracked daily to determine the day that each station was initially covered by <80% sea ice.

2.5 Statistical Analyses

All statistics were computed using R 2.14.0 (www.r-project.org), including *t*-tests and Pearson correlations (r values). Significance for all tests was set at α=0.05. Data interpolation was performed in ArcMap 10.0 (ESRI) in Lambert Azimuthal Equal Area projection to prevent the distortion of rasters at high latitudes. Inverse distance weighting was used to interpolate all pigment values to depict overall trends. Kriging was used to interpolate sediment stable carbon isotope values. Values created in between actual data points are estimates and are meant to convey patterns; no computations were made on these estimated values.

3. Results

3.1 Chlorophyll a*, pheopigments, and accessory pigments*

Since the sea ice edge fosters an intense microalgal bloom, we investigated the number of days that had elapsed between the ice edge retreat from each station and when the station was sampled (Figure 3.1). We used the MIZ demarcation, defined as 80% ice cover by the NIC, because this is an indicator of when phytoplankton blooms can occur at the ice edge (Reigstad et al., 2002). Furthermore, extensive under-ice microalgae blooms have been observed (Yager et al., 2001; Arrigo et al., 2012), so 0% ice cover is a poor timestamp for the initiation of ice edge primary production. No significant linear trends were found between days ice free prior to sampling and chlorophyll *a* concentration, but a 2nd order (parabolic) regression explained the pattern more clearly (Figure 3.2). Stations that had experienced ice retreat between 82 to 101 days prior to occupation contained the least concentrated chlorophyll *a*. Likewise, stations that transitioned from ice cover to open water conditions within a week of our occupation contained sediments with relatively low concentrations of chlorophyll *a*. However, areas within the study site that had been in open water conditions for approximately 35 to 77 days contained the highest concentrations of chlorophyll *a*.

Sediment chlorophyll *a* concentrations ranged from 10.1 to 665 mg m^{-2} (0.332 to 81.7 μg g^{-1} dry weight) (Table 3.1; Figure 3.3a). The northwestern area of our study site (stations 35, 36, 37, 1030) contained the highest concentrations of pigments (43.6 – 81.7 μg g^{-1}; 430 – 665 mg m^{-2}). The stations 108, 46, and 109 near Hanna Shoal, near-shore stations 4 and 14, and the southernmost stations 103 and 105 contained relatively low concentrations of chlorophyll *a* (0.33 – 16.0 μg g^{-1}; 12.5 – 44.8 mg m^{-2}). When pigment concentrations expressed by mg m^{-2} and μg g^{-1} were regressed, the two values for chlorophyll *a* moderately agreed (r^2=0.72).

Pheophytin *a* was in low concentrations at stations recently transitioned to open water phase (<3 days) and where open water had dominated for over 70 days, which coincided with stations where chlorophyll *a* concentrations were lowest (Figure 3.1, 3.3b). Pheophytin *a* was in relatively high concentrations in two regions: the southern

stations 103 and 105, which had experienced ice retreat 16 and 13 days prior to sampling, respectively, and in the northwest region of the study site where chlorophyll *a* was also highest (Figure 3.1, 3.3b). Pheophorbide *a*, a marker for metazoan grazing, followed a similar trend to the pheophytin distribution (Figure 3.3c). Pyropheophorbide *a*, the secondary degradation product of pheophorbide *a*, had not yet formed at the southern stations where pheophorbide was high or at stations where chlorophyll *a* was in low concentrations (Figure 3.3d). However, pyropheophorbide *a* concentrations were high in the northwest sector of the study site and in the northeast sector near the mouth of Barrow Canyon. In some cases (e.g. stations 46, 108, 1015, 27, 1010) the chlorophyll *a*:pyropheophorbide *a* (chl:pyro) ratios were <1 (Table 3.1). Total pheopigment concentrations (sum of pheophytin *a*, pheophorbide *a*, and pyropheophorbide *a*) spanned to relatively high values (>190 mg m^{-2}, 20 μg g^{-1}; Figure 3.4) and positively correlated with chlorophyll *a* concentrations ($r=0.715$, $p<0.001$; Table 2).

Despite high pheopigment concentrations at some stations, the ratio of chlorophyll to total pheopigments (chl:pheo) was >1 at 32 of 39 stations (Figure 3.4). There was no apparent temporal trend between chl:pheo ratios and ice retreat since stations that had been ice free for 1 and 100 days had chl:pheo ratios >1. Some of the stations that had experienced ice retreat less than two weeks before sampling exhibited low values (<1) indicating that either substantial chlorophyll *a* had not yet reached the seafloor and the initial onset of fresh chlorophyll *a* was rapidly degraded, or the chlorophyll *a* was degraded in the water column before it reached the sediments.

Molar concentrations of pheophytin *a* were higher than pheophorbide *a* at 25 of 39 stations (Figure 3.5). At 10 of these stations, pheophorbide *a* concentrations were below detection limit. Station 46 was the only station where pheophorbide *a* and pheophytin *a* were both undetectable. There were no clear spatial or temporal trends aligning stations that had higher pheophorbide *a* concentrations than pheophytin *a*. Both pheophytin *a* and pheophorbide *a* were significantly and positively correlated to chlorophyll *a* ($p<0.001$, $r=0.78$ and 0.54, respectively; Table 2). Pheophytin *a* was highly

correlated to fucoxanthin ($p<0.001$, $r=0.82$), whereas pheophorbide *a* was less so ($p<0.01$, $r=0.50$; Table 2).

The pigments chlorophyll *b*, chlorophyll *c*, prasinoxanthin, and 19-hex-fucoxanthin were found in very low concentrations or not at all and displayed no significant trends within the study area; therefore, these pigments are not reported here. Fucoxanthin, a biomarker for diatoms, predominated other accessory pigments in sediments (Table 3.1). Its high correlation with sedimentary chlorophyll *a* ($r=0.948$, $p<0.001$; Table 2) suggested that diatoms contributed a large proportion of the chlorophyll *a* standing stock in sediments, in addition to sedimentary pheopigments, TOC, and TN that were also highly correlated to fucoxanthin (Table 3.2). Contrarily, the dinoflagellate marker peridinin was not significantly correlated to chlorophyll *a* or any other benthic parameter measured by this study. At 19 of 47 stations, no peridinin was found (Table 3.1).

3.2 Suspended and sedimentary organic matter stable carbon isotopes

SPOM stable carbon isotope values ranged from -26.2 to -21.0‰. Replicate values varied little around the mean for all samples except for the near-seafloor SPOM at station 37, which had error bars spanning 1.4‰. At all stations, the mean near-bottom SPOM $\delta^{13}C$ value was more enriched than the near-surface value (Figure 3.6).

The sedimentary organic matter $\delta^{13}C$ values in our study area ranged from -24.9 to -22.3‰. The most ^{13}C-depleted values occurred in coastal stations (1, 4, 14, 27). A distinct gradient formed as stations further from the Alaskan coast contained sediments with more ^{13}C-enriched organic matter (Figure 3.7).

4. Discussion

4.1 Organic matter inputs and retention in the benthos

The sedimentary chlorophyll *a* concentrations quantified in this study were among the highest ever recorded globally (Table 3.3). The Chukchi Sea and other arctic seas were historically regarded as biological deserts since the photosynthetic growing season

is approximately 120 days (Sakshaug and Slagstad, 1991). However, studies in past decades showed that the arctic seas, and particularly the Chukchi Sea, undergo intense blooms of primary production that support rich and abundant benthic fauna (Wassmann and Slagstad, 1993; Ambrose and Renaud, 1995; Hargrave et al., 2002).

The Chukchi Sea is host to three factors that, in concert, allow the seafloor to become a repository of such high concentrations of photopigments. First, our entire 120,000 km^2 study area averaged 42 m deep, about half the average depth of the entire Chukchi Sea (Jakobsson, 2002). Second, the Chukchi Sea receives nitrate-rich water (20-30 $\mu g\ l^{-1}$) upwelled from the Pacific Ocean and Gulf of Anadyr (Walsh et al., 1989), facilitating relatively high primary productivity of >400 gC $m^{-2}\ yr^{-1}$, of which >160 gC $m^{-2}\ yr^{-1}$ is "new" production (see review by Sakshaug (2004)). Third, this water column primary production is largely ungrazed by zooplankton due to an "extreme mismatch" in timing of zooplankton migration to the shallow seas and the rapid sinking of phytoplankton (Sakshaug, 2004). Rates of zooplankton growth and reproduction during spring are inhibited by low temperatures, which allows a major fraction of primary production to sink directly to the seafloor ungrazed, as shown in the Bering Sea (Coyle and Pinchuk, 2002). Therefore, particle flux from the Chukchi Sea water column is extremely high. At 67 °N in the Chukchi Sea, the southern boundary of our study area, the upper estimate of particle flux was measured at 38 mmol C $m^{-2}\ d^{-1}$ (166 gC $m^{-2}\ yr^{-1}$) using $^{235}Th/^{238}U$ particle scavenging during the summer open water season (Moran et al., 1997). Near the northernmost stations in our study at 71 °N, particle export was quantified at 39 mmol C $m^{-2}\ d^{-1}$ (171 gC $m^{-2}\ yr^{-1}$) during the summer months (Moran et al., 2005). Diatoms, the dominant Chukchi Sea primary producer, can sink between 0.1 to 30 m day^{-1} depending on hydrographic and physiological conditions (Smayda, 1971). However, viable cells found >1000 meters below the compensation depth in the open ocean provide evidence for oceanographic mechanisms for accelerated sinking of phytoplankton (e.g. density inversion currents, aggregation formation, downwelling events) that rapidly export biomass to the sediments (Smayda, 1971). Since at least 1% of surface irradiance reaches 25% of the Arctic continental shelves in summer,

microalgae may not experience a light-induced buoyancy trigger (Gattuso et al., 2006). Furthermore, dissolved inorganic nitrogen (nitrate, nitrite, and ammonium) and phosphate concentrations increased with depth during our summer sampling from nutrient-poor surface waters to sediments effluxing nutrients (Grebmeier and Cooper, 2012; Souza and Dunton, in press), which can also induce negative buoyancy in microalgae (Richardson and Cullen, 1995). Laws et al. (1988) demonstrated that although 58% of water column production was lost to zooplanktonic grazing in an Alaskan bay, 40% was exported from the euphotic zone as viable cells. Moreover, even at the deeper parts of the shelf where ambient light does not reach the sediments, the highest vertical flux of phytoplankton occurs at the compensation depth, which would occur very near the seafloor in the Chukchi Sea (Wassmann et al., 2003). Based on the above ancillary evidence, we assume that a large component of organic matter produced in the euphotic zone was rapidly transported out of the shallow water column to the sediments. Regardless of whether degradation occurred in the water column during deposition or in the sediments themselves, pheopigments provide a useful marker to gauge how rapidly and to what extent chlorophyll *a* has degraded.

Though less extensive work has been conducted in the northern Chukchi Sea, previous studies have shown trends that the western boundary of our study site, influenced by the BSAW, contains sediments with lower C:N values and higher TOC and TN concentrations (Grebmeier et al., 1988; Naidu et al., 1993; Naidu et al., 2000). TOC and TN were significantly ($p<0.001$) and positively ($r = 0.55$ and 0.54, respectively) correlated with sedimentary chlorophyll *a* standing stock concentrations (Table 3.2), which indicated the consistent contribution of microalgae to the sediments in this area. The extent of the northwestward pigment gradient is incomplete since the U.S.-Russian maritime border bisecting the Chukchi Sea prevented more westward sampling. Low values of benthic faunal biomass and abundance for this northwestern region may attribute to the high retention of organic matter in sediments if low biomass is an indication of benthic grazing pressure (Grebmeier and Cooper, 2012; Ravelo et al., 2012; Schonberg and Dunton, 2012). However, the standing stock of photopigments measured

here represents only a snapshot of primary production that has reached the seafloor. The non-linear relationship of benthic chlorophyll *a* standing stock to time since ice retreated indicated benthic pigments have a dynamic temporal relationship (Figure 3.2).

4.2 Chlorophyll a*, pheopigments, and accessory pigments*

Southern stations 103 and 105 that experienced ice retreat 16 and 13 days prior to cruise occupation, respectively, showed relatively low sedimentary chlorophyll *a* values (7.75 and 16.0 μg g^{-1}), but these values were higher than stations 109, 108, and 46 (0.66, 2.08, and 0.33 μg g^{-1}, respectively) that had experienced only 1-2 days of sub-80% ice cover prior to sampling. Counterintuitive to the south-to-north sea ice retreat paradigm for the Arctic, northwestern stations experienced ice retreat earlier than the southern stations due to the formation of the Chukchi Polynya in 2010 described by Stringer and Groves (1991; Figure 3.1). The highest values of chlorophyll *a* were measured at the northwest stations, which experienced sub-80% ice cover about six to eight weeks prior to expedition occupation. This represents the approximate window of time for the initial ice edge bloom to occur and reach the benthos since stations with longer durations of sub-80% ice conditions had lower chlorophyll *a* concentrations, indicating microalgae had already begun to degrade in the benthos.

Previous studies have shown a positive correlation between water column chlorophyll *a* and sediment chlorophyll *a* (Grebmeier et al., 1988; Morata and Renaud, 2008), a trend that was reflected in our mid-summer Chukchi Sea data. When station 103, a clear outlier, was omitted from the linear regression, integrated water column chlorophyll *a* (Grebmeier and Cooper, 2012) and sedimentary chlorophyll *a* correlated with each other (r^2=0.74). The positive correlation corroborates the tight nature of pelagic-benthic coupling on shallow arctic shelves (Grebmeier and Barry, 1991; Dunton et al., 2005; Morata and Renaud, 2008). The correlation between the concentration of chlorophyll *a* in the water column and benthos implies either that a supply of fresh microalgae must continually be replenished in the water column as it is delivered to the benthos, or microalgae simultaneously undergo intense production in the water column

and sediments. Engelsen et al. (2002) demonstrated with remote sensing data that smaller blooms occur repeatedly after an initial large bloom, and the second largest bloom occurs up to 60 days post-ice retreat. The water column bloom at station 103, which occurred 16 days after ice retreat, aligns with the timeline described by Engelsen et al. (2002) where the initial ice edge bloom materializes two weeks post-ice retreat. The secondary large bloom that can occur ~60 days post-ice retreat explains the positive correlation between water column and sediment chlorophyll *a*. Stations in the 42 to 64 day post-ice retreat window (e.g., stations 21, 35, 36) had high concentrations of chlorophyll *a* in the water column and benthos simultaneously.

Although it is clear that pheophytin *a* and pheophorbide *a* are formed during chlorophyll *a* diagenesis, there are multiple degradative pathways that lead to the formation of these pigments. Pheophorbide *a* and pyropheophorbide *a* are major products of macrozooplanktonic grazing formed via the chlorophyllide pathway, not by enzymatic cleavage of the phytol chain from pheophytin *a* (Lee et al., 2000). Instead, the formation of pheophytin *a* from chlorophyll *a* is likely an end-product not further converted into pheophorbide *a*. Pheophorbide *a* is formed via the chlorophyllide pathway versus the enzymatic cleavage of the phytol chain from pheophytin *a* (Ziegler et al., 1988). Sun et al. (1993) showed that chlorophyll *a* in sediments free of macrofauna formed pheophytin *a* but did not further degrade to pheophorbide *a*. Bianchi et al. (1988) demonstrated predominant pathways of pheophytin *a* formation from microbial degradation of chlorophyll *a* in sediments, while pheophorbide *a* was formed by macrofaunal degradation of chlorophyll *a*. Contrarily, the grazing activities of the cladoceran *Daphnia pulex* rapidly produced of both pheophytin *a* and pheophorbide *a* (Daley, 1973). Copepods and salps have been shown to produce both pheophytin *a* and pheophorbide *a* after grazing on fresh microalgal material in the water column (Hallegraeff, 1981). Pheophytin *a* and, to a lesser extent, pheophorbide *a* were formed by ciliate and heterotrophic dinoflagellate grazing (Strom, 1993). Protozoan grazers were also suspected of coprophagy that would accelerate the conversion of pigments to colorless

compounds and prevent any pigments from accumulating in the sediments (Klein et al., 1986; Strom, 1993).

In this study, pheophytin *a* and pheophorbide *a* were found in relatively high concentrations at stations 103 and 105 where the ice edge bloom occurred approximately two weeks prior. The rapid accumulation of pheopigments in sediments demonstrated the efficiency of grazing pathways that degrade fresh organic matter and shunt it through the food web, whether microbial or metazoan (Sun et al., 2009; Boetius et al., 2013). The northwestern region of the study area that contained the highest chlorophyll *a* concentrations also possessed some of the highest pheopigment concentrations. Despite a lower benthic faunal biomass in this region, pheophorbide *a* still accumulated in the sediments. Pheophytin *a* concentrations were appreciably high throughout the study area except for the coastal stations that experienced the earliest ice edge conditions. In the coastal stations, not only has the benthic grazing pathways had the most time to rework the fresh carbon in the sediments, likely into colorless compounds since all pigments were found in low concentration, but these stations also occurred in the ACW, where water column production is lower than adjacent western areas in the BSAW (Walsh et al., 1989). These factors, in conjunction, are likely responsible for the low chlorophyll and pheopigment concentrations found here. The stations in the northeast of the study site approach the 50 m isobath marking the mouth of Barrow Canyon, a region of the Chukchi Sea renown for its high benthic biomass (Grebmeier et al., 2006). Here, at stations 29 and 1010, both pheophorbide *a* and pheophytin *a* are relatively concentrated.

The molar ratios of pheophytin *a* to pheophorbide *a* in the sediments (range = 0.25 to 5.00; $\bar{x}$ ± SD = 1.48 ± 1.16) at more than half of our stations exhibited a ratio >1 (Figure 3.5). 1:1 molar conversions of chlorophyll to pheopigments after heterotrophic digestion are hypothetically possible (Shuman and Lorenzen, 1975), but pheopigments are eventually converted to colorless compounds, which reduces the amount of pheopigments that can accumulate in sediments. Hawkins et al. (1986) reported 45.9 ± 26.7% of chlorophyll *a* was converted into pheopigments by the bivalve *Mytilus edulus*, while the remaining fraction was lost to colorless compounds and heterotrophic

metabolism. Helling and Baars (1985) reported a 67% recovery of pheopigments from chlorophyll after grazing by calanoid copepods. On the contrary, Kiørboe and Tiselius (1987) measured only an 8% loss to colorless compounds by the copepod *Acartia tonsa*. The large range of pheophytin:pheophorbide ratios and high concentrations of both pigments that we measured in the Chukchi Sea sediments implies dynamic heterotrophic processes of microbes, protozoans, and metazoans. For example, at stations 4, 5, 14, 15, 40, 48, and 106, pheophorbide *a* was not found, whereas pheophytin *a* was measurable. At those stations, the community of heterotrophs and subsequent degradation processes either (1) did not produce pheophorbide *a* and did produce pheophytin *a*, or (2) pheophorbide *a* was produced but degraded faster than pheophytin *a* to colorless compounds prior to our sampling. Some evidence suggests the degradation rate of pheophytin *a* may be "intrinsically slower" than the rate for chlorophyll *a* or pheophorbide *a*, which allows its accumulation in sediments (Sun et al., 1993).

Pyropheophorbide *a*, the degradation product of pheophorbide *a*, followed a lag pattern of its parent molecule. In the southern stations where high pheophorbide *a* had recently accumulated in high concentrations from benthic grazing of the recent microalgae deposition, pyropheophorbide *a* had not yet formed. Pyropheophorbide *a* was found in high concentrations where both pheophorbide *a* was high and sea ice had retreated more than three weeks prior to sampling, with the exception of the northern station 108 in the Hanna Shoal region, which had experienced ice retreat less than one week prior to sampling. Here, pyropheophorbide *a* concentrations exceeded that of all other pigments at that station. The high concentration of this pigment can be explained as either (1) the small amount of fresh organic matter that had already sunk to the shallow benthos was rapidly and thoroughly degraded, or (2) pyropheophorbide *a* was a relic pigment not associated with recently deposited organic matter. Since pyropheophorbide *a* was not found throughout much of the study area, the former hypothesis is more likely the case.

The prevalence of the diatom biomarker fucoxanthin over the dinoflagellate biomarker peridinin in the sediments demonstrates the importance of diatom carbon to

the benthic food web (Table 3.1). This concept is corroborated by the high positive correlation between chlorophyll *a*, TOC, and TN to fucoxanthin in the sediments (Table 3.2). Diatoms typically dominate the initial onset of an ice edge bloom, whereas other microalgae like dinoflagellates occur later in summer in low nutrient-low silicate conditions (Carmack and Wassmann, 2006). Siliceous tests make diatoms denser than seawater (1.050 – 1.300 g cm^{-3}, de Jonge (1979)); thus, in the Arctic, diatoms of the pennate morphology common to ice algae and benthic microalgae accumulate more rapidly than other microalgae on the seafloor (von Quillfeldt, 2000; von Quillfeldt et al., 2003; Wulff et al., 2009). Dinoflagellates might predominate secondary or tertiary late-season blooms if silicate is limiting, but dinoflagellate biomarkers have been reported in low concentrations in the Chukchi Sea water column during summer (Hill et al., 2005).

The proportion of diatoms versus dinoflagellates in sediments (% diatoms) was estimated using pigment concentrations in the equation

$$\% \text{ diatoms} = (S_{fuco:chl}/C_{fuco:chl})/[(S_{fuco:chl}/C_{fuco:chl})+(S_{peri:chl}/C_{peri:chl})] \quad (2)$$

where S represents a sample's ratio of fucoxanthin (fuco) or peridinin (peri) to chlorophyll *a* (chl). In order to account for peridinin being ~50% of total dinoflagellate pigments and fucoxanthin being ~38% of diatom total pigments, we standardized S to respective pigment ratios (C) determined by Wright et al. (1996). In this way, $C_{fuco:chl}$ = 0.60 and $C_{peri:chl}$ = 1.06. This allowed us to compare relative amounts of fucoxanthin directly to relative amounts of peridinin despite one group containing higher absolute concentration of pigments than the other. This provided a rough approximation of the abundance of diatoms and dinoflagellates since the fuco:chl and peri:chl ratios can vary for various taxa and based on environmental conditions. However, the approximation allowed us to generally compare the concentrations of the two accessory pigments to each other. When the pigments were compared, diatoms accounted for at least 80% of the sum of diatoms and dinoflagellates throughout Chukchi Sea study area, except for stations 109 (74%), 30 (62%), and 106 (42%).

4.3 Viability of the microphytobenthos

The Chukchi Sea shelf provides a possible habitat for viable microphytobenthos. The viability of the Chukchi Sea microphytobenthos was explored by Matheke and Horner (1974), who found that the high benthic microalgae biomass (55-320 mg m^{-2} chlorophyll *a*) accounted for 76% of pelagic and benthic production, but this concept has since largely been ignored in the Chukchi Sea. Most studies around the globe that report benthic chlorophyll *a* parameters are situated in deeper sites, and therefore, typically report lower values than this study (Table 3.3). The values we found for the Chukchi Sea exceeded most other temperate systems that we reviewed. Within the Arctic, the shallow coastal waters of Svalbard (Woelfel et al., 2010), Greenland (Glud et al., 2002), and the Chukchi Sea (Matheke and Horner, 1974) have values that approach those of our study. Cooper et al. (2009) reported values much lower than ours for the Chukchi Sea, but their sampling effort focused on the deep shelf break and did not sample as heavily in the shallow basin where we report high values. Of the Antarctic studies reviewed here, relatively high chlorophyll *a* concentrations were reported, which further demonstrate the intense productivity and the strong pelagic-benthic coupling of polar seas. For example, Dayton et al. (1986) found chlorophyll *a* values as high as 913 mg m^{-2} in muddy, shallow substrates off the coast of Antarctica.

Although we did not measure the photosynthetic capacity of sediments, the possibility of viable microalgae cannot be overlooked as a component of the benthic food web, nitrogen cycling, and the carbon cycle in the Chukchi Sea. The ratio of chlorophyll *a* to total pheopigments (chl:pheo) provides a metric to quantify the degree of degradation in microalgae. Most chl:pheo ratios throughout our study site were >1, which is indicative of viable cells. In areas of low chlorophyll *a* where open water conditions had existed for >100 days, chl:pheo ratios were still >1 suggesting that viable cells continud to produce and maintain their photosynthetic pigments, counteracting the degradative grazing and senescent pathways.

4.4 Sedimentary pigments as proxies for ^{13}C-enrichment for food webs

A hypothesis posited by previous studies (McConnaughey and McRoy, 1979; Lovvorn et al., 2005) implicates microbial processing, which degrades organic matter and respires ^{13}C-depleted CO_2, as a mechanism to provide ^{13}C-enriched organic matter to Chukchi Sea benthic fauna. The hypothesis, to our knowledge, has not been directly tested in the Chukchi Sea benthos, but our pigment and stable isotope data provided some insight to the relationship between the degradative processes in the sediments and the macrofaunal food web.

Depth profiles of suspended particulate organic matter (SPOM) in our study area revealed organic matter was more ^{13}C-enriched near the seafloor than in surface waters (Figure 3.6). A possible explanation of this trend was that as SPOM sinks toward the seafloor, it degraded and fractionated in its stable isotope value as it lost $^{12}CO_2$. Curiously, the $\delta^{13}C$ values of near-bottom SPOM did not account for the ^{13}C-enriched stable isotope values of the majority of benthic fauna (Chapter 1). Therefore, if organic matter degradation does occur while suspended in the water column and accounts for the measured stable carbon isotope enrichment, it must further degrade and fractionate once it reaches the seafloor if that organic matter is responsible for the consumers' $\delta^{13}C$ values.

There was a positive correlation between the $\delta^{13}C$ values of sedimentary organic matter and the concentration of both pheophytin and pheophorbide (Table 3.2). The concentration of total pheopigments was significantly and positively correlated with the $\delta^{13}C$ values of the omnivorous scavenging snow crab *Chionoecetes opilio* (Figure 3.8). However, the correlational trends of sediment and organism $\delta^{13}C$ values with pheopigment concentration may be confounded by sources of organic matter (marine vs. terrestrial) to the system and the subsequent spatial patterns of stable isotope values (i.e., isoscapes). We found the very distinct pattern of sedimentary organic matter $\delta^{13}C$ values in the Chukchi Sea also reported in the synthesis by Naidu et al. (2004) during our summer sampling (Figure 3.7). The previous findings concluded that the coastal area (stations 1, 4, 14, and 27 in this study) underlying the ACW received terrestrially-derived material that was relatively ^{13}C-depleted, whereas sediment from the areas at the western

and northern extent of our study area (e.g., stations 103, 105, 20, 21, 35, 36, 37, 1030, 38, 47, 49), which were overlaid by the BSAW, contained a more ^{13}C-enriched signal of marine phytoplankton. The pattern of ^{13}C-depleted coastal sediments to ^{13}C-enriched offshore sediments showed a striking resemblance to the pattern of sedimentary pigments, from low concentrations in the coastal sediments to high concentrations in offshore sediments. We interpreted the pattern of pigment distribution as the amount of marine primary production reaching the sediments since the BSAW is more productive than the ACW (Walsh et al., 1989). It is, then, difficult to separate the trend of *C. opilio* δ^{13}C values and pheopigments from sedimentary δ^{13}C values; however, *C. opilio* individuals were still up to 3.4‰ more enriched than sedimentary organic matter, even after accounting for a 1‰ δ^{13}C enrichment per trophic level for these third trophic level organisms (Table 3.4). Interestingly, the crabs that were not more enriched (~0‰) than sedimentary organic matter were collected at station 47 and 49, where sedimentary pheopigment concentrations were very low. The negative enrichment for the individual at station 47 suggests that the δ^{13}C enrichment factor can be less than 1‰ for the species. The individuals from station 103, where pheopigment concentrations were relatively high, were 3.2 – 3.4‰ more ^{13}C-enriched than sedimentary organic matter. Furthermore, the δ^{13}C values of organisms were linearly related to the pheopigment concentration (r^2=0.84). Although it was not experimentally determined, the correlation suggests degradation of organic matter is related to ^{13}C-enrichment, a signal transferred into the food web and better explains the anomalously ^{13}C-enriched organism values than sedimentary organic matter values alone.

Pigments are useful biomarkers for investigating the diagenetic processes of chlorophyll-containing organic matter. However, the production of major pheopigments from multiple heterotrophic pathways confounds our ability to specifically implicate the microbial food web as a major step in organic matter processing versus other protozoan and metazoan activities. Future studies should experimentally investigate predominant pigments formed by the diverse array of consumers in the marine benthic system, since most feeding-pigment studies use zooplankton. An essential question still remains for the

carbon and nitrogen cycles in the Chukchi Sea: what are the steps leading to the assimilation of organic matter by benthic consumers? The pigment and stable isotope data presented here suggest diagenetic intricacies, but direct experimentation and measurement of these hypothetical processes are still needed.

Table 3.1. Concentrations of sedimentary pigments in the northeast Chukchi Sea determined by HPLC (both on a dry weight and areal basis).

Station	Chlorophyll *a*		Pheophytin *a*		Pheophorbide *a*	
	μg g^{-1}	mg m^{-2}	μg g^{-1}	mg m^{-2}	μg g^{-1}	mg m^{-2}
1	7.34	117	1.45	23.3	3.98	63.9
4	0.47	25.6	0.52	29.3	0.00	0.00
5	1.43	21.1	0.45	6.65	0.00	0.00
6	8.44	103	1.34	16.4	1.53	18.7
9	30.6	438	6.39	91.5	2.35	33.7
10	2.74	30.9	1.83	20.7	1.55	17.5
11	13.5	196	1.52	22.0	1.45	21.0
14	0.49	12.5	0.11	2.75	0.00	0.00
15	75.0	191	9.39	23.9	0.00	0.00
19	2.96	26.1	1.56	13.8	0.53	4.71
20	28.5	296	4.87	50.8	2.32	24.2
21	9.19	109	3.14	37.5	0.60	7.15
22	2.40	29.8	0.67	8.30	1.00	12.5
24	23.8	125	1.79	9.43	1.94	10.3
27	6.27	107	0.94	16.0	0.14	2.43
29	36.3	114	3.62	11.4	1.53	4.83
30	5.07	55.6	1.54	16.9	0.64	6.97
35	81.7	603	7.80	57.6	4.88	36.0
36	46.5	616	5.14	68.1	2.03	26.9
37	43.6	430	3.89	38.5	3.98	39.3
38	12.0	118	1.24	12.2	0.46	4.52
39	10.9	148	2.90	39.5	0.77	10.6
40	4.97	74.0	1.07	16.0	0.00	0.00
41	4.76	68.9	1.92	27.7	0.75	10.8
46	0.33	10.2	0.00	0.00	0.00	0.00
47	3.09	25.0	1.42	11.5	0.00	0.00
48	3.50	35.6	0.91	9.27	0.00	0.00
49	10.2	87.1	5.48	46.6	1.87	16.0
103	7.75	35.2	8.11	36.8	6.88	31.2
105	16.0	44.8	6.04	16.9	5.65	15.8
106	4.80	73.5	2.11	32.3	0.00	0.00
108	2.08	43.3	0.40	8.29	0.22	4.62
109	0.66	15.3	0.27	6.39	0.00	0.00
1010	51.1	284	5.53	30.9	4.68	26.1
1013	2.69	36.1	0.93	12.5	0.75	10.1
1014	3.51	43.4	0.60	7.39	0.41	5.06
1015	1.68	33.3	0.12	2.32	0.23	4.60
1016	0.71	14.8	0.08	1.71	0.01	0.23
1030	79.2	665	5.84	49.1	5.55	46.7

Table 3.1 cont.

Station	Pyropheophorbide *a*		Peridinin		Fucoxanthin	
	μg g^{-1}	mg m^{-2}	μg g^{-1}	mg m^{-2}	μg g^{-1}	mg m^{-2}
1	2.41	38.7	0.00	0.00	3.92	62.90
4	0.00	0.00	0.16	9.20	0.45	25.4
5	0.00	0.00	0.17	2.53	0.73	10.7
6	3.25	39.7	1.10	13.5	2.35	28.8
9	4.75	68.0	0.00	0.00	9.85	141
10	0.00	0.00	0.30	3.34	1.92	21.7
11	0.00	0.00	1.01	14.7	4.22	61.2
14	0.00	0.00	0.12	3.13	0.38	9.66
15	0.00	0.00	0.63	1.61	31.4	79.9
19	0.63	5.56	0.00	0.00	0.41	3.61
20	0.00	0.00	0.26	2.68	6.51	67.8
21	0.00	0.00	0.50	6.01	2.05	24.4
22	0.00	0.00	0.39	4.85	0.90	11.2
24	7.99	42.2	0.00	0.00	6.94	36.6
27	3.87	66.2	0.00	0.00	1.79	30.7
29	1.85	5.85	0.00	0.00	7.70	24.3
30	0.00	0.00	1.13	12.4	1.04	11.4
35	0.00	0.00	0.37	2.74	22.0	162
36	1.51	20.0	0.00	0.00	11.8	156
37	2.33	23.0	0.00	0.00	10.8	106
38	0.65	6.39	0.00	0.00	2.14	21.0
39	2.38	32.4	0.00	0.00	1.98	26.9
40	0.74	11.0	0.00	0.00	1.16	17.3
41	0.80	11.5	0.00	0.00	1.02	14.7
46	0.51	15.7	0.00	0.00	0.11	3.50
47	0.00	0.00	0.00	0.00	1.95	15.8
48	0.00	0.00	0.53	5.42	2.28	23.2
49	0.84	7.12	0.00	0.00	2.09	17.8
103	0.00	0.00	0.63	2.87	4.58	20.8
105	0.00	0.00	0.41	1.14	9.01	25.2
106	0.00	0.00	2.01	30.9	0.85	13.0
108	2.58	53.5	0.00	0.00	0.60	12.5
109	0.00	0.00	0.24	5.61	0.38	8.87
1010	9.77	54.5	0.00	0.00	16.33	91.1
1013	0.00	0.00	0.09	1.25	1.31	17.6
1014	0.00	0.00	0.31	3.86	1.53	18.9
1015	2.68	53.2	0.00	0.00	0.45	8.9
1016	0.00	0.00	0.01	0.14	0.40	8.39
1030	1.94	16.3	0.00	0.00	17.6	147

Table 3.2. Pearson correlation matrix (r values) relating benthic pigment concentrations, biological characteristics, and environmental factors. TOC=total organic matter; TN=total nitrogen; IP25=concentration of Ice Proxy 25 (ng/g); Chl a=chlorophyll *a*; Tpheo=total pheopigments. IP25 concentrations from K. Taylor and R. Harvey (pers. comm.). Infauna biomass and abundance data for H' calculation from Schonberg and Dunton (2012). Only significant statistics are shown. Significance denoted as: *p<0.05; **p<0.01; ***p<0.001. Non-significant relationships not reported.

Explanatory Variable	Fucoxanthin	Pheophytin *a*	Pheophorbide *a*	Tpheo	IP25	TOC	TN
Fucoxanthin		0.819***	0.500**	0.709***		0.520***	0.511**
Chlorophyll *a*	0.948***	0.774***	0.541***	0.715***		0.554***	0.537***
Sediment $\delta^{13}C$		0.462**	0.337*		0.563***	0.562***	0.640***
Infauna Diversity (H')					-0.692***	-0.493**	-0.552***
Infauna Biomass							
Days ice retreat					-0.452**		
C. opilio $\delta^{13}C$				0.917*			

Table 3.3. Selected primary literature values for sedimentary chlorophyll *a* and pheopigment concentrations. Values are grouped by region. Method, location, and depth of each study are listed. *pheophytin + pheophorbide; **pheophytin + pyropheophytin; ***estimated from a figure.

Study	Location	Method	Season	Depth (m)	Values
Antarctic studies					
Mincks et al. 2005	Antarctica, Western Antarctic Penninsula	HPLC and fluorometry	Austral summer – winter	550 – 680	0.1 – 3.07 μg g^{-1} chl *a*
Dayton et al. 1986	Antarctic, McMurdo Sound	Spectrophotometry	Austral summer	6 - 43	47.3 – 913 mg m^{-2} chl *a*; 0.43 – 10.5 chl:pheo
Gilbert 1991	Signey Island, Antarctica	Spectrophotometry	July – June	8	10 – 500 mg m^{-2} chl *a****
Arctic studies					
Matheke and Horner 1974	Barrow, Alaska (Chukchi Sea)	Spectrophotometry	February – August	~5	55 – 320 mg m^{-2} chl *a*
Horner and Schrader 1982	Stefanson Sound, Alaska (Beaufort Sea)	Fluorometry	April – June	7	<1 – 28 mg m^{-2} chl *a*
Glud et al. 2002	Young Sound, Greenland	Spectrophotometry	July – August	5 – 30	66 – 186 mg m^{-2} chl *a*
Ambrose and Renaud 1995	Northeast Water Polynya, Greenland	Fluorometry	July – August	125 – 515	7.22 – 45.62 mg m^{-2} total pigments
Clough et al. 2005	Chukchi Sea and Arctic Ocean	Fluorometry	June – August	44 – 2500	0.001 – 2.78 ug cm^{-1} surface chl *a* 0.03 – 23.61 ug cm^{-1} surface pheophytin
Cooper et al. 2005	Chukchi Sea (shelf break)	Fluorometry	May – August	34 – 3197	1 – 37 mg m^{-2} chl *a****
Cooper et al. 2009	Chukchi Sea (shelf break)	Fluorometry	May – August	49 – 3760	0 – 20 mg m^{-2} chl *a*

Table 3.3 cont.

Woelfel et al. 2010	Kongsfjorden, Svalbard	Spectrophotometry	June – August	5 – 30	13 – 317 mg m^{-2} chl *a*
Morata and Renaud 2008	Western Barents Sea, Svalbard	HPLC	May – August	195-503	0.163-2.801 μg g^{-1} chl *a*; 0.010 – 1.810 μg g^{-1} pheophorbide; 0.134 – 3.491 μg g^{-1} pheophytin; 0.006 – 0.454 μg g^{-1} pyropheophorbide; 0.073 – 0.595 chl:pheo
Renaud et al. 2007	Franklin Bay, Beaufort Sea	Fluorometry	December – June	231	10 mg m^{-2} chl *a**** 78 – 110 mg m^{-2} pheopigments***
Renaud et al. 2008	Western Barents Sea, Svalbard	Fluorometry	May – August	195 – 503	0.6±0.3 – 40.2±5.4 mg m^{-2} chl *a*; 4.7±2.2 – 79.3±5.3 mg m^{-2} pheopigments
Morata et al. 2011	Franklin Bay, Beaufort Sea	Fluorometry	January – June	250	1.5 – 2.2 mg m^{-2} chl *a* *** 0.06 – 0.09 chl:pheo***
This study	Chukchi Sea	HPLC	July – August	22-60	0.33 – 81.7 μg g^{-1} chl *a*; 10.2 – 665 mg m^{-2} chl *a*; 0.52 – 8.0 chl:pheo
Temperate studies					
Pinckney et al. 1994	North Inlet Estuary, South Carolina	HPLC Spectrophotometry Fluorometry	April – June	*Spartina* zone, mud flats, sand flats, intertidal zone	1 – 240 mg m^{-2} chl *a* (HPLC)
Brotas et al. 2007	Tagus Estuary, Portugal	HPLC Spectrophotometry	September – May	shallow mesotidal sediments	<10 – 150 μg g^{-1} chl *a* (HPLC) 0 – 16 μg g^{-1} pheophorbide

Table 3.3. cont.

Cahoon et al. 1994	North Carolina, Cape Hatteras (continental slope)	Spectrophotometry	August – September	530 – 2003	2.10 ± 2.88 to 65.2 ± 10.2 mg m^{-2} chl *a*; 0.08 ± 0.10 to 2.29 ± 3.44 μg g^{-1} chl *a*
Cartaxana et al. 2003	Tagus Estuary, Portugal	HPLC	not specified	shallow mesotidal sediments	61.3 ± 5.1 μg g^{-1} chl *a*; 48.1 ± 4.7 μg g^{-1} fucoxanthin; 8.62 ± 1.30 μg g^{-1} pheophytin; 16.0 ± 1.7 μg g^{-1} pheophorbide
Grippo et al. 2010	North Gulf of Mexico, Louisiana	HPLC	April – October	5 – 18	8 – 77 mg m^{-2} chl *a*; 6.8 ± 0.88 – 58.0 ±23.2 mg m^{-2} Tpheo*; 0.19 – 2.27 chl:pheo
Josefson et al. 2012	Bothnian Bay, Scandinavia	HPLC	May – June	68 – 108	0.04 ± 0.02 μg cm^{-3} chl *a*; 0.74 μg cm^{-3} pheophytin**
	Bothnian Sea, Scandinavia			104 – 286	3.41 ± 3.86 μg cm^{-3} chl *a*; 1.47 μg cm^{-3} pheophytin**
	Gulf of Finland			47 – 70	8.92 ± 3.49 μg cm^{-3} chl *a*; 4.51 μg cm^{-3} pheophytin**
	Eastern Gotland Basin, Scandinavia			47 – 90	0.81 ± 0.38 μg cm^{-3} chl *a*; 1.90 μg cm^{-3} pheophytin**
de Jonge and Colijn 1994	Ems Estuary, Netherlands	Spectrophotometry	May – August	intertidal mud and sandflats	5 – 425 mg m^{-2} chl *a****

Table 3.4. Comparison of $\delta^{13}C$ values of sedimentary organic matter and *Chionoecetes opilio* individuals collected at the same stations. The $\delta^{13}C$ enrichment accounts for a 1‰ enrichment per trophic level for the third trophic level *C. opilio*.

Station	Sediment $\delta^{13}C$ (‰)	*C. opilio* $\delta^{13}C$ (‰)	$\delta^{13}C$ enrichment* (‰)
1	-24.7	-18.9	2.8
1	-24.7	-19.0	2.9
21	-22.7	-18.5	1.2
30	-23.2	-19.1	1.1
30	-23.2	-19.2	1.0
47	-22.5	-19.9	-0.4
49	-22.9	-19.9	0.0
103	-22.3	-15.9	3.4
103	-22.3	-16.0	3.3
103	-22.3	-16.1	3.2

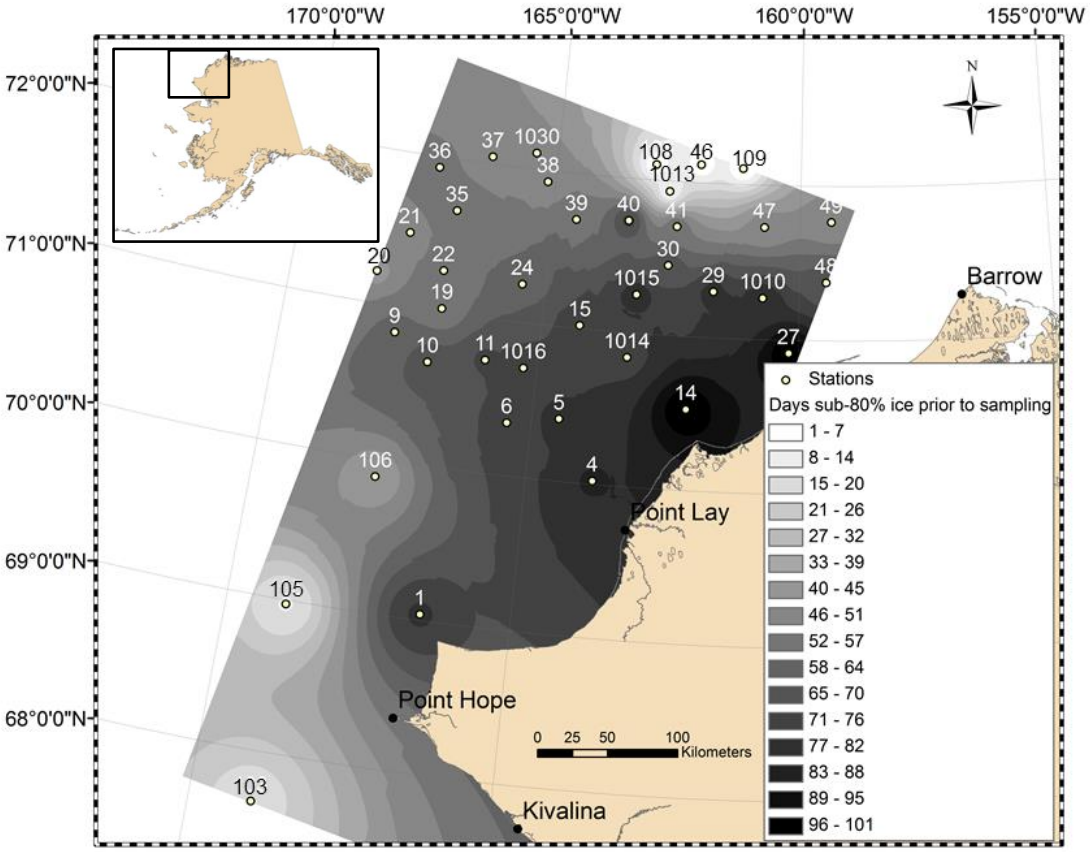

Figure 3.1. Location of sampling stations in the Northeast Chukchi Sea with the timing of sea ice retreat in 2010. The black to white gradient represents the earliest to most recent retreat. Station numbers appear on the map, while colors represent values.

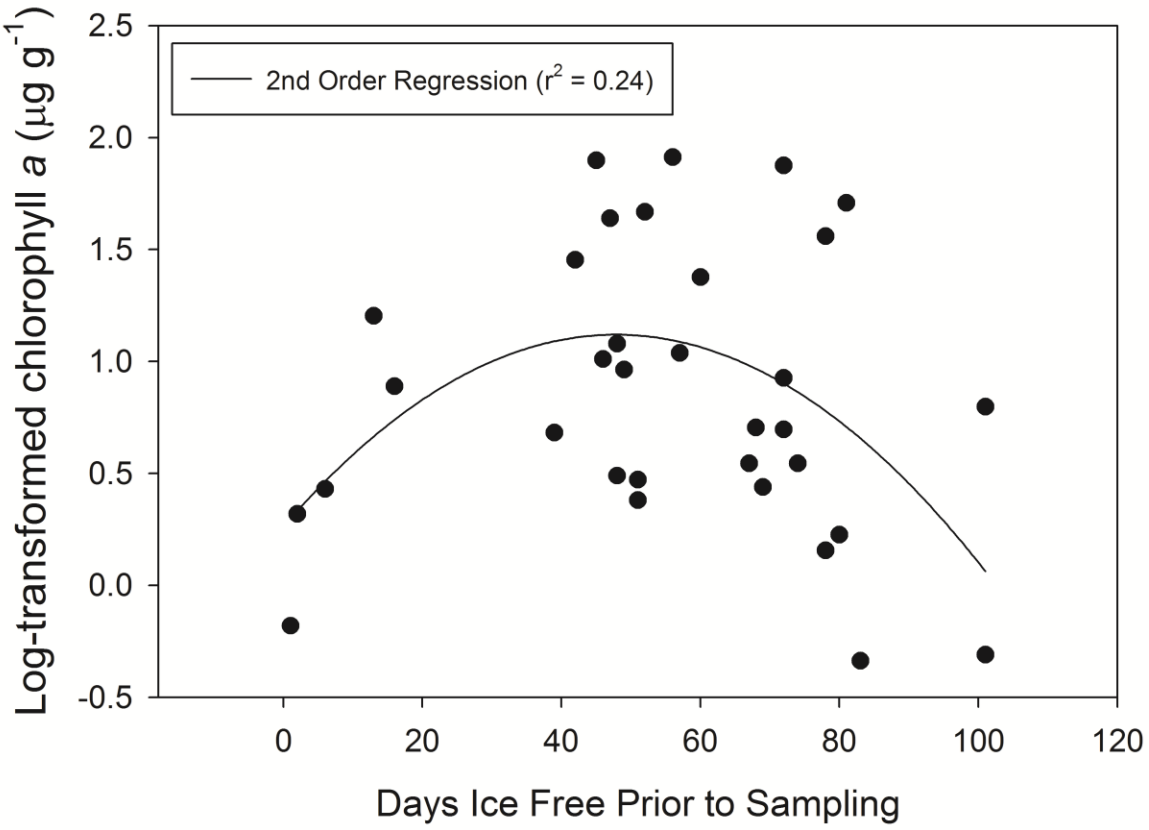

Figure 3.2. Second order regression depicting the trend between time (in days) since ice retreat and sedimentary chlorophyll *a* concentration. Days of initial ice retreat defined once ice extent is defined as <80% sea ice (NIC).

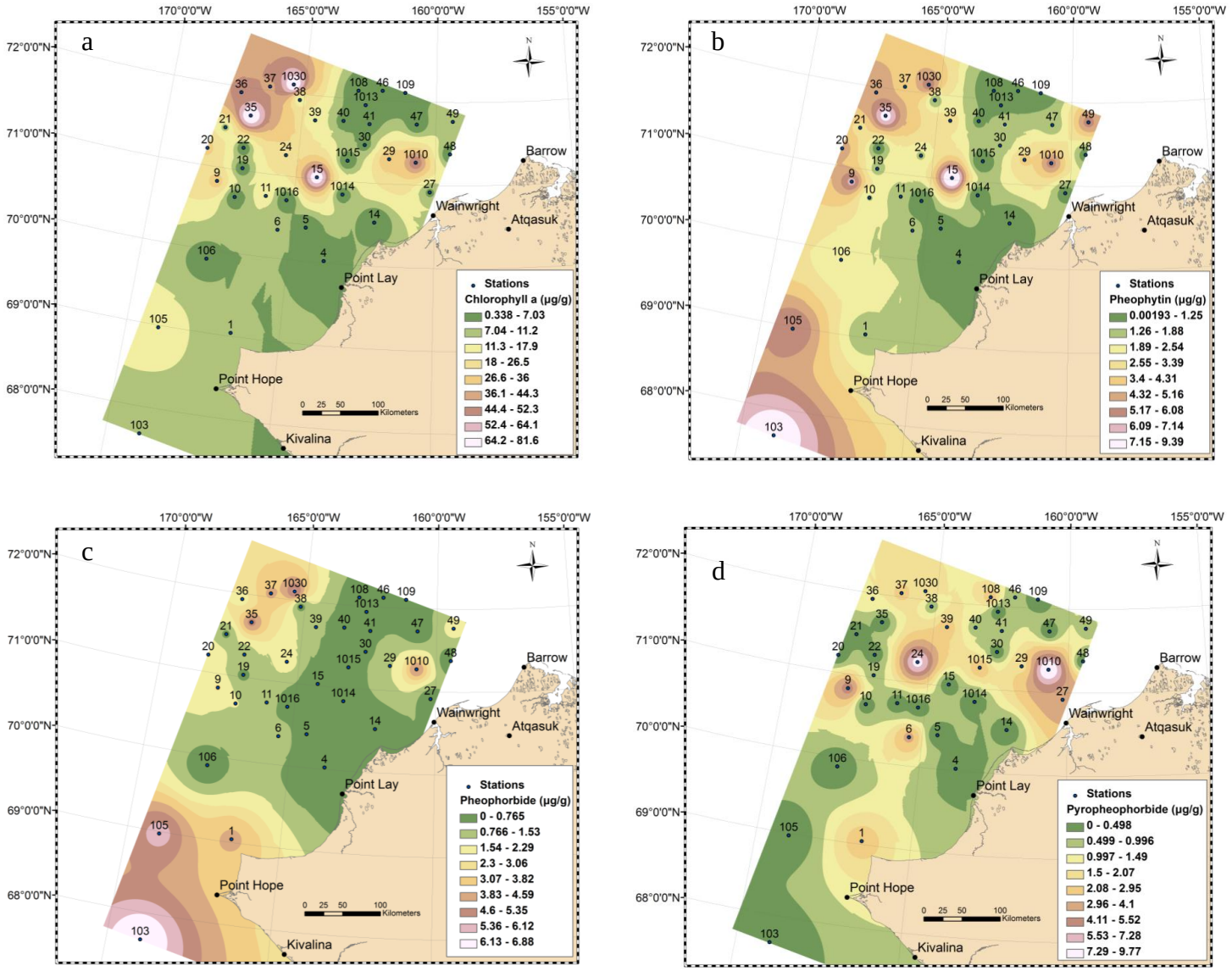

Figure 3.3. Interpolation of sedimentary pigments chlorophyll *a* (a), pheophytin *a* (b), pheophorbide *a* (c), and pyropheophorbide (d). Numbers on map represent station numbers. The color scheme represents pigment concentration (µg g^{-1}).

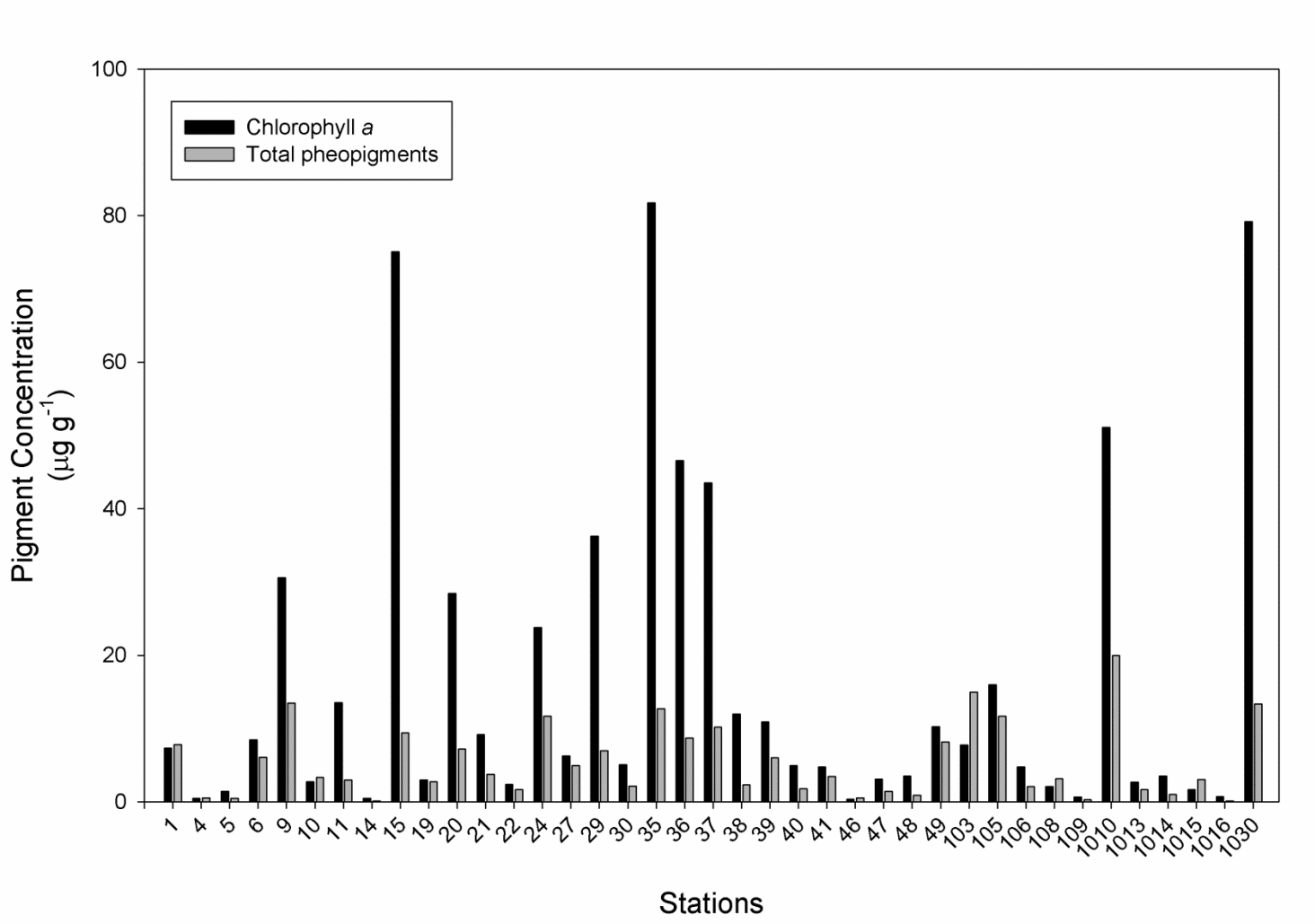

Figure 3.4. Concentration of chlorophyll *a* and total pheopigments (sum of pheophytin, pheophorbide, and pyropheophorbide) at each station. Stations 1, 4, 10, 46, 103, 108, and 1015 contain less chlorophyll *a* than total pheopigments.

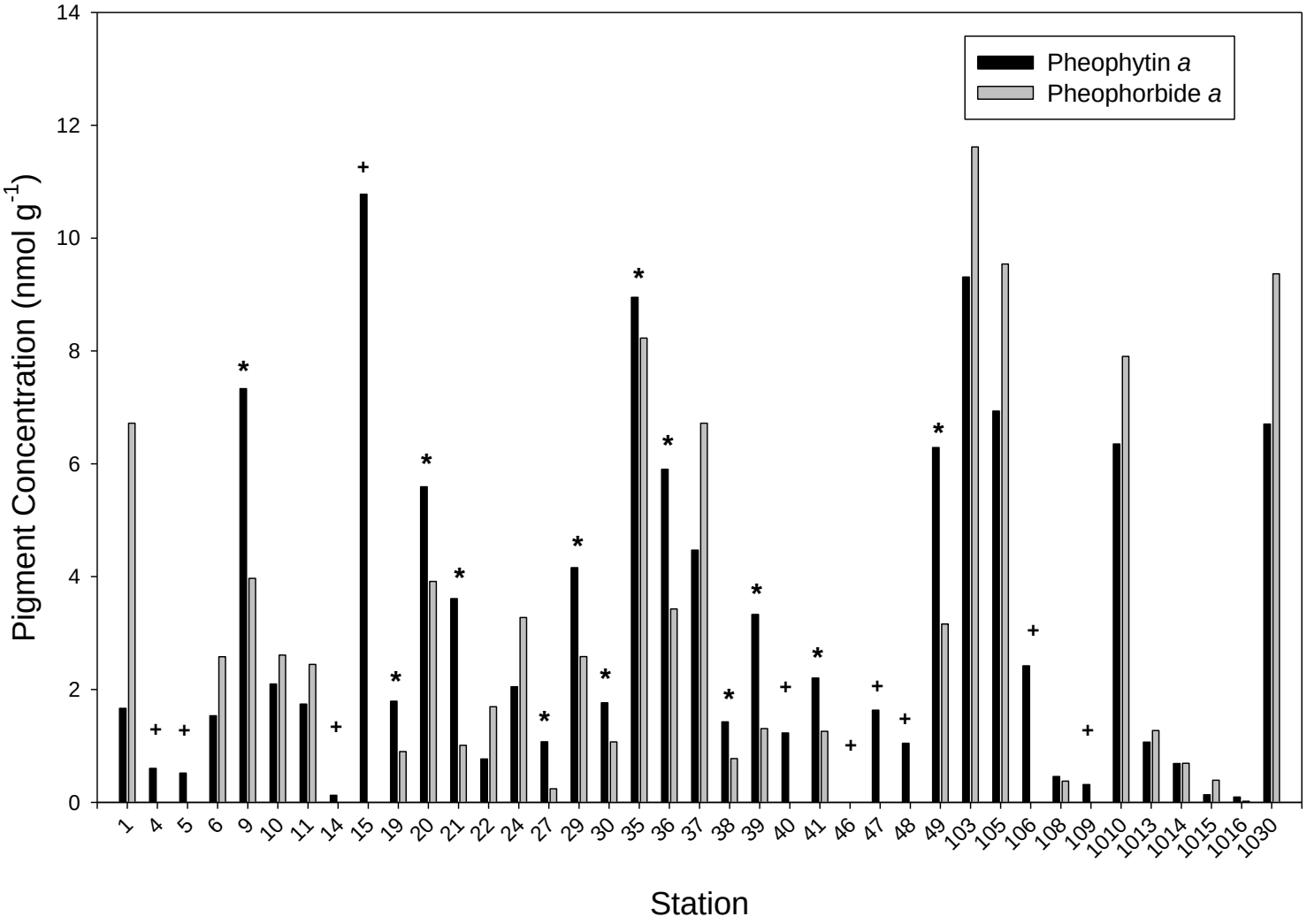

Figure 3.5. Comparison of pheophytin *a* to pheophorbide *a* ratios within sediments in the Chukchi Sea. * denotes ratios of pheophytin:pheophorbide >1. + denotes pheophorbide *a* in concentrations below detection limit.

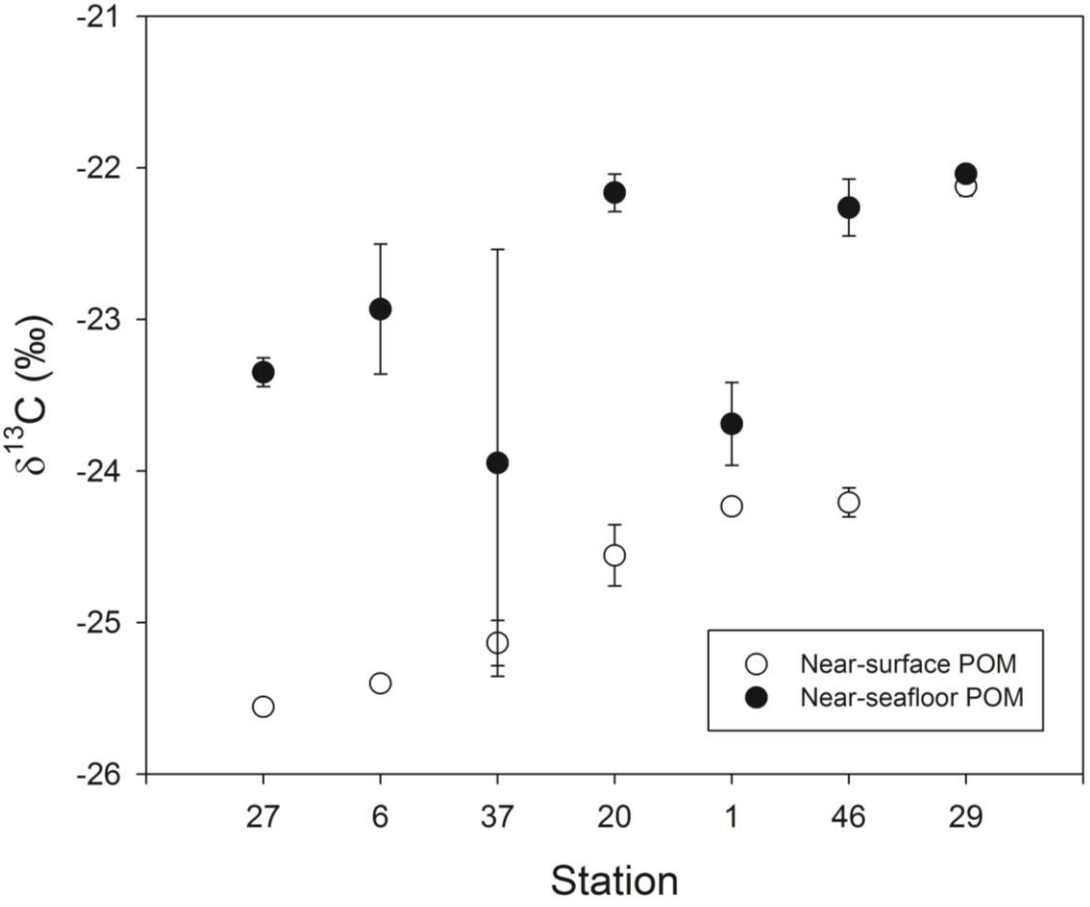

Figure 3.6. Depth profiles of SPOM $\delta^{13}C$ values. Near-surface SPOM is shown in open circles, while near-bottom SPOM is shown in closed circles. Values are mean ± SE.

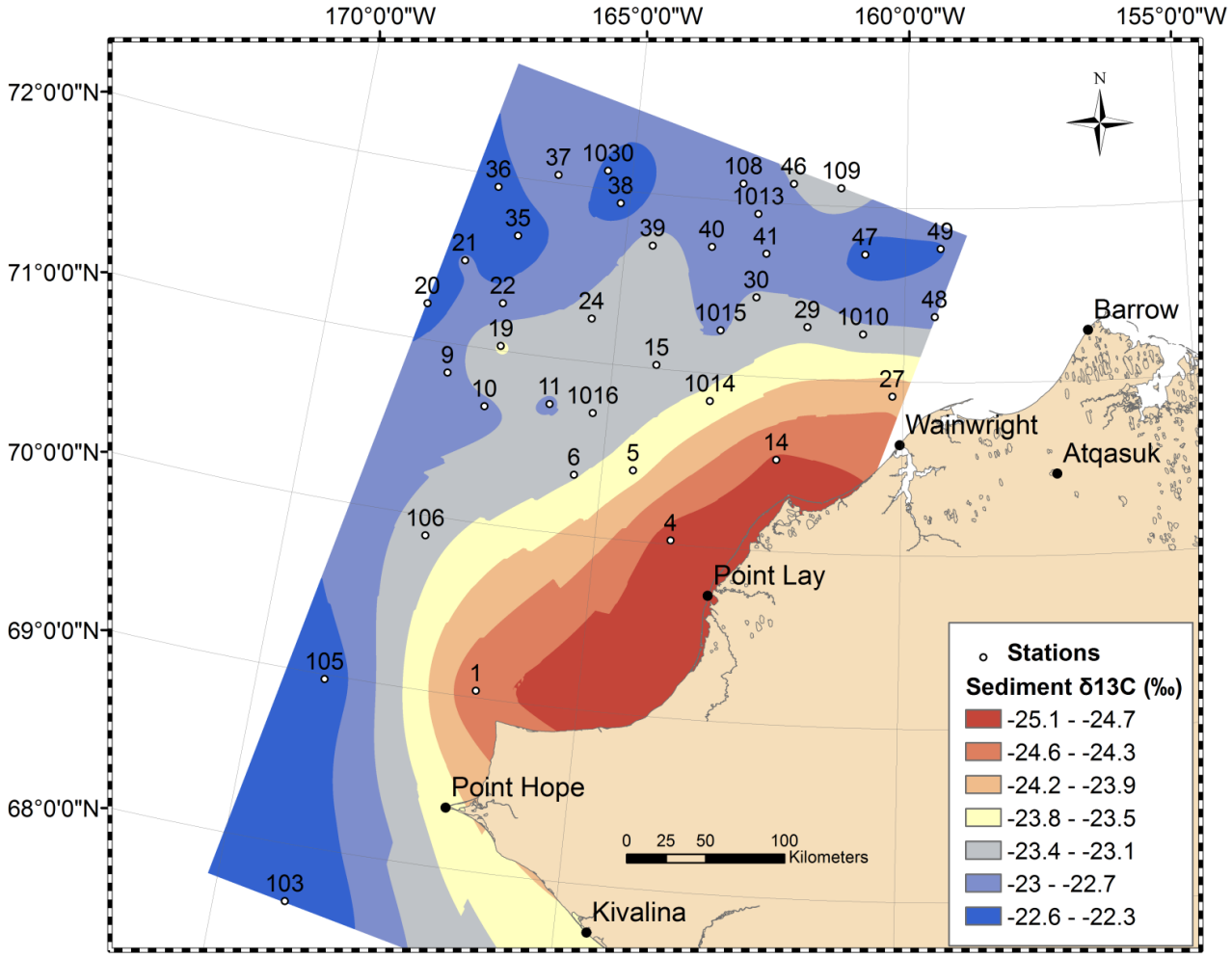

Figure 3.7. Interpolated $\delta^{13}C$ values of sedimentary organic matter within the study site. Numbers on map are stations. Color scheme represents gradient of $\delta^{13}C$ values (‰).

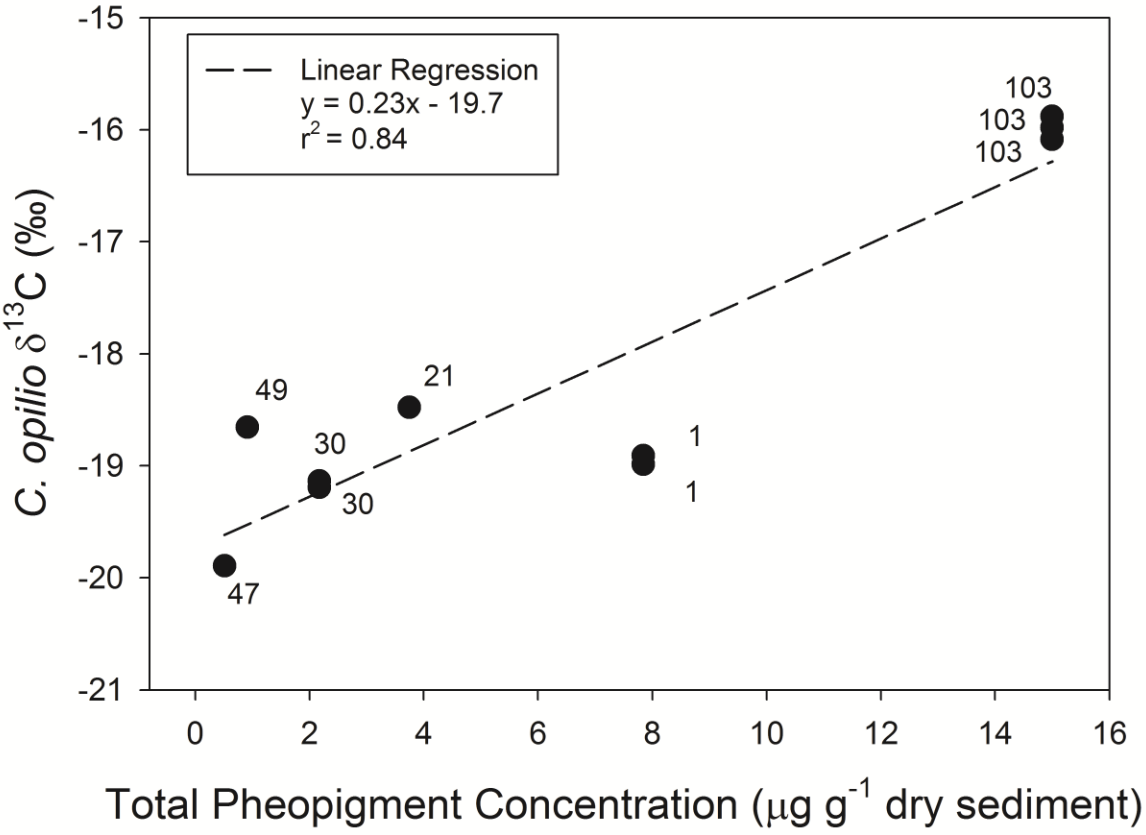

Figure 3.8. Relationship between *Chionoecetes oplio* $\delta^{13}C$ values and sedimentary pheopigments ($p<0.05$, $r=0.917$, $n=10$). Numbers next to data points are the stations where each individual was collected.

Chapter 4

Problems and revisions to the spectrophotometric equations to estimate chlorophyll *a* and pheophytin *a* in the marine environment: a perspective from sedimentary pigments

Abstract

The monochromatic spectrophotometric technique to determine chlorophyll *a* and pheophytin *a* concentrations is one of the most commonly applied technique in the marine environment. Nominal differences occurred when comparing chlorophyll *a* concentrations between the spectrophotometric technique and high-performance liquid chromatography (HPLC), a technique that chemically separates compounds prior to analysis. However, dramatic differences were noted when the two techniques measured pheophytin *a* in marine sediments. Various aspects of the method were assessed to determine improvements that would better reflect the values attained using HPLC. The minimal acid strength required to completely convert the chlorophyll *a* in a sample to pheophytin *a* was reassessed for sediment samples. By deriving the coefficients *K* and *R* from the chlorophyll and pheopigment equations, it was determined that the pheophytin *a* equation requires the coefficient ($K - 1$) instead of simply *K*. Independently determining *K* and *R* for each instrument as opposed to using the given values in the literature improved accuracy of spectrophotometric chlorophyll equation. The impacts of the chlorophyll:pheophytin ratio on the efficacy of the spectrophotometric equation to determine pigments was assessed, but there was no effect from pigment ratio using purified standards. It is hypothesized that pheophorbide *a*, another pheopigment common in marine sediments, interferes with the spectrophotometric reading since we did not find any issues with the method to measure purified standards, but it grossly overestimated pheophytin *a* from field samples.

1. Introduction

The monochromatic spectrophotometric equation developed by Lorenzen (1967) is one of the most commonly used methods to determine concentrations of chlorophyll *a* and one of its major degradation products pheophytin *a* in the marine environment, cited 1,998 times at the time of this writing (Thomson Reuters, 2013). The method prescribes the use of 750 nm (background) corrected absorbance readings at 665 nm before (665_o) and after (665_a) acidification to determine chlorophyll *a* and pheophytin *a* using the equations

$$\text{Chlorophyll } a \text{ (mg)} = A * K * (665_o - 665_a) \quad (1)$$

and

$$\text{Pheophytin } a \text{ (mg)} = A * K * [(R * 665_a) - 665_o] \quad (2)$$

where: *A*=the absorption coefficient of chlorophyll, 11.0; *K*=the factor to equate the reduction in absorbency to initial chlorophyll, 1.7/0.7, or 2.43; and *R*=the maximum ratio of 665_o:665_a in the absence of pheopigments, 1.7. The terms for volume of extract, volume of water filtered, and cuvette path length have been omitted since those terms are equal between the two equations.

The acidification step that the technique employs chemically converts all chlorophyll *a* to pheophytin *a* by removing the Mg^{2+} ion from chlorophyll *a* and replacing it with two hydrogen atoms (Lorenzen, 1967). The decrease in absorbance at 665 nm after chlorophyll *a* is reduced to pheophytin *a* post-acidification allows the deduction of both pigment concentrations despite the two compounds absorbing visible light at the same wavelength. Since this technique can discern chlorophyll *a* from chlorophyll degradation products (pheopigments), it is advantageous compared to others such as the trichromatic equation developed by Jeffrey and Humphrey (1975) that cannot decipher chlorophyll *a* from pheopigments and, subsequently, will overestimate

chlorophyll *a* in the presence of pheopigments. Despite the merits of a spectrophotometric technique that can rapidly and inexpensively estimate pigment concentrations, concerns have been reported with quantifying pheophytin *a* in field samples, especially sediments (Brown et al., 1981; Plante-Cuny et al., 1993; Brotas et al., 2007).

High-performance liquid chromatography (HPLC), which chemically separates compounds to measure their concentrations, generally produces chlorophyll *a* estimates that agree with monochromatic spectrophotometry. Pinckney et al. (1994) reported a 16% overestimation of chlorophyll by spectrophotometry compared to HPLC, but found a constant trend between the two ($r^2 = 0.99$). Daemen (1986) reported reliable, but overestimated chlorophyll by the monochromatic equation compared to HPLC (HPLC:spectrophotometer chlorophyll ratios = 0.70 ± 0.05). Plante-Cuny et al. (1993) found chlorophyll *a* estimations between HPLC and spectrophotometry similar, but pheophytin *a* concentrations in sediments were severely overestimated by spectrophotometry. Brotas et al. (2007) found similar results in sediments where spectrophotometry and HPLC approximated similar concentrations of chlorophyll *a* (slope of linear regression = 1.05; $r^2 = 0.91$), but the monochromatic equation calculated pheophytin *a* concentrations five times larger than HPLC in both muddy and sandy substrates. Brown et al. (1981) compared pigment estimations between fluorometry, spectrophotometry, and HPLC from sediment extractions. The authors found that spectrophotometry slightly overestimates chlorophyll *a* concentration compared to HPLC, but grossly overestimates pheophytin *a* by a factor of 3.75. If using spectrophotometric analysis to indicate the "freshness" of organic matter by chlorophyll:pheophytin ratios, an enlarged pheophytin value will cause understimation of the chlorophyll:pheophytin. Despite the myriad of discrepancies in reporting pheophytin *a* using spectrophotometry, most conclusions simply advise using the more laborious and expensive HPLC or thin layer chromatography (TLC) to assess more accurately pigment concentrations instead of examining potential corrections that can be applied to the spectrophotometric method. Moed and Hallegraeff (1978) addressed issues with the

method such as negative values computed from pheopigments, larger "acid ratios" than the prescribed 1.7 by Lorenzen (1967), and no literature consensus regarding acid strength, volume, and duration of treatment. The authors experimented with differing acid concentrations and found that complete conversion to pheophytin was achieved with a small volume of moderately dilute acid, but they did not test whether their prescribed acid concentrations resolved issues with reporting pheophytin by the monochromatic equation. The use of a minimum acid volume and strength is necessary since acid too concentrated (greater than 0.003 M in the sample) causes peak shifts in the absorbance spectrum and interference by accessory pigments like the acidified by-products of fucoxanthin (Riemann, 1978). One technique that showed promise to discriminate chlorophyll *a* and pheophytin *a* used a phase separation technique to isolate nonpolar compounds (chlorophyll *a* and pheophytin *a*) in hexane from polar compounds like pheophorbide *a*, chlorophyllide *a*, and other carotenoids that might cause interference with the spectrophotometric readings (Whitney and Darley, 1979). The successful execution of this method involved required determination of new values for the coefficients *K* and *R* for the hexane phase on their spectrophotometer.

Fluorometric determinations of sedimentary pigments have been proposed (e.g., Yentsch and Menzel, 1963; Tietjen, 1968), but the sensitivity of fluorometry results in dilutions factors ranging from 1:10,000 to 1:100,000 necessary to reach the linear detection limit of the instrument when measuring concentrated sedimentary photopigments compared to water column samples (Pinckney et al. 1994). Therefore, we did not consider fluorometry here.

The present investigation was undertaken to examine how the sedimentary pigment estimation by the monochromatic spectrophotometric equation could be improved to better reflect the estimations achieved by HPLC. Since, hypothetically, all chlorophyll *a* can be converted to pheophytin *a*, we assessed the mechanics of the monochromatic equation to provide explanation for the overestimation of pheophytin *a* in field samples. First, we independently assessed the strength of acid required to achieve complete conversion to pheophytin of a sediment extract. Next, we investigated the

relationship between monochromatic and HPLC estimation of chlorophyll *a* and pheophytin *a* (hereafter, chlorophyll and pheophytin). We assessed the monochromatic equation by deriving the equations to better grasp the given values of the constants *K* and *R* by Lorenzen (1967). We tested the hypothesis that the ratio of chlorophyll:pheophytin in a sample will result in a differing efficacy of the equation to estimate pigment concentration. Finally, we compared pigment concentrations obtained with the original equation to new values achieved with a revised equation and independently determined coefficients.

2. Methods

2.1 Sample collection

Sediment samples were collected from the Chukchi Sea, AK during the Chukchi Sea Offshore Monitoring in Drilling Areas-Chemical and Benthos (COMIDA-CAB) project in 2010 aboard the *R/V Moana Wave*. Sediments were collected using a 20 cm^3 syringe barrel (1.8 cm diameter, 2 cm depth) from intact, undisturbed surface sediments retrieved by a van Veen grab (0.1 m^2). Sediment aliquots were placed in pre-labeled polyethylene Falcon tubes (BD, USA) and immediately frozen in darkness to -20°C. Sediment was transported to the University of Texas Marine Science Institute (UTMSI, USA) and preserved at -80°C until prepared for pigment analysis.

2.2 Pigment extraction

Pigments were extracted from the sediments using 10 mL of 100% acetone since residual porewater in the sample dilutes the acetone concentration (Sun et al., 1991). Volume of porewater was determined and accounted for in extract volume. Samples were sonicated in chilled water for 15 min in darkness. After centrifuging samples for 5 min at 4000 rpm, supernatant was decanted and filtered through 0.2 μm nylon filters. To ensure the complete extraction of pigments from sediments in the event of solvent saturation, each sample was extracted twice and the extracts were combined. If the

combined extract was cloudy, the entire 20 mL was re-filtered through a 0.2 μm nylon filter.

2.3 Pigment estimation

One sub-sampled aliquot of supernatant was analyzed using spectrophotometry (Shimadzu UV-2401PC), including the entire spectrum from 750 to 400 nm. For the acidification step, HCl (Fisher Scientific, USA) was used and diluted to specific molarities with ultrapure water.

The HPLC pigment analysis followed protocol of DHI (DHI Water and Environment, Denmark). Briefly, a binary gradient of 28 mM tetrabuyl ammonium acetate (TBA) in methanol (30%:30%, v:v) (eluent A) and methanol (eluent B) was used. Eluant B was ramped from 5% to 95% in 22 min, and held for 7 min before falling back to 5% within 2 min. A C_8 HPLC column (Agilent Eclipse XDB, 3.5 μm, 4.6 mm x 150 mm) was used, and the eluted pigment was detected by UV-vis absorbance (wavelength = 450 nm). Concentrations were determined by comparing pigment peaks of equal retention time to those of certified commercial standards (DHI, VWR, and Sigma-Aldrich, USA).

2.4 Statistics

All statistics were computed in R 2.14.0 (www.r-project.org). Significance was set at $\alpha = 0.05$. When necessary for multiple comparisons, α was lowered according to a Bonferroni correction. For experiments that used chlorophyll and pheophytin standards, *n* for each method tested in each treatment (mixture of pigments) was 1. Replication of this experiment would allow us to put confidence limits around our values, but the volume of required pigment standards limited our experimental design. Instead of approaching this as differences between methods in each treatment (mixture of pigments), we employed a paired t-test to determine if there were differences overall between methods ($n = 5$). For field samples, $n = 39$.

3. Results

3.1 Effect of acid strength on sediment extracts

Sedimentary chloropigment extract was divided into four aliquots and subjected to different acid strengths to investigate if the concentration of acid recommended for water column samples causes complete pheophytinization in sediment extracts. Three acid treatments were used in 3 mL of extract: 90 μL of 0.1 M HCl (as prescribed by EPA Method 446), 30 μL of 0.5 M HCl, and 30 μL of 1.0 M HCl. There was no effect of acid strength on the sample (Figure 4.1). All acid treatments produced the same absorbance spectra, and the peak at ~665nm was reduced by about 50% compared to the control that contained chlorophyll. Therefore, the minimal acid strength we tested here was used throughout the rest of our analyses.

3.2 Effect of varying proportions of chlorophyll and pheophytin

Chlorophyll and pheophytin standard solutions were mixed, respectively, in 100:0, 75:25, 50:50, 25:75, and 0:100 proportions, and the absorbance spectrum was measured before and after acid treatment (Figure 4.2a,b). As the proportion of chlorophyll standard was decreased (and replaced by pheophytin), the absorbance at the red-end of the spectrum (660-680 nm) was proportionally reduced (Figure 4.2a). There was a minor right-shift in peak absorbance for chlorophyll from 662 nm for 100:0 to 665 nm for 0:100. Post-acidification, all five spectra, regardless of pigment proportions, were identical at the red-end of the spectrum indicating complete pheophytinization (Figure 4.2b). Our measured acid ratio (665_o:665_a for the chlorophyll standard) was 1.9.

A distinct shift of the blue absorption maximum of chlorophyll at 430 nm to the pheophytin absorption maximum at 410 nm was also observed as the ratio of the two pigments changed (Figure 4.1, 4.2a). The dissolution of the 430 nm peak was complete since pheophytin has almost no absorbance at the wavelength. The absorbance of chlorophyll at 410 nm is ~30% reduced from its absorbance at 430 nm, but the pheophytin absorbance at 410 nm is almost equal to that of chlorophyll at 430 nm.

Curiously, when the mixtures of standards were acid-treated, all absorption maxima were aligned at 410 nm but at slightly different intensities.

3.3 Equation derivation

Essentially, Lorenzen (1967) assumed that the absorbance at 665 nm before the acid treatment (665_o) was from two components: chlorophyll (*x*) and pheophytin (*y*). After acidification, the new absorbance at 665 nm (665_a) is composed of the original pheophytin component (*y*) unchanged from the acid treatment plus the newly formed pheophytin from the original chlorophyll (*x*), which is equivalent to the absorbance of chlorophyll reduced by the "acid ratio" *R*, or $\frac{x}{R}$. Therefore, we can derive the monochromatic equations from the following two equations:

$$x + y = 665_o \quad (3)$$

$$\frac{x}{R} + y = 665_a \quad (4)$$

By subtracting Equation 4 from Equation 3, we negate the *y* component to obtain the expression:

$665_o - 665_a = x - \frac{x}{R}$.

We isolated *x* in two steps:

$$665_o - 665_a = x\left(\frac{R}{R} - \frac{1}{R}\right)$$

$$(665_o - 665_a) * \frac{R}{R-1} = x$$

If using the value for *R* determined by Lorenzen (1967), we found that $\frac{R}{R-1}$ is $\frac{1.7}{0.7}$, or 2.43, which is the given value for the constant *K*. Therefore, the equation was simplified to:

$$x = K * (665_o - 665_a) \quad (5)$$

Equation 5 is identical to Equation 1 except that the absorption coefficient *A* has not yet been included. To derive the pheopigment equation, we solved for *y* with the newly derived *x* from Equation 5. First we rearranged Equation 3 to isolate *y*:

$$y = 665_o - x$$

Then we substituted *x* for its equivalent in Equation 5 to form

$$y = 665_o - K(665_o - 665_a).$$

Once *K* was distributed, we obtained

$$y = (1 - K)665_o + K(665_a),$$

which was rearranged so that 665_a is subtracted from 665_o:

$$y = K(665_a) - (K - 1)665_o.$$

Lastly, when the (*K* – 1) term was removed from 665_o, we found *y* expressed as

$$y = (K - 1) * (\left(\frac{K}{K-1}\right) * \ 665_a - 665_o). \quad (6)$$

If using the *K* value from Lorenzen (1967), then $\left(\frac{K}{K-1}\right)$ is $\frac{2.43}{2.43-1}$, or 1.7, the given value for *R*. Importantly, Equation 4 differed from Equation 2 provided by Lorenzen (1967). We derived a factor (*K* - 1) for the pheopigment equation versus Equation 2 that contains only *K*. Hereafter, the "revised" monochromatic equation for chlorophyll refers to Equation 1 with our independently determined *K*, and the "revised" monochromatic equation for pheophytin refers to Equation 6 with our independently determined *K* and *R*. For the revised equations, *R* = 1.9 and *K* = *R*/(*R*-1), or 2.12, based on our instrument and chlorophyll standard, and Equation 6 was used for pheophytin estimation.

3.4 Comparison of original and revised techniques to estimate pigment concentrations

The chlorophyll and pheophytin standards were mixed into five proportions (see prior section), and their concentrations were measured using HPLC and spectrophotometry. To compare pigment estimation techniques (i.e., original and revised monochromatic spectrophotometric equations, and HPLC), the "actual" concentration of pure chlorophyll and pheophytin standards were first determined using the the Beer-Lambert equation (A=ebc). The equation exploits the principle that pigment concentration (c) is related to the molar absorptivity of each compound (e), the path length of the cuvette (b), and the maximum absorbance at a specified wavelength (A). The molar absorptivity of a compound is equal to the molecular weight multiplied by the specific absorption coefficient of that molecule in a given solvent (α). In 90% acetone, α for chlorophyll is 87.7 $l \cdot g^{-1}$ cm^{-1} (Jeffrey and Humphrey, 1975) and the molecular weight is 893 g mol^{-1}. The molecular weight for pheophytin is 869 g mol^{-1} and α is 49.5 $l \cdot g^{-1}$ cm^{-1} (Lorenzen and Downs, 1986). Both the original equations for chlorophyll and pheophytin from Lorenzen (1967) with prescribed constants (*K* and *R*) were compared to the newly derived pheophytin equation with independently determined *K* and *R*.

Chlorophyll estimations using HPLC, the original monochromatic equation, and the revised monochromatic equations were not significantly different from the "actual" value determined by the Beer-Lambert equation for any of the mixtures of chlorophyll

and pheophytin standards (Figure 4.3a, Table 4.1). Both monochromatic equations produced positive, non-zero values for chlorophyll concentration in the 0:100 chlorophyll:pheophytin mixture.

For pheophytin estimation, HPLC and the revised monochromatic equation were not significantly different from the actual values determined by the Beer-Lambert equation (Figure 4.3b, Table 4.1). The original monochromatic equation from Lorenzen (1967) produced significantly different concentrations from actual values (Table 4.1). In the 100:0 chlorophyll:pheophytin mixture, negative pheophytin concentrations were computed using the original monochromatic equation (Figure 4.3b).

3.5 Chukchi Sea field samples

The original monochromatic equation, when applied to field samples, estimated chlorophyll moderately well based on a comparison of linear regressions (Figure 4.4a). Slight underestimation was observed for most samples that contained high chlorophyll concentrations, but the original monochromatic equation followed the trend of those values determined by HPLC analysis ($y = 0.76x + 0.16$; $r^2=0.78$). When values were recalculated with the independently derived *K*, the slope of the linear regression for the spectrophotometric and HPLC values became slightly shallower ($y = 0.66x + 0.14$; $r^2=0.78$). Chlorophyll values for both the original and modified equations were significantly different than the 1:1 curve (ANCOVA interaction term, $p<0.001$).

The original monochromatic equation grossly overestimated pheophytin concentrations in field samples (Figure 4.4b). The slope of the linear regression for the values computed by the original equation was 6.9, and most values were an order of magnitude larger than those determined by HPLC. Despite the large overestimation, values determined by the two techniques formed a linear correlation ($r^2=0.75$). However, when the revised equation with independently determined constants was applied to estimate pheophytin, the values were less overestimated (Figure 4.4b). A shallower slope of the regression (4.6) revealed a closer approximation and values correlated slightly better ($r^2=0.80$) than with the original values, but pheophytin was still overestimated.

4. Discussion

4.1 Errors associated with the monochromatic equation and suggested modifications

Significant errors were observed when spectrophotometry was used to determine the concentration of pigments from sediment field samples (Figure 4.4a,b). The errors were primarily in sediment samples since no significant differences were detected when both the original and revised monochromatic equations were used to determine the concentration of chlorophyll from purified standards (Table 4.1). Notably, both original and revised monochromatic equations reported positive values for chlorophyll when only pheophytin was present (0:100), whereas HPLC could detect differences because it chemically separates compounds before measuring absorbance (Figure 4.3a). The positive, non-zero values were perceived by the equations since absorbance of pure pheophytin changed from 0.047 to 0.044 after acidification. Hypothetically, this change in absorbance should not occur since the acid induces only the loss of the Mg^{2+} ion from the porphyrin ring of chlorophyll, which pheophytin already lacks. Nevertheless, this change in absorbance of 0.003 is greater than the instrumental analytical error. Otherwise, if no change in absorbance had occurred, then both spectrophotometric equations would report chlorophyll concentration of zero in the presence of pheophytin.

When only chlorophyll was present (100:0), HPLC and the revised monochromatic equation produced concentrations of zero for pheophytin, whereas the original monochromatic equation produced a negative value (Figure 4.3b). The spectrophotometric method relies on the "acid ratio" (R=665_o:665_a) to correct for the presence of pheophytin by accounting for the reduction in absorbance at 665 nm after acidification. For example, the absorbance of the chlorophyll standard prior to acidification (665_o) was 0.068. After acidification (665_a), when the standard was completely converted to pheophytin, the absorbance was reduced to 0.036. Therefore, after the "acid ratio" 665_o:665_a is multiplied by 665_a, then 665_o is obtained. In the case of pure chlorophyll, the difference of $(R * 665_a)$ and 665_o should be zero. However, negative values were observed when the prescribed "acid ratio" of 1.7 was used because

our measured 665_a of the chlorophyll standard multiplied by 1.7 was less than our measured 665_o (see Equation 2). Therefore, it is advisable to determine an "acid ratio" for each unique instrument ($R = 665_o:665_a$ for a chlorophyll standard) to prevent the determination of negative pigment values. HPLC estimation of pigments in 100:0 and 0:100 mixtures of standards detected only the presence of one pigment, unlike spectrophotometry. After examining the chromatograms from the HPLC analysis, chlorophyll and pheophytin were the only peaks present in all our samples during this experiment; thus we do not suspect interference from other pigments caused this unexpected error.

We also determined that accuracy is increased by considering the full absorbance spectrum, especially 600-667 nm, rather than making measurements at a single wavelength. By manually choosing absorption maxima, inaccuracy was reduced by 11-19%. In this study, pure chlorophyll had maximum absorbance at 662 nm versus 665 nm recommended by Lorenzen (1967) or 664 nm by Jeffrey and Humphrey (1975). The pheophytin standard had peak absorbance at 665 nm, so the mixtures with proportionally more pheophytin had a peak absorbance closer to 665 nm (e.g., for a 25:75 mixture, the maximum absorbance was at 664 nm). The peak absorbance for all acidified samples was also 665 nm, which matched the pheophytin standard.

Despite pheophytin and its parent molecule, chlorophyll, sharing an almost identical absorption maximum wavelength in the red spectrum, there was a spectral distinction in the blue spectrum between the two molecules (Figure 4.2a). The use of the blue spectrum to discriminate chlorophyll and pheophytin seems possible, but the accessory pigment fucoxanthin, a common biomarker for diatoms, absorbs between 410 and 430 nm (Riemann, 1978). The interference of fucoxanthin was apparent in our samples since the spectral behavior of our sediment extractions in the blue spectrum (Figure 4.1) was different than the spectra of purified standards that did not contain fucoxanthin (Figure 4.2a).

4.2 Pheophytin overestimation in sediment samples and potential causes

Despite the revisions suggested for the monochromatic equation, pheophytin concentrations in field samples were still severely overestimated compared to HPLC (Figure 4.4b). Chlorophyll concentrations in field samples were also in error as they were underestimated compared to HPLC (Figure 4.4a). Assuming that the proposed revision of the equation and the values for *K* and *R* are correct (see Results), then either the absorbance at 665_o or 665_a can be considered the source of the disparities in pigment concentrations. The conclusion is based on Equations 1 and 6, and indicates either an elevated reading of 665_a or a lower reading of 665_o could simultaneously cause an underestimation of chlorophyll and overestimation of pheophytin since 665_a is subtracted from 665_o in Equation 1 and 665_o is subtracted from $(R * 665_a)$ in Equation 6.

The possibility of an inflated 665_a term was pursued as the primary cause of the error since it is measured after chemical alterations have occurred to the sample. To evaluate this assumption, hypothetical values for 665_a were derived by setting Equation 6 equal to the value of pheophytin determined by HPLC (hereafter, 665_{an}). We found a range of values for 665_a:665_{an} (1.11 to 1.69) that demonstrated that 665_a was always overestimated in field samples. To determine the accuracy of these newly derived values, we used 665_{an} to recalculate the concentration of chlorophyll using Equation 1 with our independently determined *K*. When the new chlorophyll concentrations were regressed to the concentrations of chlorophyll determined by HPLC in sediment samples, a 1:1 relationship was found between the two estimations (Figure 4.5). This improved agreement between spectrophotometry and HPLC (compared to that for chlorophyll in Figure 4.4a) provides confidence that 665_a was overestimated during analysis.

Causes of the apparent overestimation of 665_a are beyond the scope of this study, although the molarity of acid used during acidification is not a factor (Figure 4.1). Some correlational data may provide the foundation of future studies to elucidate the causes of overestimated 665_a readings. Since there was no interference between HPLC and the revised monochromatic equation when using purified standards (Figure 4.3b), it is inferred that the issues that caused the overestimation of 665_a were related to sediment

characteristics and were likely related to interference by other compounds extracted by the acetone solvent. Of the pigments we measured during HPLC analysis of field samples, pheophorbide *a* (hereafter, pheophorbide) was found in appreciable concentrations and reflected pheophytin concentrations (Figure 4.6). Pheophorbide is a pheopigment oftentimes reported as one of the most common chlorophyll degradation products that can accumulate in sediments in the presence of herbivorous grazers (Daley, 1973; Bianchi et al., 1988). Like pheophytin, it does not possess the Mg^{2+} ion in the porphyrin ring, but additionally lacks the phytol chain common to both chlorophyll and pheophytin. Therefore, upon acidification, no change should occur to this molecule (Lorenzen, 1967). Spectrally, the specific absorption coefficient (α) for pheophorbide (69.8) is midway between that for chlorophyll (87.7) and pheophytin (49.5) (Lorenzen and Downs, 1986). Since α is positively related to the absorbance of a substance and acidification will not alter pheophorbide, a sample that contains pheophorbide will absorb at a greater maximum post-acidification than one that contains only chlorophyll and pheophytin, potentially overestimating 665_a. To demonstrate the possibility of pheophorbide interference, we regressed pheophorbide concentrations with the difference between 665_a and 665_{an}, which showed that every 1 μg of pheophorbide per gram of dry sediment will increase the absorbance of 665_a by 0.010 (Figure 4.7). Therefore, pheophorbide likely contributes to interference in 665_o.

By conducting experiments similar to ours that use chlorophyll, pheophytin, and pheophorbide standards, the interference of pheophorbide with 665_a could be experimentally determined. Since pheophorbide is unaltered during acidification because it does not contain the Mg^{2+} ion and its specific absorption coefficient is different than that of pheophytin at 665 nm, it may be impossible to correct for the presence of pheophorbide in Equations 1 and 6 without first knowing the concentration of pheophorbide in a sample. Therefore, the improvements to the monochromatic spectrophotometric equation suggested here can improve the accuracy chlorophyll and pheophytin measurements, but attention should be also directed toward the method itself based on the possibility that severe inaccuracies can occur in the presence of

pheophorbide. Other factors may also interfere with the spectrophotometric readings of sedimentary pigments that are related to the sediment matrix (e.g., the extraction of other compounds like humic substances); these effects too cannot be ruled out as contributing to the issues addressed here, and further study is needed.

In summary, for sediment pigment extracts, we found that a small volume of 0.1 M HCl (90 μL in 3 mL of sample, as recommended by EPA Method 446) was sufficient to completely convert all chlorophyll to pheophytin. We also derived the term ($K - 1$) for the pheophytin equation instead of only K. By independently measuring the "acid ratio" R for our instrument and standard, and subsequently, calculating K based on R, more accuracy was achieved for the monochromatic estimation of pheophytin. The ratio of chlorophyll:pheophytin did not alter the efficacy of the monochromatic equation. Based on that finding and our correlational data presented here, we hypothesize that pheophorbide may contribute to the inflated 665_a reading that causes severe overestimation of pheophytin.

Table 4.1. Results of paired t-tests comparing estimation techniques to actual concentrations determined by the Beer-Lambert equation (see Figure 3a-b). Since six pairwise comparisons were made, α was adjusted from 0.05 to 0.008 according to Bonferroni corrections. An asterisk notes significant differences.

Actual values compared to	Pigment	p-value
HPLC	Chlorophyll	0.056
Original monochromatic	Chlorophyll	0.021
Revised monochromatic	Chlorophyll	0.794
HPLC	Pheophytin	0.403
Original monochromatic	Pheophytin	0.002*
Revised monochromatic	Pheophytin	0.928

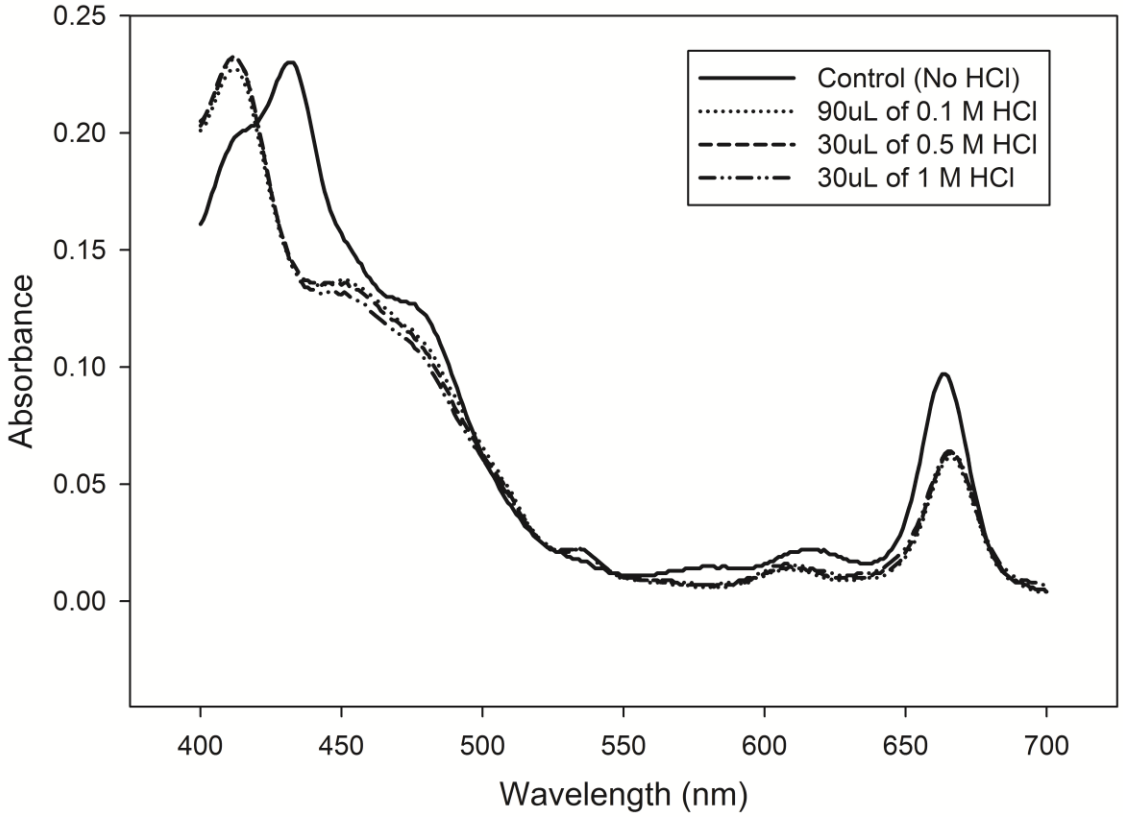

Figure 4.1. Absorption spectra of a sediment pigment control sample before (solid line) and after (dashed lines) acid treatment of different molarities.

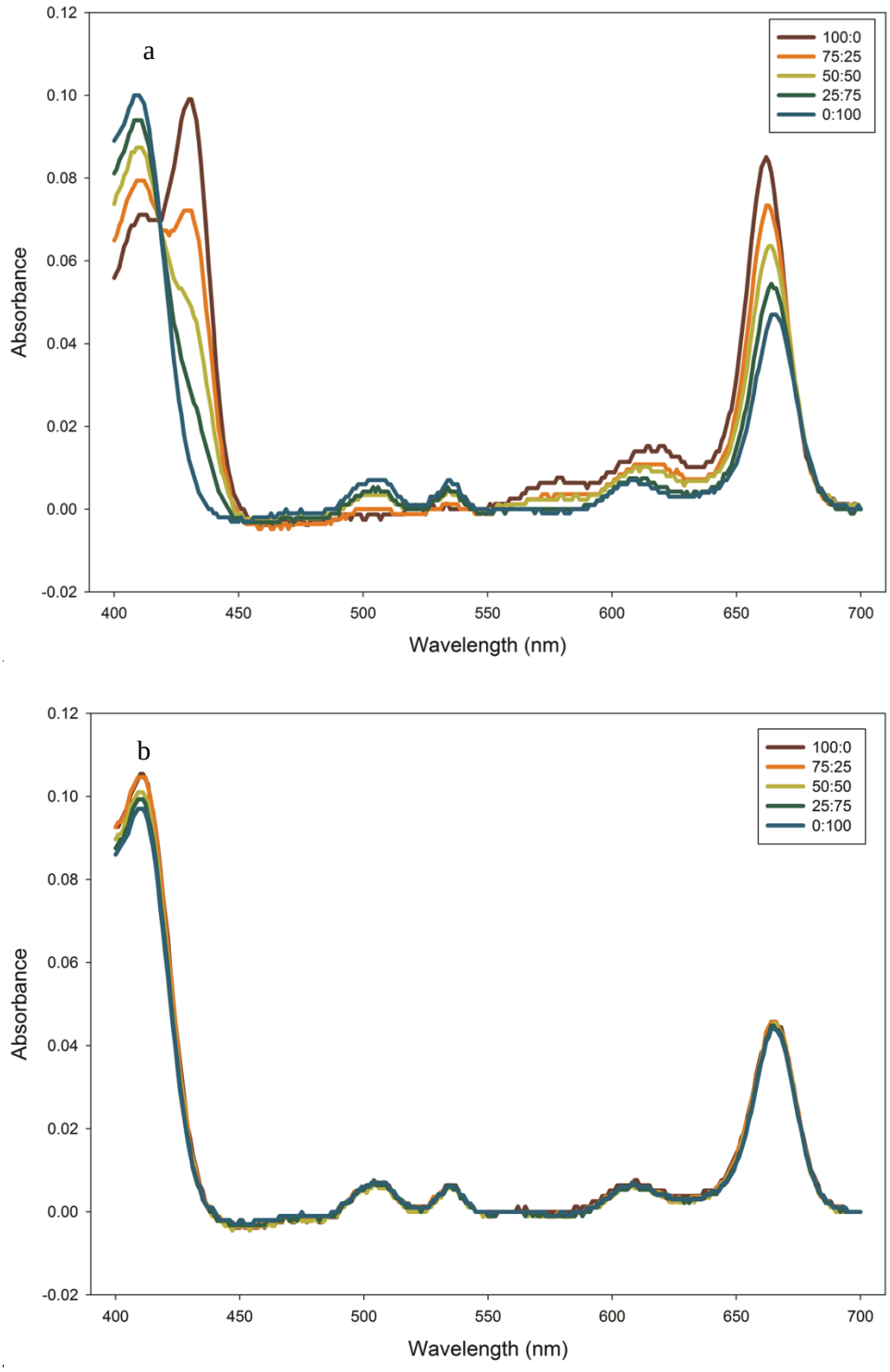

Figure 4.2. Absorption spectra of five mixtures of chlorophyll and pheophytin standards before (a) and after (b) acid treatment.

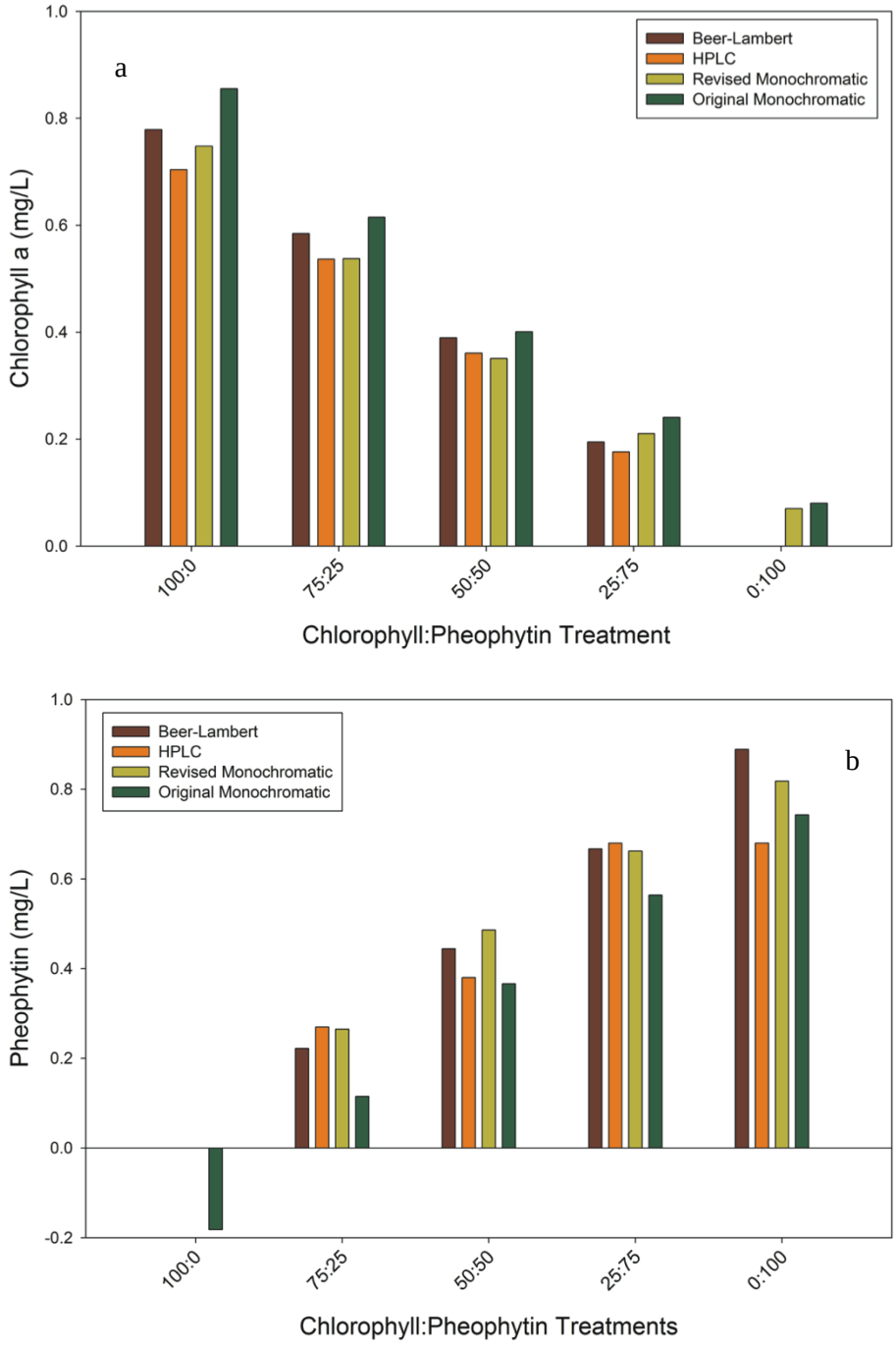

Figure 4.3. Concentrations of chlorophyll (a) and pheophytin (b) determined by the Beer-Lambert equation, HPLC, the revised monochromatic equation (using independently determined *K* for chlorophyll, and *K*, *R*, and Equation 6 for pheophytin), and the original monochromatic equations (Equations 1 and 2 for chlorophyll and pheophytin, respectively) with prescribed constants.

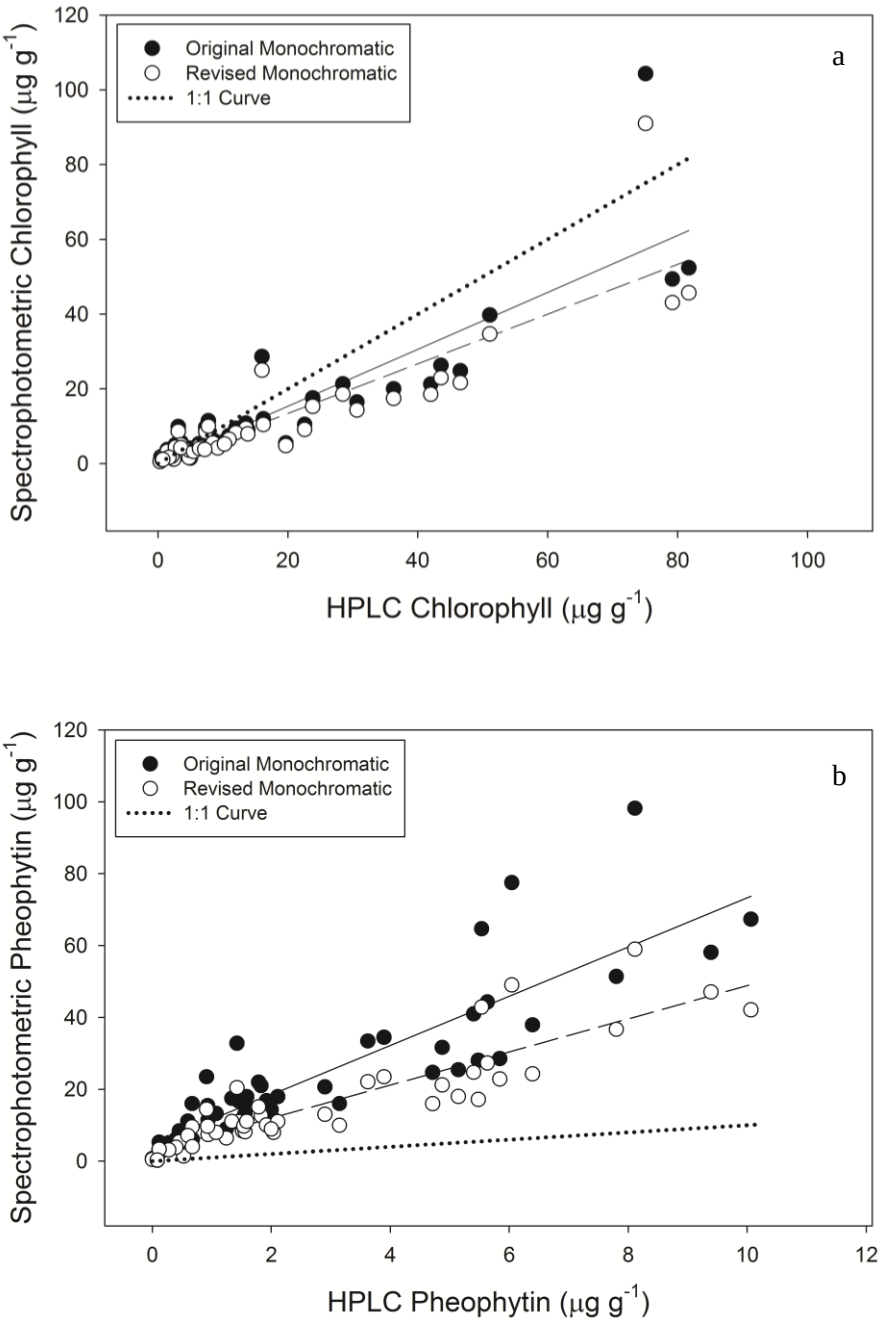

Figure 4.4. Comparison of concentrations determined by the original monochromatic equations (closed circles) and revised monochromatic equations (open circles) for chlorophyll (a) and pheophytin (b). The modified monochromatic values for chlorophyll were calculated with an independently determined *K*, and the modified monochromatic values for pheophytin were calculated with independently determined *K*, *R*, and Equation 6. Linear regressions for closed circles are solid lines. Linear regressions for open circles are dashed lines. 1:1 curves are dotted lines.

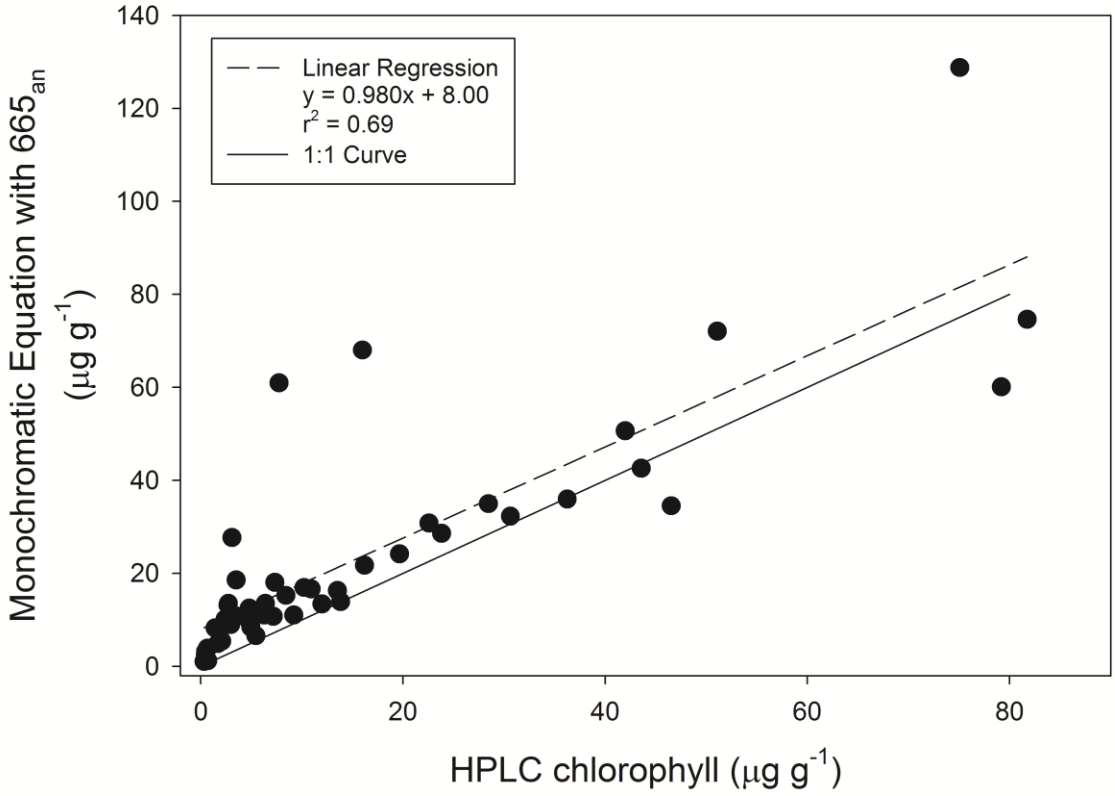

Figure 4.5. A 1:1 curve compared to a linear regression of chlorophyll concentrations determined by HPLC and recalculated chlorophyll concentrations using 665_{an}.

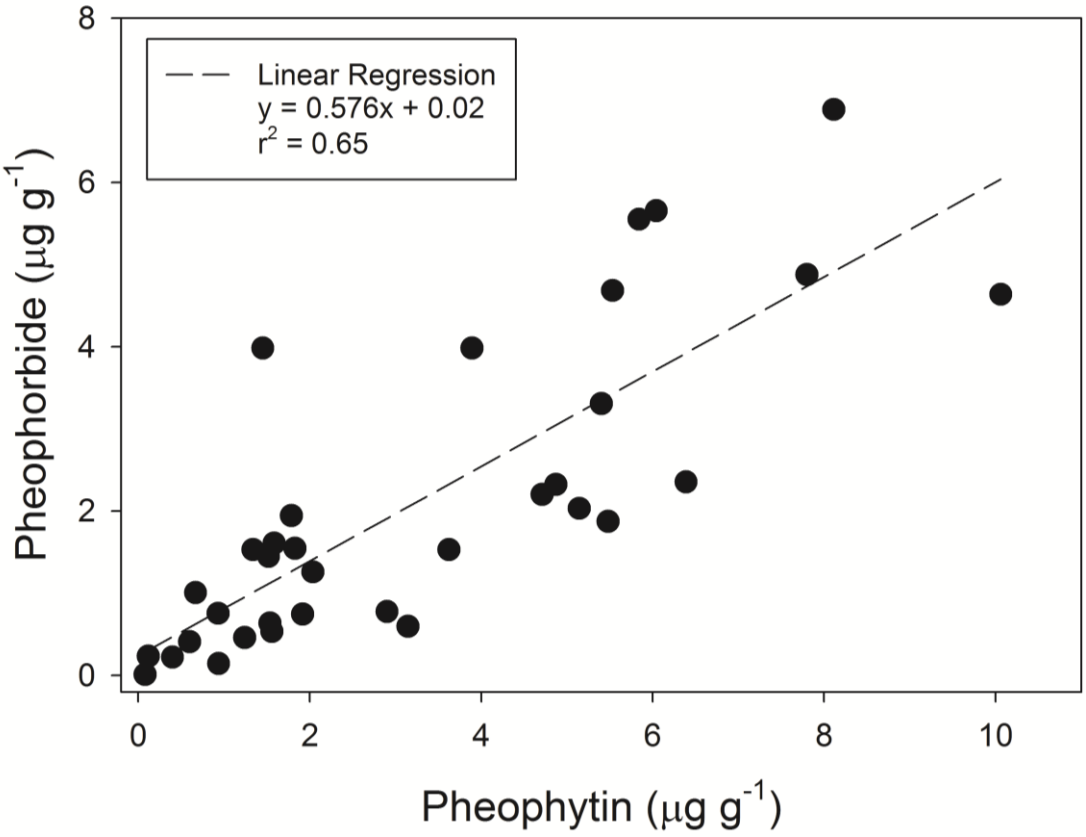

Figure 4.6. Linear regression of pheophytin and pheophorbide concentrations from sediment samples.

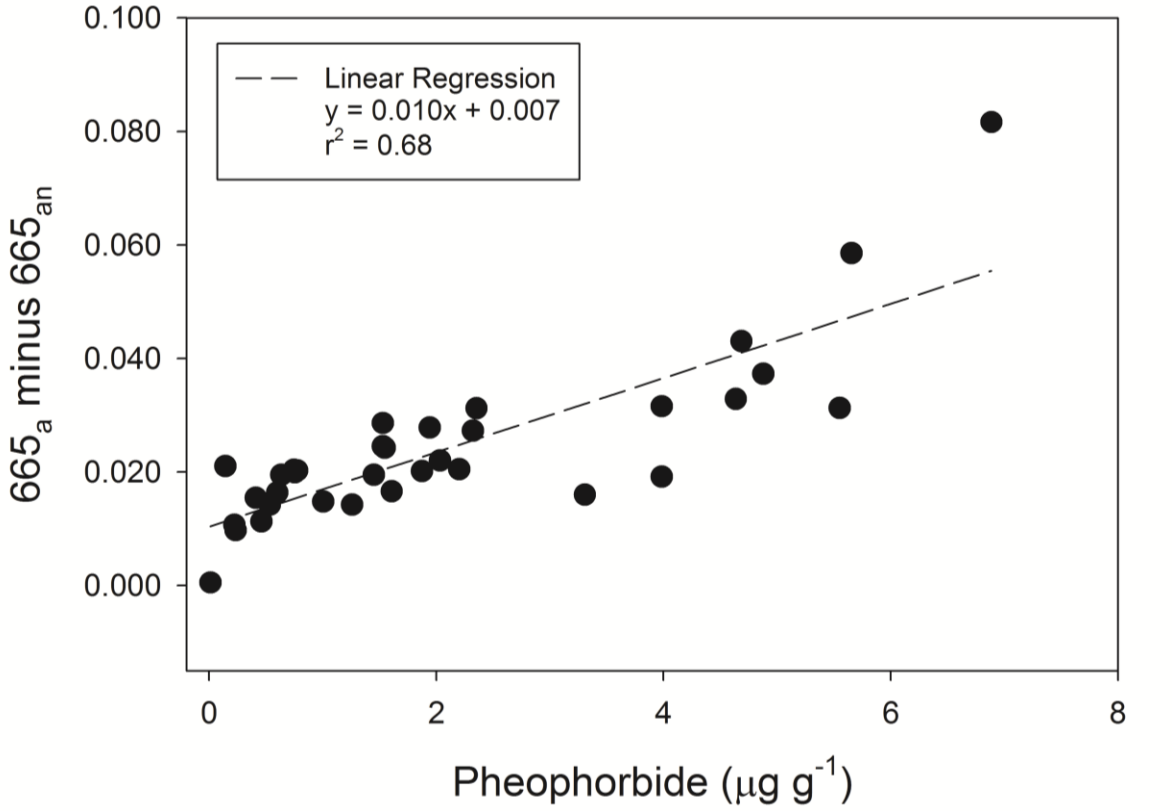

Figure 4.7. Linear regression of pheophorbide concentrations and the difference of 665_a and 665_{an}.

References

Abrantes, K., and Sheaves, M. (2009) Food web structure in a near-pristine mangrove area of the Australian Wet Tropics. *Estuar. Coast. Shelf Sci.*, 82, 597-607.

ACIA (2005). *Arctic Climate Impact Assessment*. Cambridge: Cambridge University Press.

Ambrose, W.G., Jr., and Renaud, P.E. (1995) Benthic response to water column productivity patterns: evidence for benthic-pelagic coupling in the Northeast Water Polynya. *Journal of Geophysical Research*, 100, 4411-4421.

Appeltans, W., Bouchet, P., Boxshall, G., De Broyer, C., de Voogd, N., Gordon, D., Hoeksema, B., Horton, T., Kennedy, M., Mees, J., Poore, G., Read, G., Stöhr, S., Walter, T., and Costello, M. (2012). World Register of Marine Species.

Arrigo, K.R., Perovich, D.K., Pickart, R.S., Brown, Z.W., van Dijken, G.L., Lowry, K.E., Mills, M.M., Palmer, M.A., Balch, W.M., Bahr, F., Bates, N.R., Benitez-Nelson, C., Bowler, B., Brownlee, E., Ehn, J.K., Frey, K.E., Garley, R., Laney, S.R., Lubelczyk, L., Mathis, J., Matsuoka, A., Mitchell, B.G., Moore, G.W.K., Ortega-Retuerta, E., Pal, S., Polashenski, C.M., Reynolds, R.A., Schieber, B., Sosik, H.M., Stephens, M., and Swift, J.H. (2012) Massive phytoplankton blooms under arctic sea ice. *Science*, 336, 1408-1408.

Arrigo, K.R., Van Dijken, G., and Pabi, S. (2008) Impact of a shrinking Arctic ice cover on marine primary production. *Geophys. Res. Lett.*, 35, L19603.

Bearhop, S., Adams, C.E., Waldron, S., Fuller, R.A., and Macleod, H. (2004) Determining trophic niche width: a novel approach using stable isotope analysis. *Journal of Animal Ecology*, 73, 1007-1012.

Bergmann, M., Dannheim, J., Bauerfeind, E., and Klages, M. (2009a) Trophic relationships along a bathymetric gradient at the deep-sea observatory HAUSGARTEN. *Deep-Sea Res. I*, 56, 408-424.

Bergmann, M., Dannheim, J., Bauerfeind, E., and Klages, M. (2009b) Trophic relationships along a bathymetric gradient at the deep-sea observatory HAUSGARTEN. *Deep-Sea Res Pt I*, 56, 408-424.

Bianchi, T.S., Dawson, R., and Sawangwong, P. (1988) The effects of macrobenthic deposit-feeding on the degradation of chloropigments in sandy sediments. *J. Exp. Mar. Biol. Ecol.*, 122, 243-255.

Blanchard, G.F. (1990) Overlapping microscale dispersion patterns of meiofauna and microphytobenthos. *Mar. Ecol. Prog. Ser.*, 68, 101-111.

Bluhm, B., Iken, K., Mincks Hardy, S., Sirenko, B., and Holladay, B. (2009) Community structure of epibenthic megafauna in the Chukchi Sea. *Aquat. Biol.*, 7, 269-293.

Bluhm, B.A., Gebruk, A.V., Gradinger, R., Hopcroft, R.R., Huettmann, F., Kosobokova, K.N., Sirenko, B.I., and Weslawski, J.M. (2011) Arctic marine biodiversity: an update of species richness and examples of biodiversity change. *Oceanography*, 24, 232-248.

Boetius, A., Albrecht, S., Bakker, K., Bienhold, C., Felden, J., Fernandez-Mendez, M., Hendricks, S., Katlein, C., Lalande, C., Krumpen, T., Nicolaus, M., Peeken, I.,

Rabe, B., Rogacheva, A., Rybakova, E., Somavilla, R., and Wenzhofer, F. (2013) Export of algal biomass from the melting arctic sea ice. *Science*, 339, 1430-1432.
Borja, A., Muxika, I., and Franco, J. (2003) The application of a Marine Biotic Index to different impact sources affecting soft-bottom benthic communities along European coasts. *Marine Pollution Bulletin*, 46, 835-845.
Brotas, V., Mendes, C.R., and Cartaxana, P. (2007) Microphytobenthic biomass assessment by pigment analysis: comparison of spectrophotometry and High Performance Liquid Chromatography methods. *Hydrobiologia*, 587, 19-24.
Brown, L.M., Hargrave, B.T., and MacKinnon, M.D. (1981) Analysis of chlorophyll *a* in sediments by high-pressure liquid chromatography. *Can. J. Fish. Aquat. Sci.*, 38, 205-214.
Budge, S.M., Wooller, M.J., Springer, A.M., Iverson, S.J., McRoy, C.P., and Divoky, G.J. (2008) Tracing carbon flow in an arctic marine food web using fatty acid-stable isotope analysis. *Oecologia*, 157, 117-129.
Cahoon, L.B. (1999). The role of benthic microalgae in neritic ecosystems. *Oceanography and Marine Biology, Vol 37*, Vol. 37 (pp. 47-86).
Carmack, E., Macdonald, R., and Jasper, S. (2004) Phytoplankton productivity on the Canadian Shelf of the Beaufort Sea. *Mar. Ecol. Prog. Ser.*, 277, 37-50.
Carmack, E., and Wassmann, P. (2006) Food webs and physical-biological coupling on pan-Arctic shelves: Unifying concepts and comprehensive perspectives. *Prog Oceanogr*, 71, 446-477.
Carman, K.R., Fleeger, J.W., and Pomarico, S.M. (1997) Response of a benthic food web to hydrocarbon contamination. *Limnol. Oceanog.*, 42, 561-571.
Cartaxana, P., Jesus, B., and Brotas, V. (2003) Pheophorbide and pheophytin a-like pigments as useful markers for intertidal microphytobenthos grazing by Hydrobia ulvae. *Estuar. Coast. Shelf Sci.*, 58, 293-297.
Cavalieri, D.J., Parkinson, C.L., Gloersen, P., and Zwally, H.J. (2009). Sea Ice Concentration from Nimus-7 SMMR and DMSP SSM/I-SSMIS Passive Microwave Data, 05/01/2009-07/31/2009. Boulder, Colorado USA: National Snow and Ice Data Center.
Cavalieri, D.J., Parkinson, C.L., Gloersen, P., and Zwally, H.J. (2010). Sea Ice Concentration from Nimus-7 SMMR and DMSP SSM/I-SSMIS Passive Microwave Data, 05/01/2010-07/31/2010. Boulder, Colorado USA: National Snow and Ice Data Center.
Chanton, J.P., Cherrier, J., Wilson, R.M., Sarkodee-Adoo, J., Bosman, S., Mickle, A., and Graham, W.M. (2012) Radiocarbon evidence that carbon from the Deepwater Horizon spill entered the planktonic food web of the Gulf of Mexico. *Environmental Research Letters*, 7.
Clough, L.M., Renaud, P.E., and Ambrose, W.G. (2005) Impacts of water depth, sediment pigment concentration, and benthic macrofaunal biomass on sediment oxygen demand in the western Arctic Ocean. *Can. J. Fish. Aquat. Sci.*, 62, 1756-1765.
Coachman, L.K., Aagaard, K., and Tripp, R.B. (1975). *Bering Strait: The regional physical oceanography*. Seattle: University of Washington Press.

Coffin, R.B., Velinsky, D.J., Devereux, R., Price, W.A., and Cifuentes, L.A. (1990) Stable carbon isotope analysis of nucleic-acids to trace sources of dissolved substrates used by estuarine bacteria. *Appl. Environ. Microbiol.*, 56, 2012-2020.

Cooper, L.W., Lalande, C., Pirtle-Levy, R., Larsen, I.L., and Grebmeier, J.M. (2009) Seasonal and decadal shifts in particulate organic matter processing and sedimentation in the Bering Strait Shelf region. *Deep-Sea Res. II*, 56, 1316-1325.

Cota, G.F., Pomeroy, L.R., Harrison, W.G., Jones, E.P., Peters, F., Sheldon, W.M., and Weingartner, T.R. (1996) Nutrients, primary production and microbial heterotrophy in the southeastern Chukchi Sea: Arctic summer nutrient depletion and heterotrophy. *Mar. Ecol. Prog. Ser.*, 135, 247-258.

Coull, B.C., and Chandler, G.T. (1992) Pollution and meiofauna - field, laboratory, and mesocosm studies. *Oceanography and Marine Biology*, 30, 191-271.

Coyle, K.O., and Cooney, R.T. (1988) Estimating carbon flux to pelagic grazers in the ice-edge zone of the eastern Bering Sea. *Mar. Biol.*, 98, 299-306.

Coyle, K.O., and Pinchuk, A.I. (2002) Climate-related differences in zooplankton density and growth on the inner shelf of the southeastern Bering Sea. *Prog. Oceanogr.*, 55, 177-194.

Crawford, R.E., and Jorgenson, J.K. (1993) Schooling behavior of arctic cod, *Boreogadus saida*, in relation to drifting pack ice. *Envir. Biol. Fish.*, 36, 345-357.

Currin, C.A., Newell, S.Y., and Paerl, H.W. (1995) The role of standing dead *Spartina alterniflora* and benthic microalgae in salt marsh food webs - considerations based on multiple stable isotope analysis. *Mar. Ecol. Prog. Ser.*, 121, 99-116.

Daemen, E. (1986) Comparison of methods for the determination of chlorophyll in estuarine sediments. *Netherlands Journal of Sea Research*, 20, 21-28.

Daley, R.J. (1973) Experimental characterization of lacustrine chlorophyll diagenesis .ii. bacterial, viral and herbivore grazing effects. *Archiv fur Hydrobiologie*, 72, 409-439.

Davies, J.M., Addy, J.M., Blackman, R.A., Blanchard, J.R., Ferbrache, J.E., Moore, D.C., Somerville, H.J., Whitehead, A., and Wilkinson, T. (1984) Environmental effects of the use of oil-based drilling muds in the North Sea. *Marine Pollution Bulletin*, 15, 363-370.

Dayton, P.K., Watson, D., Palmisano, A., Barry, J.P., Oliver, J.S., and Rivera, D. (1986) Distribution patterns of benthic microalgal standing stock at McMurdo Sound, Antarctia. *Polar Biol.*, 6, 207-213.

de Jonge, V.N. (1979) Quantitative separation of benthic diatoms from sediments using density gradient centrifugation in the colloidal silica Ludox-TM. *Mar. Biol.*, 51, 267-278.

Deegan, L.A., and Garritt, R.H. (1997) Evidence for spatial variability in estuarine food webs. *Mar. Ecol. Prog. Ser.*, 147, 31-47.

DeNiro, M., and Epstein, S. (1978) Influence of diet on distribution of carbon isotopes in animals. *Geochim. Cosmochim. Acta*, 42, 495-506.

DeNiro, M., and Epstein, S. (1981) Influence of diet on the distribution of nitrogen isotopes in animals. *Geochim. Cosmochim. Acta*, 45, 341-351.

Dennard, S.T., McMeans, B.C., and Fisk, A.T. (2009) Preliminary assessment of Greenland halibut diet in Cumberland Sound using stable isotopes. *Polar Biol.*, 32, 941-945.

Doi, H., Kikuchi, E., Shikano, S., and Takagi, S. (2010) Differences in nitrogen and carbon stable isotopes between planktonic and benthic microalgae. *Limnology*, 11, 185-192.

Dubois, S., Jean-Louis, B., Bertrand, B., and Lefebvre, S. (2007) Isotope trophic-step fractionation of suspension-feeding species: Implications for food partitioning in coastal ecosystems. *J. Exp. Mar. Biol. Ecol.*, 351, 121-128.

Dunton, K.H. (2001) delta N-15 and delta C-13 measurements of Antarctic peninsula fauna: Trophic relationships and assimilation of benthic seaweeds. *American Zoologist*, 41, 99-112.

Dunton, K.H., Goodall, J.L., Schonberg, S.V., Grebmeier, J.M., and Maidment, D.R. (2005) Multi-decadal synthesis of benthic-pelagic coupling in the western arctic: Role of cross-shelf advective processes. *Deep-Sea Res. II*, 52, 3462-3477.

Dunton, K.H., Saupe, S.M., Golikov, A.N., Schell, D.M., and Schonberg, S.V. (1989) Trophic relationships and isotopic gradients among arctic and subarctic marine fauna. *Mar. Ecol. Prog. Ser.*, 56, 89-97.

Dunton, K.H., and Schell, D.M. (1987) Dependence of consumers on macroalgal (*Laminaria solidungula*) carbon in an arctic kelp community - $\delta^{13}C$ evidence. *Mar. Biol.*, 93, 615-625.

Dunton, K.H., Schonberg, S.V., and Cooper, L.W. (2012) Food Web Structure of the Alaskan Nearshore Shelf and Estuarine Lagoons of the Beaufort Sea. *Estuaries. Coast.*, 35, 416-435.

Ellers, O., and Telford, M. (1984) Collection of food by oral-surface podia in the sand dollar, *Echinarachnius-parma* (Lamarck). *Biol. Bull.*, 166, 574-582.

Engelsen, O., Hegseth, E.N., Hop, H., Hansen, E., and Falk-Petersen, S. (2002) Spatial variability of chlorophyll-a in the Marginal Ice Zone of the Barents Sea, with relations to sea ice and oceanographic conditions. *J. Mar. Syst.*, 35, 79-97.

Fanelli, E., Cartes, J.E., Badalamenti, F., Rumolo, P., and Sprovieri, M. (2009a) Trophodynamics of suprabenthic fauna on coastal muddy bottoms of the southern Tyrrhenian Sea (western Mediterranean). *Journal of Sea Research*, 61, 174-187.

Fanelli, E., Cartes, J.E., Rumolo, P., and Sprovieri, M. (2009b) Food-web structure and trophodynamics of mesopelagic–suprabenthic bathyal macrofauna of the Algerian Basin based on stable isotopes of carbon and nitrogen. *Deep-Sea Res. I*, 56, 1504-1520.

Feder, H.M., and Blanchard, A. (1998) The deep benthos of Prince William Sound, Alaska, 16 months after the Exxon Valdez oil spill. *Marine Pollution Bulletin*, 36, 118-130.

Feder, H.M., Iken, K., Blanchard, A.L., Jewett, S.C., and Schonberg, S. (2011) Benthic food web structure in the southeastern Chukchi Sea: an assessment using $\delta^{13}C$ and $\delta^{15}N$ analyses. *Polar Biol.*, 34, 521-532.

Fisk, A.T., Hobson, K.A., and Norstrom, R.J. (2001) Influence of chemical and biological factors on trophic transfer of persistent organic pollutants in the

northwater polynya marine food web. *Environmental Science & Technology*, 35, 732-738.

Fourqurean, J.W., Moore, T.O., Fry, B., and Hollibaugh, J.T. (1997) Spatial and temporal variation in C:N:P ratios, delta N-15 and delta C-13 of eelgrass Zostera marina as indicators of ecosystem processes, Tomales Bay, California, USA. *Mar. Ecol. Prog. Ser.*, 157, 147-157.

Fox, A.L., Hughes, E.A., Trocine, R.P., Trefry, J.H., Schonberg, S.V., McTigue, N.D., Lasorsa, B.K., Konar, B., and Cooper, L.W. (in press) Mercury in the northeastern Chukchi Sea: Distribution patterns in seawater and sediments and biomagnification in the benthic food web. *Deep-Sea Res. II*.

France, R., Chandler, M., and Peters, R. (1998) Mapping trophic continua of benthic foodwebs: body size -15N relationships. *Mar. Ecol. Prog. Ser.*, 174, 301-306.

France, R.L. (1995) Carbon-13 enrichment in benthic compared to planktonic algae: foodweb implications. *Mar. Ecol. Prog. Ser.*, 124, 307-312.

Fry, B., Joern, A., and Parker, P.L. (1978) Grasshopper food web analysis - use of carbon isotope ratios to examine feeding relationships among terrestrial herbivores. *Ecology*, 59, 498-506.

Fry, B., and Sherr, E.B. (1984) $\delta^{13}C$ measurements as indicators of carbon flow in marine and freshwater ecosystems. *Contrib. Mar. Sci.*, 27, 13-47.

Gattuso, J.P., Gentili, B., Duarte, C.M., Kleypas, J.A., Middelburg, J.J., and Antoine, D. (2006) Light availability in the coastal ocean: impact on the distribution of benthic photosynthetic organisms and their contribution to primary production. *Biogeosciences*, 3, 489-513.

Gautier, D.L., Bird, K.J., Charpentier, R.R., Grantz, A., Houseknecht, D.W., Klett, T.R., Moore, T.E., Pitman, J.K., Schenk, C.J., Schuenemeyer, J.H., Sorensen, K., Tennyson, M.E., Valin, Z.C., and Wandrey, C.J. (2009) Assessment of undiscovered oil and gas in the Arctic. *Science*, 324, 1175-1179.

Gilbert, N.S. (1991) Primary production by benthic microalgae in nearshore marine sediments of Signy Island, Antarctica. *Polar Biol.*, 11, 339-346.

Gillies, C.L., Stark, J.S., Johnstone, G.J., and Smith, S.D.A. (2012) Carbon flow and trophic structure of an Antarctic coastal benthic community as determined by $\delta^{13}C$ and $\delta^{15}N$. *Estuar. Coast. Shelf Sci.*, 97, 44-57.

Glud, R.N., Kuhl, M., Wenzhofer, F., and Rysgaard, S. (2002) Benthic diatoms of a high Arctic fjord (Young Sound, NE Greenland): importance for ecosystem primary production. *Mar. Ecol. Prog. Ser.*, 238, 15-29.

Glud, R.N., Woelfel, J., Karsten, U., Kuhl, M., and Rysgaard, S. (2009) Benthic microalgal production in the Arctic: applied methods and status of the current database. *Botanica Marina*, 52, 559-571.

Gomez, I., Wulff, A., Roleda, M.Y., Huovinen, P., Karsten, U., Quartino, M.L., Dunton, K., and Wiencke, C. (2009) Light and temperature demands of marine benthic microalgae and seaweeds in polar regions. *Botanica Marina*, 52, 593-608.

Gradinger, R. (2009) Sea-ice algae: Major contributors to primary production and algal biomass in the Chukchi and Beaufort Seas during May/June 2002. *Deep-Sea Res. II*, 56, 1201-1212.

Gradinger, R., Kaufman, M., and Bluhm, B. (2009). Pivotal role of sea ice sediments in the seasonal development of near-shore Arctic fast ice biota. *Mar. Ecol. Prog. Ser.*, Vol. 394 (pp. 49-63).

Graeve, M., Kattner, G., and Piepenburg, D. (1997) Lipids in Arctic benthos: Does the fatty acid and alcohol composition reflect feeding and trophic interactions? *Polar Biol.*, 18, 53-61.

Grebmeier, J.M., and Barry, J.P. (1991) The influence of oceanographic processes on pelagic-benthic coupling in polar regions: A benthic perspective. *J. Mar. Syst.*, 2, 495-518.

Grebmeier, J.M., and Cooper, L.W. (2012). Water column chlorophyll, benthic infauna and sediment markers. In K.H. Dunton, *Chukchi Sea Offshore Monitoring in Drilling Area (COMIDA): Chemical and Benthos (CAB) Final Report* (pp. 103-142). Port Aransas: Univeristy of Texas Marine Science Institute.

Grebmeier, J.M., Cooper, L.W., Feder, H.M., and Sirenko, B.I. (2006) Ecosystem dynamics of the Pacific-influenced northern Bering, Chukchi, and East Siberian Seas. *Prog. Oceanogr.*, 71, 331-361.

Grebmeier, J.M., Feder, H.M., and McRoy, C.P. (1989) Pelagic-benthic coupling on the shelf of the northern Bering and Chukchi Seas. II. Benthic community structure. *Mar. Ecol. Prog. Ser.*, 51, 253-268.

Grebmeier, J.M., McRoy, C.P., and Feder, H.M. (1988) Pelagic-Benthic Coupling on the Shelf of the Northern Bering and Chukchi Seas .I. Food-Supply Source and Benthic Biomass. *Mar. Ecol. Prog. Ser.*, 48, 57-67.

Hallegraeff, G.M. (1981) Seasonal study of phytoplankton pigments and species at a coastal station off Sydney - importance of diatoms and the nanoplankton. *Mar. Biol.*, 61, 107-118.

Hammerschlag-Peyer, C.M., Yeager, L.A., Araujo, M.S., and Layman, C.A. (2011) A hypothesis-testing framework for studies investigating ontogenetic niche shifts using stable isotope ratios. *PLoS One*, 6.

Hansen, J., and Josefson, A. (2004) Ingestion by deposit-feeding macro-zoobenthos in the aphotic zone does not affect the pool of live pelagic diatoms in the sediment. *J. Exp. Mar. Biol. Ecol.*, 308, 59-84.

Hansen, J.L.S., and Josefson, A.B. (2001) Pools of chlorophyll and live planktonic diatoms in aphotic marine sediments. *Mar. Biol.*, 139, 289-299.

Hargrave, B.T., Walsh, I.D., and Murray, D.W. (2002) Seasonal and spatial patterns in mass and organic matter sedimentation in the North Water. *Deep-Sea Res. II*, 49, 5227-5244.

Hawkins, A.J.S., Bayne, B.L., Mantoura, R.F.C., Llewellyn, C.A., and Navarro, E. (1986) Chlorophyll degradation and absorption throughout the digestive system of the blue mussel *Mytilus edulis J. Exp. Mar. Biol. Ecol.*, 96, 213-223.

Hecky, R.E., and Hesslein, R.H. (1995) Contributions of benthic algae to lake food webs as revealed by stable isotope analysis. *Journal of the North American Benthological Society*, 14, 631-653.

Helling, G.R., and Baars, M.A. (1985) Changes of the concentrations of chlorophyll and phaeopigment in grazing experiments. *Hydrobiological Bulletin*, 19, 41-48.

Hennig, C. (2010) Methods for merging Gaussian mixture components. *Adv. Data Anal. Classif.*, 4, 3-34.

Herman, P.M.J., Middelburg, J.J., Widdows, J., Lucas, C.H., and Heip, C.H.R. (2000) Stable isotopes as trophic tracers: combining field sampling and manipulative labelling of food resources for macrobenthos. *Mar. Ecol. Prog. Ser.*, 204, 79-92.

Highsmith, R.C., Coyle, K.O., Bluhm, B.A., Konar, B. (2006). Gray whales in the Bering and Chukchi Seas. In J.A. Estes, DeMaster, D.P., Doak, D.F., Williams, T.M., Brownell, R.L., *Whales, Whaling and Ocean Ecosystems* (pp. 303-313). Berkeley: University of California Press.

Hill, V., Cota, G., and Stockwell, D. (2005) Spring and summer phytoplankton communities in the Chukchi and Eastern Beaufort Seas. *Deep-Sea Res. Part II-Top. Stud. Oceanogr.*, 52, 3369-3385.

Hjorth, M., Vester, J., Henriksen, P., Forbes, V., and Dahllof, I. (2007) Functional and structural responses of marine plankton food web to pyrene contamination. *Mar. Ecol. Prog. Ser.*, 338, 21-31.

Hobson, K.A., Fisk, A.T., Karnovsky, N., Holst, M., Gagnon, J.-M., and Fortier, M. (2002) A stable isotope ($\delta^{13}C$, $\delta^{15}N$) model for the North Water food web: implications for evaluating trophodynamics and the flow of energy and contaminants. *Deep-Sea Res. II*, 49, 5131-5150.

Hobson, K.A., and Welch, H.E. (1992) Determination of trophic relationships within a high arctic marine food web using $\delta^{13}C$ and $\delta^{15}N$ analysis. *Mar. Ecol. Prog. Ser.*, 84, 9-18.

Hoch, M.P., Fogel, M.L., and Kirchman, D.L. (1994) Isotope Fractionation During Ammonium Uptake By Marine Microbial Assemblages. *Geomicrobiol. J.*, 12, 113-127.

Hoekstra, P.F., O'Hara, T.M., Fisk, A.T., Borga, K., Solomon, K.R., and Muir, D.C.G. (2003) Trophic transfer of persistent orgranochlorine contaminants (OCs) within an Arctic marine food web from the southern Beaufort-Chukchi Seas. *Environ. Pollut.*, 124, 509-522.

Horner, R., and Schrader, G.C. (1982) Relative contributions of ice algae, phytoplankton and benthic microalgae to primary production in nearshore regions of the Beaufort Sea. *Arctic*, 35, 485-503.

Iken, K., and 405 (2001) Food web structure of the benthic community at the Porcupine Abyssal Plain (NE Atlantic): a stable isotope analysis. *Prog. Oceanogr.*, 50, 383-405.

Iken, K., Bluhm, B., and Dunton, K. (2010) Benthic food-web structure under differing water mass properties in the southern Chukchi Sea. *Deep-Sea Res. II*, 57, 71-85.

Iken, K., Bluhm, B.A., and Gradinger, R. (2005) Food web structure in the high Arctic Canada Basin: evidence from $\delta^{13}C$ and $\delta^{15}N$ analysis. *Polar Biol.*, 28, 238-249.

Jakobsson, M. (2002) Hypsometry and volume of the Arctic Ocean and its constituent seas. *Geochemistry Geophysics Geosystems*, 3, 1-18.

Jardine, T.D., Kidd, K.A., and Fisk, A.T. (2006) Applications, considerations, and sources of uncertainty when using stable isotope analysis in ecotoxicology. *Environmental Science & Technology*, 40, 7501-7511.

Jeffrey, S.W., and Humphrey, G.F. (1975) New spectrophotometric equations for determining chlorophylls a, b, c1 and c2 in higher-plants, algae and natural phytoplankton. *Biochemie Und Physiologie Der Pflanzen*, 167, 191-194.

Jensen, L.K., and Carroll, J. (2010) Experimental studies of reproduction and feeding for two Arctic-dwelling *Calanus* species exposed to crude oil. *Aquatic Biology*, 10, 261-271.

Jepsen, D.B., and Winemiller, K.O. (2002) Structure of tropical river food webs revealed by stable isotope ratios. *Oikos*, 96, 46-55.

Kahru, M., Brotas, V., Manzano-Sarabia, M., and Mitchell, B.G. (2011) Are phytoplankton blooms occurring earlier in the Arctic? *Glob. Change Biol.*, 17, 1733-1739.

Karsten, U., Schumann, R., Rothe, S., Jung, I., and Medlin, L. (2006) Temperature and light requirements for growth of two diatom species (Bacillariophyceae) isolated from an Arctic macroalga. *Polar Biol.*, 29, 476-486.

Kaufman, L., and Rousseeuw, P. (1990). *Finding groups in data: an introduction to cluster analysis*. New York: John Wiley & Sons, Inc.

Kaufman, M.R., Gradinger, R.R., Bluhm, B.A., and O'Brien, D.M. (2008) Using stable isotopes to assess carbon and nitrogen turnover in the Arctic sympagic amphipod *Onisimus litoralis*. *Oecologia*, 158, 11-22.

Kiørboe, T., and Tiselius, P.T. (1987) Gut clearance and pigment destruction in a herbivorous copepod, *Acartia tonsa*, and the determination of in situ grazing rates. *Journal of Plankton Research*, 9, 525-534.

Klein, B., Gieskes, W.W.C., and Kraay, G.G. (1986) Digestion of chlorophylls and carotenoids by the marine protozoan *Oxyrrhis marina* studied by HPLC analysis of algal pigments. *Journal of Plankton Research*, 8, 827-836.

Kwak, T.J., and Zedler, J.B. (1997) Food web analysis of southern California coastal wetlands using multiple stable isotopes. *Oecologia*, 110, 262-277.

Lalande, C., Grebmeier, J.M., Wassmann, P., Cooper, L.W., Flint, M.V., and Sergeeva, V.M. (2007) Export fluxes of biogenic matter in the presence and absence of seasonal sea ice cover in the Chukchi Sea. *Cont. Shelf Res.*, 27, 2051-2065.

Laws, E.A., Bienfang, P.K., Ziemann, D.A., and Conquest, L.D. (1988) Phytoplankton population-dynamics and the fate of production during the spring bloom in Auke Bay, Alaska. *Limnol. Oceanog.*, 33, 57-65.

Layman, C.A., Araujo, M.S., Boucek, R., Hammerschlag-Peyer, C.M., Harrison, E., Jud, Z.R., Matich, P., Rosenblatt, A.E., Vaudo, J.J., Yeager, L.A., Post, D.M., and Bearhop, S. (2012) Applying stable isotopes to examine food-web structure: an overview of analytical tools. *Biol. Rev.*, 87, 545-562.

Layman, C.A., Arrington, D.A., Montana, C.G., and Post, D.M. (2007a) Can stable isotope ratios provide for community-wide measures of trophic structure? *Ecology*, 88, 42-48.

Layman, C.A., Quattrochi, J.P., Peyer, C.M., and Allgeier, J.E. (2007b) Niche width collapse in a resilient top predator following ecosystem fragmentation. *Ecology Letters*, 10, 937-944.

Leakey, C.D.B., Attrill, M.J., Jennings, S., and Fitzsimons, M.F. (2008) Stable isotopes in juvenile marine fishes and their invertebrate prey from the Thames Estuary, UK, and adjacent coastal regions. *Estuar. Coast. Shelf Sci.*, 77, 513-522.

Lee, C., Wakeham, S.G., and Hedges, J.I. (2000) Composition and flux of particulate amino acids and chloropigments in equatorial Pacific seawater and sediments. *Deep-Sea Res. I*, 47, 1535-1568.

Lorenzen, C.J. (1967) Determination of chlorophyll and pheo-pigments: spectrophotometric equations. *Limnol. Oceanog.*, 12, 343-346.

Lorenzen, C.J., and Downs, J.N. (1986) The specific absorption coefficients of chlorophyllide *a* and pheophorbide *a* in 90% acetone, and comments on the fluorometric determination of chlorophyll and pheopigments. *Limnol. Oceanog.*, 31, 449-452.

Lovvorn, J.R., Cooper, L.W., Brooks, M.L., De Ruyck, C.C., Bump, J.K., and Grebmeier, J.M. (2005) Organic matter pathways to zooplankton and benthos under pack ice in late winter and open water in late summer in the north-central Bering Sea. *Mar. Ecol. Prog. Ser.*, 291, 135-150.

Lovvorn, J.R., Richman, S.E., Grebmeier, J.M., and Cooper, L.W. (2003) Diet and body condition of spectacled elders wintering in pack ice of the Bering Sea. *Polar Biol.*, 26, 259-267.

Maberly, S.C., Raven, J.A., and Johnston, A.M. (1992) Discrimination between 12C and 13C by marine plants. *Oecologia*, 91, 481-492.

Macdonald, R.W., Sakshaug, E., and Stein, R. (2004). The Arctic Ocean: Modern status and recent climate change. In R. Stein, & R.W. Macdonald, *The Organic Carbon Cycle in the Arctic Ocean* (pp. 6-21). Berlin: Springer-Verlag.

Macdonald, T.A., Burd, B.J., Macdonald, V.I., and van Roodselaar, A. (2010). Taxonomic and feeding guild classification for the marine benthic macroinvertebrates of the Strait of Georgia, British Columbia. *Can. Tech. Rep. Fish. Aquat. Sci.*, Vol. 2874 (pp. 1-63).

Machas, R., Santos, R., and Peterson, B. (2003) Tracing the flow of organic matter from primary producers to filter feeders in Ria Formosa lagoon, southern Portugal. *Estuaries*, 26, 846-856.

Macko, S., and Estep, M. (1984) Microbial alteration of stable nitrogen and carbon isotopic compositions of organic matter. *Org. Geochem.*, 6, 787-790.

Macko, S.A., Fogel, M.L., Hare, P.E., and Hoering, T.C. (1987) Isotopic fractionation of nitrogen and carbon in the synthesis of amino-acids by microorganisms. *Chem. Geol.*, 65, 79-92.

Matheke, G.E.M., and Horner, R. (1974) Primary productivity of the benthic microalgae in the Chukchi Sea near Barrow, Alaska. *J. Fish. Res. Bd. Canada*, 31, 1779-1786.

McCall, B.D., and Pennings, S.C. (2012) Disturbance and recovery of salt marsh arthropod communities following BP Deepwater Horizon oil spill. *Plos One*, 7, 1-7.

McClelland, J.W., Valiela, I., and Michener, R.H. (1997) Nitrogen-stable isotope signatures in estuarine food webs: A record of increasing urbanization in coastal watersheds. *Limnol. Oceanog.*, 42, 930-937.

McConnaughey, T., and McRoy, C.P. (1979) Food web structure and the fractionation of carbon isotopes in the Bering Sea. *Mar. Biol.*, 53, 257-262.

McGee, D., Laws, R.A., and Cahoon, L.B. (2008) Live benthic diatoms from the upper continental slope: extending the limits of marine primary production. *Mar. Ecol. Prog. Ser.*, 356, 103-112.

McMahon, K.W., Ambrose, W.G., Johnson, B.J., Sun, M.Y., Lopez, G.R., Clough, L.M., and Carroll, M.L. (2006) Benthic community response to ice algae and phytoplankton in Ny Alesund, Svalbard. *Mar. Ecol. Prog. Ser.*, 310, 1-14.

Mincks, S.L., Smith, C.R., and DeMaster, D.J. (2005) Persistence of labile organic matter and microbial biomass in Antarctic shelf sediments: evidence of a sediment 'food bank'. *Mar. Ecol. Prog. Ser.*, 300, 3-19.

Mincks, S.L., Smith, C.R., Jeffreys, R.M., and Sumida, P.Y.G. (2008) Trophic structure on the West Antarctic Peninsula shelf: Detritivory and benthic inertia revealed by $\delta^{13}C$ and $\delta^{15}N$ analysis. *Deep-Sea Res. II*, 55, 2502-2514.

Mintenbeck, K., Jacob, U., Knust, R., Arntz, W.E., and Brey, T. (2007) Depth-dependence in stable isotope ratio $\delta^{15}N$ of benthic POM consumers: The role of particle dynamics and organism trophic guild. *Deep-Sea Res. I*, 54, 1015-1023.

Moed, J.R., and Hallegraeff, G.M. (1978) Some problems in the estimation of chlorophyll *a* and phaeopigments from pre-acidification and post-acidification spectrophotometric measurements. *Internationale Revue Der Gesamten Hydrobiologie*, 63, 787-800.

Moncreiff, C.A., and Sullivan, M.J. (2001) Trophic importance of epiphytic algae in subtropical seagrass beds: evidence from multiple stable isotope analyses. *Mar. Ecol. Prog. Ser.*, 215, 93-106.

Moran, S.B., Ellis, K.M., and Smith, J.N. (1997) Th-234/U-238 disequilibrium in the central Arctic Ocean: implications for particulate organic carbon export. *Deep-Sea Res. II*, 44, 1593-1606.

Moran, S.B., Kelly, R.P., Hagstrom, K., Smith, J.N., Grebmeier, J.M., Cooper, L.W., Cota, G.F., Walsh, J.J., Bates, N.R., and Hansell, D.A. (2005) Seasonal changes in POC export flux in the Chukchi Sea and implications for water column-benthic coupling in Arctic shelves. *Deep-Sea Res. Part II-Top. Stud. Oceanogr.*, 52, 3427-3451.

Morata, N., Poulin, M., and Renaud, P.E. (2011) A multiple biomarker approach to tracking the fate of an ice algal bloom to the sea floor. *Polar Biol.*, 34, 101-112.

Morata, N., and Renaud, P.E. (2008) Sedimentary pigments in the western Barents Sea: A reflection of pelagic-benthic coupling? *Deep-Sea Res. II*, 55, 2381-2389.

Naeem, S. (1998) Species redundancy and ecosystem reliability. *Conservation Biology*, 12, 39-45.

Naidu, A.S., Cooper, L.W., Finney, B.P., Macdonald, R.W., Alexander, C., and Semiletov, I.P. (2000) Organic carbon isotope ratios (delta C-13) of Arctic

Amerasian continental shelf sediments. *International Journal of Earth Sciences*, 89, 522-532.

Naidu, A.S., Cooper, L.W., Grebmeier, J.M., Whitledge, T.E., and Hameedi, M.J. (2004). The continental margin of the north Bering-Chukchi Sea: Concentrations, fluxes, accumulation and burial rates of organic carbon. In R. Stein, & R.W. Macdonald, *The Organic Carbon Cycle in the Arctic Ocean* (pp. 193-203). Berlin: Springer-Verlag.

Naidu, A.S., Scalan, R.S., Feder, H.M., Goering, J.J., Hameedi, M.J., Parker, P.L., Behrens, E.W., Caughey, M.E., and Jewett, S.C. (1993) Stable organic carbon isotopes in sediments of the north Bering-south Chukchi seas, Alaskan-Soviet Arctic Shelf. *Cont. Shelf Res.*, 13, 669-691.

Nayar, S., Goh, B.P.L., and Chou, L.M. (2005) Environmental impacts of diesel fuel on bacteria and phytoplankton in a tropical estuary assessed using in situ mesocosms. *Ecotoxicology*, 14, 397-412.

Newsome, S.D., del Rio, C.M., Bearhop, S., and Phillips, D.L. (2007) A niche for isotopic ecology. *Frontiers in Ecology and the Environment*, 5, 429-436.

Nyssen, F., Brey, T., Lepoint, G., Bouquegneau, J.M., De Broyer, C., and Dauby, P. (2002) A stable isotope approach to the eastern Weddell Sea trophic web: focus on benthic amphipods. *Polar Biol.*, 25, 280-287.

Olsgard, F., and Gray, J.S. (1995) A comprehensive analysis of the effects of offshore oil and gas exploration and production on the benthic communities of the Norwegian continental-shelf. *Mar. Ecol. Prog. Ser.*, 122, 277-306.

Perovich, D.K. (2011) The changing arctic sea ice cover. *Oceanography*, 24, 162-173.

Peterson, B.J. (1999) Stable isotopes as tracers of organic matter input and transfer in benthic food webs: A review. *Acta Oecologica*, 20, 479-487.

Peterson, B.J., and Fry, B. (1987) Stable isotopes in ecosystem studies. *Annual Review of Ecology and Systematics*, 18, 293-320.

Pinckney, J., Papa, R., and Zingmark, R. (1994) Comparison of high-performance liquid-chromatographic, spectrophotometric, and fluorometric methods for determining chlorophyll a concentrations in estuarine sediments. *Journal of Microbiological Methods*, 19, 59-66.

Pinnegar, J.K., and Polunin, N.V.C. (2000) Contributions of stable isotope data to elucidating food webs of Mediterranean rocky littoral fishes. *Oecologia*, 122, 399-409.

Pirtle-Levy, R., Grebmeier, J.M., Cooper, L.W., and Larsen, I.L. (2009) Chlorophyll *a* in Arctic sediments implies long persistence of algal pigments. *Deep-Sea Res. II*, 56, 1326-1338.

Plante-Cuny, M.R., Barranguet, C., Bonin, D., and Grenz, C. (1993) Does chlorophyllide-a reduce reliability of chlorophyll *a* measurements in marine coastal sediments? *Aquatic Sciences*, 55, 19-30.

Post, D. (2002) Using stable isotopes to estimate trophic position: Models, methods, and assumptions. *Ecology*, 83, 703-718.

Post, D.M., Layman, C.A., Arrington, D.A., Takimoto, G., Quattrochi, J., and Montana, C.G. (2007) Getting to the fat of the matter: models, methods and assumptions for dealing with lipids in stable isotope analyses. *Oecologia*, 152, 179-189.

Rasmussen, J.B., Rowan, D.J., Lean, D.R.S., and Carey, J.H. (1990) Food-chain structure in Ontario lakes determines PCB levels in lake trout (*Salvelinus namaycush*) and other pelagic fish. *Can. J. Fish. Aquat. Sci.*, 47, 2030-2038.

Rau, G.H., Riebesell, U., and Wolf-Gladrow, D. (1996) A model of photosynthetic ^{13}C fractionation by marine phytoplankton based on diffusive molecular CO_2 uptake. *Mar. Ecol. Prog. Ser.*, 133, 275-285.

Ravelo, A., Konar, B., Trefry, J.H., and Grebmeier, J.M. (in press) Epibenthic community variability in the northeast Chukchi Sea. *Deep-Sea Res. II*.

Ravelo, A.M., Konar, B., Trefry, J.H., and Grebmeier, J.M. (2012). Epibenthic community variability in the Chukchi Sea. In K.H. Dunton, *Chukchi Sea Offshore Monitoring in Drilling Area (COMIDA): Chemical and Benthos (CAB) Final Report* (pp. 161-181). Port Aransas: University of Texas Marine Science Institute.

Raymond, P.A., McClelland, J.W., Holmes, R.M., Zhulidov, A.V., Mull, K., Peterson, B.J., Striegl, R.G., Aiken, G.R., and Gurtovaya, T.Y. (2007) Flux and age of dissolved organic carbon exported to the Arctic Ocean: A carbon isotopic study of the five largest arctic rivers. *Global Biogeochem. Cycles*, 21, GB4011, doi:4010.1029/2007GB002934.

Reigstad, M., Wassmann, P., Riser, C.W., Oygarden, S., and Rey, F. (2002) Variations in hydrography, nutrients and chlorophyll a in the marginal ice-zone and the central Barents Sea. *J. Mar. Syst.*, 38, 9-29.

Reum, J.C.P., and Essington, T.E. (2008) Seasonal variation in guild structure of the Puget Sound demersal fish community. *Estuaries. Coast.*, 31, 790-801.

Richardson, T.L., and Cullen, J.J. (1995) Changes in buoyancy and chemical composition during growth of a coastal marine diatom: Ecological and biogeochemical consequences. *Mar. Ecol. Prog. Ser.*, 128, 77-90.

Riemann, B. (1978) Carotenoid interference in spectrophotometric determination of chlorophyll degradation products from natural-populations of phytoplankton. *Limnol. Oceanog.*, 23, 1059-1066.

Root, R.B. (1967) The niche exploitation pattern of the blue-gray gnat catcher. *Ecol. Monogr.*, 37, 317 - 350.

Rowe, G.T., and Phoel, W.C. (1992) Nutrient regeneration and oxygen demand in Bering Sea continental shelf sediments. *Cont. Shelf Res.*, 12, 439-449.

Saitoh, S., Iida, T., and Sasaoka, K. (2002) A description of temporal and spatial variability in the Bering Sea spring phytoplankton blooms (1997-1999) using satellite multi-sensor remote sensing. *Prog. Oceanogr.*, 55, 131-146.

Sakshaug, E. (2004). Primary and secondary production in the Arctic Seas. In R. Stein, & R.W. Macdonald, *The Organic Carbon Cycle in the Arctic Ocean* (pp. 57-81). New York: Springer.

Sakshaug, E., and Slagstad, D. (1991) Light and productivity of phytoplankton in polar marine ecosystems - a physiological view. *Polar Research*, 10, 69-85.

Sakshaug, E., and Slagstad, D. (1992) Sea ice and wind: effects on primary productivity in the Barents Sea. *Atmosphere-Ocean*, 30, 579-591.

Sanchez, F., Velasco, F., Cartes, J.E., Olaso, I., Preciado, I., Fanelli, E., Serrano, A., and Gutierrez-Zabala, J.L. (2006) Monitoring the Prestige oil spill impacts on some key species of the Northern Iberian shelf. *Marine Pollution Bulletin*, 53, 332-349.

Schonberg, S.V., Clarke, J.T., and Dunton, K.H. (in press) Distribution, abundance, biomass, and diversity of benthic infauna in the northeast Chukchi Sea, Alaska in realation to environmental variables and marine mammal predators. *Deep-Sea Res. II*.

Schonberg, S.V., and Dunton, K.H. (2012). The distribution, abundance, and diversity of the benthic fuana of the northeastern Chukchi Sea. In K.H. Dunton, *Chukchi Sea Offshore Monitoring in Drilling Area (COMIDA): Chemical and Benthos (CAB) Final Report* (pp. 143-160). Port Aransas: University of Texas Marine Science Institute.

Shuman, F.R., and Lorenzen, C.J. (1975) Quantitative degradation of chlorophyll by a marine herbivore. *Limnol. Oceanog.*, 20, 580-586.

Slattery, M., McClintock, J.B., and Bowser, S.S. (1997) Deposit feeding: A novel mode of nutrition in the Antarctic colonial soft coral *Gersemia antarctica*. *Mar. Ecol. Prog. Ser.*, 149, 299-304.

Smayda, T.J. (1971) Normal and accelerated sinking of phytoplankton in the sea. *Marine Geology*, 11, 105-122.

Solórzano, L. (1969) Determination of Ammonia in Natural Waters by Phenolhypochlorite Method. *Limnol. Oceanog.*, 14, 799-801.

Souza, A.C., and Dunton, K.H. (in press) Rates of nitrification and ammonium regeneration and uptake in northeastern Chukchi Sea shelf waters. *Deep-Sea Res. II*.

Stein, R., and Macdonald, R.W. (2004). Geochemical proxies used for organic carbon source identification in Arctic Ocean sediments. In R. Stein, & R.W. Macdonald, *The Organic Carbon Cycle in the Arctic Ocean*, Vol. 1 (pp. 24-32). Berlin: Springer.

Stringer, W.J., and Groves, J.E. (1991) Location and areal extent of polynyas in the Bering and Chukchi Seas. *Arctic*, 44, 164-171.

Strom, S.L. (1993) Production of pheopigments by marine protozoa - results of laboratory experiments analyzed by HPLC. *Deep-Sea Res. I*, 40, 57-80.

Sun, M.-Y., Clough, L.M., Carroll, M.L., Dai, J., Jr, W.G.A., and Lopez, G.R. (2009) Different responses of two common Arctic macrobenthic species (*Macoma balthica* and *Monoporeia affinis*) to phytoplankton and ice algae: Will climate change impacts be species specific? *J. Exp. Mar. Biol. Ecol.*, 376, 110-121.

Sun, M.Y., Aller, R.C., and Lee, C. (1991) Early diagenesis of chlorophyll-*a* in Long Island Sound sediments - A measure of carbon flux and particle reworking. *J. Mar. Res.*, 49, 379-401.

Sun, M.Y., Carroll, M.L., Ambrose, W.G., Clough, L.M., Zou, L., and Lopez, G.R. (2007) Rapid consumption of phytoplankton and ice algae by Arctic soft-sediment

benthic communities: Evidence using natural and C-13-labeled food materials. *J. Mar. Res.*, 65, 561-588.
Sun, M.Y., Lee, C., and Aller, R.C. (1993) Anoxic and oxic degradation of 14C-labeled chloropigments and a 14C-labeled diatom in Long Island Sound sediments. *Limnol. Oceanog.*, 38, 1438-1451.
Thomson Reuters (2013) *Web of Science*. Retrieved from http://webofknowledge.com on 9 October 2013.
Tietjen, J.H. (1968) Chlorophyll and pheo-pigments in estuarine sediments. *Limnol. Oceanog.*, 13, 189-192.
Trefry, J.H., Dunton, K.H., Trocine, R.P., Schonberg, S.V., McTigue, N.D., Hersh, E.S., and McDonald, T.J. (2013) Chemical and biological assessment of two offshore drilling sites in the Alaskan Arctic. *Marine Environmental Research*, 86, 35-45.
Vallentyne, J.R. (1955) Sedimentary chlorophyll determination as a paleobotanical method. *Canadian Journal of Botany*, 33, 304-313.
Vander Zanden, M., and Rasmussen, J. (2001) Variation in delta N-15 and delta C-13 trophic fractionation: Implications for aquatic food web studies. *Limnol Oceanogr*, 46, 2061-2066.
Velando, A., Munilla, I., Lopez-Alonso, M., Freire, J., and Perez, C. (2010) EROD activity and stable isotopes in seabirds to disentangle marine food web contamination after the Prestige oil spill. *Environ. Pollut.*, 158, 1275-1280.
von Quillfeldt, C.H. (2000) Common diatom species in arctic spring blooms: Their distribution and abundance. *Botanica Marina*, 43, 499-516.
von Quillfeldt, C.H., Ambrose, W.G., and Clough, L.M. (2003) High number of diatom species in first-year ice from the Chukchi Sea. *Polar Biol.*, 26, 806-818.
Wakeham, S.G., Lee, C., Hedges, J.I., Hernes, P.J., and Peterson, M.L. (1997) Molecular indicators of diagenetic status in marine organic matter. *Geochim. Cosmochim. Acta*, 61, 5363-5369.
Walker, B.H. (1992) Biodiversity and ecological redundancy. *Conservation Biology*, 6, 18-23.
Walker, C.H., Hopkin, S.P., Sibly, R.M., and Peakall, D.B. (2006). *Principles of Ecotoxicology*. Boca Raton: CRC Press.
Walsh, J.J., McRoy, C.P., Coachman, L.K., Goering, J.J., Nihoul, J.J., Whitledge, T.E., Blackburn, T.H., Parker, P.L., Wirick, C.D., Shuert, P.G., Grebmeier, J.M., Springer, A.M., Tripp, R.D., Hansell, D.A., Djenidi, S., Deleersnijder, E., Henricksen, K., Lund, B.A., Andersen, P., Müller-Karger, F.E., and Dean, K. (1989) Carbon and nitrogen cycling within the Bering/Chukchi Seas: Source regions for organic matter effecting AOU demands of the Arctic Ocean. *Prog. Oceanogr.*, 22, 277-359.
Wassmann, P., Olli, K., Wexels Riser, C., and Svensen, C. (2003). Ecosystem function, biodiversity and vertical flux regulation in the twilight zone. In G. Wefer, F. Lamy, & F. Mantoura, *Marine Science Frontiers for Europe* (pp. 279-287). Verlag Berlin Heidelberg New York: Springer.
Wassmann, P., and Reigstad, M. (2011) Future Arctic Ocean seasonal ice zones and implications for pelagic-benthic coupling. *Oceanography*, 24, 220-231.

Wassmann, P., and Slagstad, D. (1993) Seasonal and annual dynamics of particulate carbon flux in the Barents Sea: A model approach. *Polar Biol.*, 13, 363-372.

White, D., Kimerling, J.A., and Overton, S.W. (1992) Cartographic and geometric components of a global sampling design for environmental monitoring. *Cartogr. Geogr. Inf. Sci.*, 19, 5-22.

White, J.W., and Ruttenberg, B.I. (2007) Discriminant function analysis in marine ecology: some oversights and their solutions. *Mar. Ecol. Prog. Ser.*, 329, 301-305.

Whitney, D.E., and Darley, W.M. (1979) Method for the determination of chlorophyll *a* in samples containing degradation products. *Limnol. Oceanog.*, 24, 183-186.

Woelfel, J., Schumann, R., Peine, F., Flohr, A., Kruss, A., Tegowski, J., Blondel, P., Wiencke, C., and Karsten, U. (2010) Microphytobenthos of Arctic Kongsfjorden (Svalbard, Norway): biomass and potential primary production along the shore line. *Polar Biol.*, 33, 1239-1253.

Woodward, G., Thompson, R., Townsend, C.R., and Hildrew, A.G. (1995). Pattern and process in food webs: evidence from running waters. In A. Belgrano, U.M. Scharler, J. Dunne, & R.E. Ulanowicz, *Aquatic Food Webs: An Ecosystem Approach* (pp. 51-66). Oxford: Oxford University Press.

Wulff, A., Iken, K., Quartino, M.L., Al-Handal, A., Wiencke, C., and Clayton, M.N. (2009) Biodiversity, biogeography and zonation of marine benthic micro- and macroalgae in the Arctic and Antarctic. *Botanica Marina*, 52, 491-507.

Yager, P.L., Connelly, T.L., Mortazavi, B., Wommack, K.E., Bano, N., Bauer, J.E., Opsahl, S., and Hollibaugh, J.T. (2001) Dynamic bacterial and viral response to an algal bloom at subzero temperatures. *Limnol. Oceanog.*, 46, 790-801.

Yentsch, C.S., and Menzel, D.W. (1963) A method for the determination of phytoplankton chlorophyll and phaeophytin by fluorescence. *Deep-Sea Research*, 10, 221-231.

Ziegler, R., Blaheta, A., Guha, N., and Schonegge, B. (1988) Enzymatic formation of pheophorbide and pyropheophorbide during chlorophyll degradation in a mutant of *Chlorella fusca* Shihira et Kraus. *Journal of Plant Physiology*, 132, 327-332.